MASTER'S THESIS

Modelling the dynamic greenhouse gas emission intensity of the Dutch electricity mix

Bas J. Jansen

UNIVERSITY OF TWENTE.

Faculty of Electrical Engineering, Mathematics and Computer Science (EEMCS)

Master's thesis Sustainable Energy Technology

Modelling the dynamic greenhouse gas emission intensity of the Dutch electricity mix

Bas J. Jansen

Chair Prof.dr. J.L. Hurink
EEMCS
University of Twente

Supervisor Dr.ir. G. Hoogsteen
EEMCS
University of Twente

Supervisor Ir. E.W. Schaefer
Sustainable Energy Systems
Saxion University of Applied Sciences

External Ir. M.E. Toxopeus
Engineering Technology
University of Twente

July 18, 2023

"Soms denk ik uren na en heb ik nog niks op papier, een andere keer bereik ik precies datzelfde in vijf minuten."
Herman Finkers

Bas J. Jansen
Modelling the dynamic greenhouse gas emission intensity of the Dutch electricity mix
Master's thesis Sustainable Energy Technology, July 18, 2023
Supervising Committee: Prof.dr. J.L. Hurink, Dr.ir. G. Hoogsteen, Ir. E.W. Schaefer and Ir. M.E. Toxopeus

University of Twente
Faculty of Electrical Engineering, Mathematics and Computer Science (EEMCS)
Drienerlolaan 5
7522NB Enschede

Abstract

Electrical power in the grid is generated by an increasingly dynamic composition of sources. This is a result of a growing share intermittent renewable energy sources and dynamic power consumption. Different types of generation show large variations in life cycle environmental impact. Therefore, the environmental impact of electricity use is time dependent. This thesis aims to model the dynamic global warming potential of electricity consumption.

This thesis presents a methodology for determining the dynamic Greenhouse Gas (GHG) emission intensity of an electricity grid. Additionally a model tracking the GHG emission intensity of the Dutch grid, the Open Dynamic Electricity Composition Tracker, is presented and validated with measured data. The ODECT results show a steady decline as well as growing volatility of the GHG emission intensity of the Dutch grid.

In conclusion, current methods of carbon accounting fail to show the large potential for GHG emission reduction present in the dynamic aspects of the electricity mix. Insight in these dynamic aspects allows for lowering the carbon footprint of power consumption though the use of demand side management. Time granular carbon accounting and electricity pricing provide fair methods of allocating emissions to consumers, incentivising change in consumption behaviour. Furthermore, the transition towards a low-carbon electricity supply will be accelerated by standard open methodology as opposed to the current incomplete models.

Samenvatting

Elektriciteit wordt opgewekt door een steeds meer dynamische mix van verschillende bronnen. Dit komt onder andere door weersafhankelijke bronnen en dynamische vraag naar elektriciteit. Verschillende bronnen kennen grote variaties in gerelateerde ketenemissies. Hierdoor is het opwarmingspotentieel van elektriciteitsconsumptie tijdsafhankelijk. Het doel van deze thesis is het modelleren van het dynamische aardopwarmingsvermogen van elektriciteitsgebruik.

Deze thesis presenteert een nieuwe methode voor het bepalen van de dynamische broeikasgasintensiteit van het Nederlandse elektriciteitsnet. Een model dat de broeikasgasintensiteit volgt, de Open Dynamische Elektriciteits Compositie Tracker (ODECT), is ontwikkeld en gevalideerd met meetdata. De ODECT resultaten laten een stabiele afname en een groeiende volatiliteit van de broeikasgasintensiteit zien.

In conclusie, huidige methodes van koolstofboekhouding geven de grote potentie voor het terugdringen van elektriciteit gerelateerde emissies niet weer. Inzicht in de dynamische aspecten van de elektriciteitsmix maakt het mogelijk de koolstofvoetafdruk van elektriciteitsconsumptie te verlagen door middel van het afstemmen van verbruik. Tijdsafhankelijke koolstofboekhouding en tijdsafhankelijk beprijzen van gebruik vormt een eerlijke manier voor het toewijzen van emissies aan consumenten. Ten slotte zal de energietransitie versneld worden door een gestandaardiseerde en open methode voor het bepalen van de broeikasgasintensiteit in plaats van de vele incomplete modellen die momenteel beschikbaar zijn.

Dankwoord

In September 2017 fietste ik voor het eerst als student de campus van de UT op, de enige plek in Twente waar je een "Twents accent" kunt hebben. Nu, zes jaar later, rond ik trots mijn studietijd af met deze thesis. Mijn grote interesse in de energiesector heeft me geholpen bij het schrijven van deze thesis, maar dit valt in het niet bij de hulp en steun die ik van de volgende mensen heb gekregen:

Allereerst wil ik mijn thesis begeleiders, Gerwin en Edmund, bedanken. Jullie betrokkenheid en oprechte interesse in het onderwerp en de voortgang motiveerde enorm om een zo goed mogelijk resultaat neer te zetten. Ook het stukje verwachtingsmanagement, de opdracht moet tenslotte ergens een afronding hebben en kan niet oneindig diep zijn, heeft me geholpen tot dit verslag te komen. Beiden ontzettend bedankt, ik hoop dat we elkaar nog vaak tegen zullen komen.

The same holds for the entire research group. It was refreshing to experience the great sense of community and your sincere interest in my work. Although the population density could be quite high in the Energie-hok, I continuously enjoyed the presence of everyone. The many many cakes and treats were also a great addition.

Aan mijn vrienden, Tim, Mirko, Bram, Nathan, Ian, Cas, alle inwoners van Huize BIEM en natuurlijk de Sappige Mannen. Bedankt dat jullie me uren hebben laten ratelen over mijn projecten. Naast het feit dat jullie graag mee filosofeerden over het onderwerp, was het lekker om af en toe een pilsje te openen en even van het werk af te stappen. Dat heeft zeker geholpen bij het hoog houden van de motivatie tijdens het werken aan mijn thesis.

Als laatste wil ik mijn ouders, zussen en mijn vriendin Anne bedanken. Jullie hebben me altijd gesteund tijdens mijn studie, gaven me motivatie als ik deze nodig had, maar relativeerden ook het belang van de opdracht wanneer ik deze soms te hoog inschatte. Ook hielp het proeflezen enorm bij het wegwerken van de laatste schoonheidsfoutjes. Zonder jullie had ik deze thesis nooit kunnen maken.

Allemaal bedankt. Veel leesplezier.

Contents

1 Introduction

The relationship between humankind and its environment is changing. After scientists linked negative effects such as global warming, air pollution and loss of biodiversity to human action, a movement towards behavioural change has developed. Instead of depleting the resources and life present on our planet, humankind should steer towards a sustainable, symbiotic relationship with its natural environment. As an essential part of this transition, emissions of Greenhouse Gases (GHGs) should be reduced to prevent the ecological destruction by global warming.

Generation of electricity is one of the main sources of GHG emissions worldwide. In 2019, 32% of the human-caused GHG emissions were the result of global generation of electricity and heat [1]. In the Netherlands, the generation of electricity accounted for 22% of the national GHG emissions over the period of 2017 until 2021 [2]. Considering this scale of emissions and the growing human dependency on electricity as result of electrification of energy demand, reducing the GHG emissions of the electricity sector forms one of the key challenges in the mitigation of global warming.

Electricity can be generated from a range of sources. The predominant share of electricity related GHG emissions originates from burning fuels such as hard coal, lignite, natural gas, biomass, waste and oil [3]. Renewable Energy Sources (RESs) such as Photovoltaic (PV) panels, wind turbines, hydropower and geothermal power are characterised by low GHG emission intensity [4, 5]. Most developed countries have committed to the transition towards a GHG emission-free electricity supply, replacing fossil sources with RESs [6]. Solar, wind and some type of hydropower are weather dependent and fluctuate constantly. This intermittent generation profile as well as the low operational costs of these RESs lead to a dynamic electricity mix and a dynamic GHG emission intensity [3] [7]. Therefore, the timing of consumption affects the consumer's footprint.

Current carbon accounting methods that aim to allocate emissions to consumers of electricity are based on Guarantees of Origin (GOs) or annual Average Emission Factors (AEFs) which do not incorporate the dynamic aspects of electricity related GHG emissions. While these methods provided a first step towards electricity related emission accountability, they do not reflect the physical system and therefore disregard system boundaries such as capacity limits, temporal and geographical matching of supply and demand or even lack of physical connection between generator and consumer. As it is impossible to trace the origin of electrons consumed by individual loads, the electricity mix is considered to be equal for all consumers connected to a shared electricity grid [3, 8]. Even during behind-the-meter PV generation, consumed power behind the same meter might come from the grid through a different phase. Therefore, the GO backed claim of electricity 100% generated by RES does not hold in the physical domain. The current carbon accounting methods inevitably lack monetary and moral incentive for electricity consumer to align their consumption profile with the generation profile of RESs. A shift towards dynamic carbon accounting methods is needed to progress the transition towards a GHG emission-free electricity supply. Before dynamic GOs are realised, accurate dynamic GHG emission intensity factors are needed to provide insight for consumption adaptation to governments, consumers and related organisations.

The topic of dynamic emission factors has been widely researched in the last decades (Related Works, Section 3.2). However, a standardised methodology to calculate dynamic emission factors does currently not exist. Most models focus on a specific aspect of the calculation, and rely on general assumptions for other aspects, limiting their overall accuracy. For example, some models focus on broad coverage of zones while overlooking zone specific aspects such as missing data. Furthermore, many implemented models provide no or only limited insight in their methodology, data sources and resulting data. As a result of this lack of transparency, no foundation can be given for conclusions based on this data. In order to provide qualitative data that is fit for research and decision making, it should be accompanied by a descriptive methodology. The use of public data and full methodological transparency will maximise impact of a dynamic GHG emission intensity method by allowing for broad use, comparison and debate.

1.1 Research questions

The objective of this work is to present a methodology for the calculation of the dynamic GHG emission intensity of the Dutch electricity grid using public data. The dynamic GHG emission can be used as input for time granular methods of carbon accounting and demand side management. By creating insight in the dynamic aspects of the electricity mix and its related GHG emissions, possibilities arise for adaptation, development and planning towards a future-proof, GHG emission free electricity supply. The main research question of this thesis is:

How can the dynamic GHG emission intensity of the Dutch electricity mix be modelled using publicly available data sources?

The answer to the research question can be found by answering the following sub-questions:

1. How is the production and consumption of electrical power organised?
2. How are dynamic GHG emission intensity factors calculated by existing methods and models?
3. How can the GHG emission intensity of the electricity mix be determined from publicly available data?
4. What is the validity of the developed methodology?

1.2 Outline

This thesis is structured as follows: In Chapter 2 the background of the presented methodology will be laid out. The background details current methods of power generation, transmission and consumption of electrical power as well as the functioning of electrical power markets and involved stakeholders. Furthermore, sources of GHG emissions related to the generation of electrical power and standard carbon accounting methods are presented. In Chapter 3 the existing dynamic GHG emission intensity factor methodologies will be compared, available data will be presented. Furthermore, this chapter presents a new methodology for determining the GHG emission intensity of the Dutch electricity mix and a derived model: the Open Dynamic Electricity Composition Tracker (ODECT). In Chapter 4, the data generated by ODECT is analysed and the validity of the model is assessed. Finally, in Chapters 5 and 6 the main conclusions of this work as well as recommendations for future work are presented.

Background

2

Electricity is used to power a wide range of appliances, from LED light bulbs (5W) to large industrial e-boilers (50 MW). Complex systems of generation, trade and transmission are hidden behind the seemingly self-evident supply of electricity. In this chapter, the processes between power generation from initial energy sources to the delivery of power to the consumer are described. Section 2.1 describes the physical route of electrical power from generation by various types of power plants to the consumption. In Section 2.2, electricity markets as link between generation and consumption and its stakeholders are discussed. Finally, in Section 2.3 the sources of GHG emissions related to electricity generation are presented along with carbon accounting methods for assigning these emission to responsible parties.

2.1 Electricity grid

2.1.1 Generation

Electricity is not a natural resource than can be harvested. It has to be generated by conversion of other forms of energy. For example, when generating electricity from coal incineration, the chemical energy stored in the coal is transformed into thermal energy which is converted into electrical energy. With a greater scope, it can be observed that the chemical energy in the coal is originally obtained from radiant (solar) energy and millions of years of thermal and gravitational energy. The generation type composition of the power in the electricity grid is referred to as the electricity mix. As electrical energy can be generated from the various types of energy available on earth, electricity mixes consist of a broad range of generation types. Figure 2.1 shows the relative global generation per generation type and time period. Generation types can be categorised as either renewable or non-renewable, with the exception of waste which can be organic (renewable) and non-organic waste (non-renewable). Because of its unknown composition and non-organic fraction, waste will be categorised as non-renewable throughout this thesis. While nuclear energy uses radioactive fuels, it is categorised as renewable in this thesis considering its emission characteristics and abundant reserves of uranium [9]. The generation types in Figure 2.1 are also grouped by the type of energy that is converted into electricity. By far the largest share of electricity is generated from thermal energy through the use of various types of turbines. The thermal heat is produced by the burning of fuels such as coal and gas, nuclear fission or extraction of heat from solar irradiation. Additionally, heat can be extracted as geothermal energy from the earths crust. Generally, heat is stored in a working fluid which leads to a pressure increase. The fluid is then forced through a turbine, resulting in a rotational torque that powers a generator. Apart from heat, smaller shares of electrical power originate from the direct conversion of mechanical energy in the form of wind- and hydro power. A third method of electrical power generation in the form of the conversion of radiant energy by PV panels is responsible for a growing share of the electricity generation. The working principles of all generation types and their respective sub-types are elaborated in Appendix A.

Apart from the energy type that is converted to electricity, the generation type can be categorised amongst others by the cost of generation, emission intensity and ramp speeds. Cost of electricity is commonly expressed in Levelised Cost of Electricity (LCOE) which includes all lifetime costs of installing, operating and dismantling the power generating installation. The emission intensity of generation types is expressed in mass of specific emissions per kWh [10]. In the case of greenhouse gases (GHGs), the emission intensity is expressed in gCO_2eq/kWh [10]. This unit includes the equivalent values of all emitted GHG emissions analysed within a specific scope, which is elaborated in Section 2.3.1. The ramp speed is the extent to which a power generating installation is able to increase or decrease its generation per unit of time, often measured in %/min. Besides exploiting other options such as batteries and DSM, including generation sources with high ramp speed is crucial for a robust and agile electricity supply, because the generation can quickly respond to unexpected events, continuously matching supply and demand.

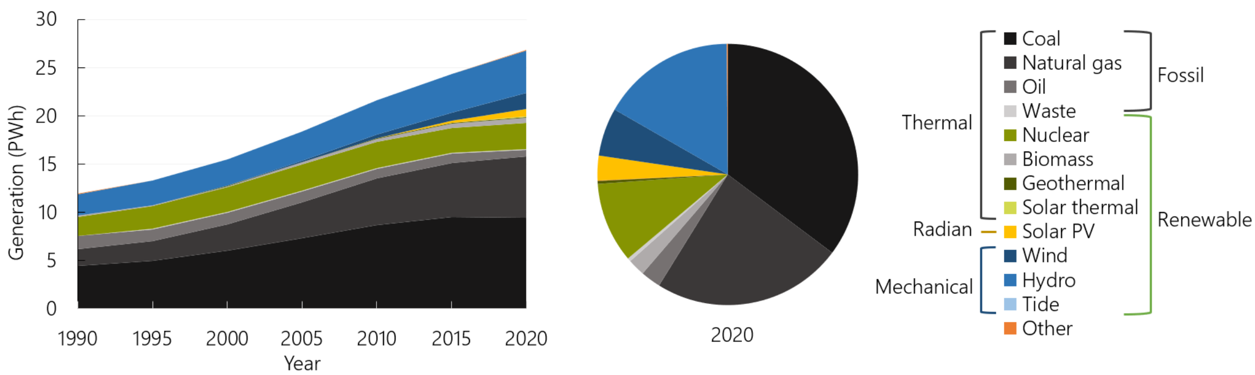

Fig. 2.1.: Overview of global electricity generation by source [11]. The sources are grouped in their respective domain of transferred energy i.e. the energy type that is converted to electricity.

2.1.2 Grid infrastructure

The previous section covered the common electricity generation types. In order to use the electricity for lighting, cooking, heating and many other appliances, it has to be transported to the end users and converted to a usable voltage level. This is done through the electricity grid. In this thesis the electricity grid is defined as the entire infrastructure between generators and electricity consuming appliances. The electricity grid is a large and complex network designed to efficiently transmit and distribute electricity. The system components consist of various types of transmission lines for different voltage levels and substations housing voltage changing transformers and equipment for monitoring and protecting the operation of the grid. In order to transmit the power efficiently, the voltage is increased for transmission over larger distances. This fact as well as safety and demand requirements result in several interconnected grid layers with different scales and voltages, i.e. the voltage of these layers and the distance of transmission are related. These levels are illustrated in Figure 2.2. The spatially largest grid layer, on an international level, is the synchronous grid. The synchronous grid connects countries and transmits power delivered by large electrical power plants, e.g. nuclear power plants, to transmission grids. On a (semi-) national, the transmission grid connects regions and transmits power delivered by electricity producing generators, e.g. natural gas fired power plants, and the synchronous grid to large industrial consumers and distribution grids. The distribution grid delivers the produced power to end users on a local level. An increasing share of decentral generators such as PV panels or small onshore wind turbines is added to the distribution grid, adding to the bidirectionality of power transmission.

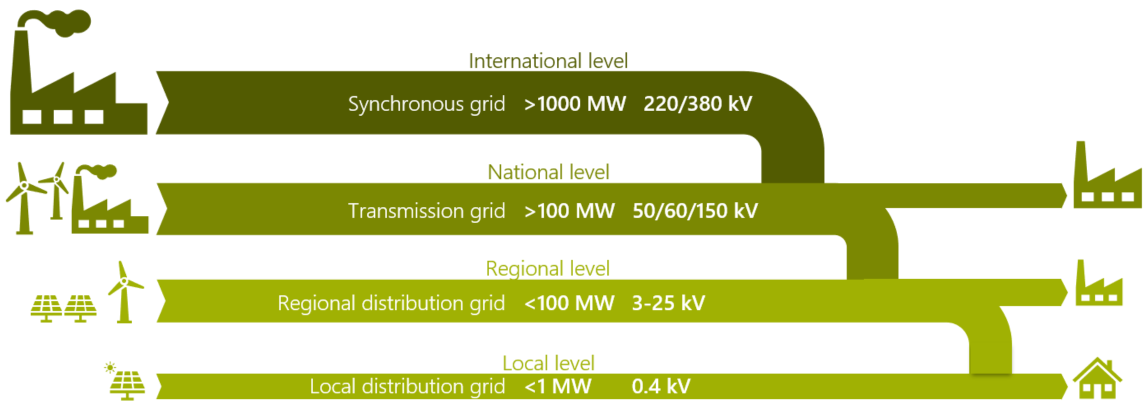

Fig. 2.2.: Overview of different bidirectional transmission levels of the electricity grid. Adapted from [12].

In Figure 2.3, the Dutch high-voltage grid is shown. The Dutch electricity grid is connected to neighbouring countries through nine cross-border connections (four with Germany, two with Belgium, and one with Norway, Denmark and Great Britain each).

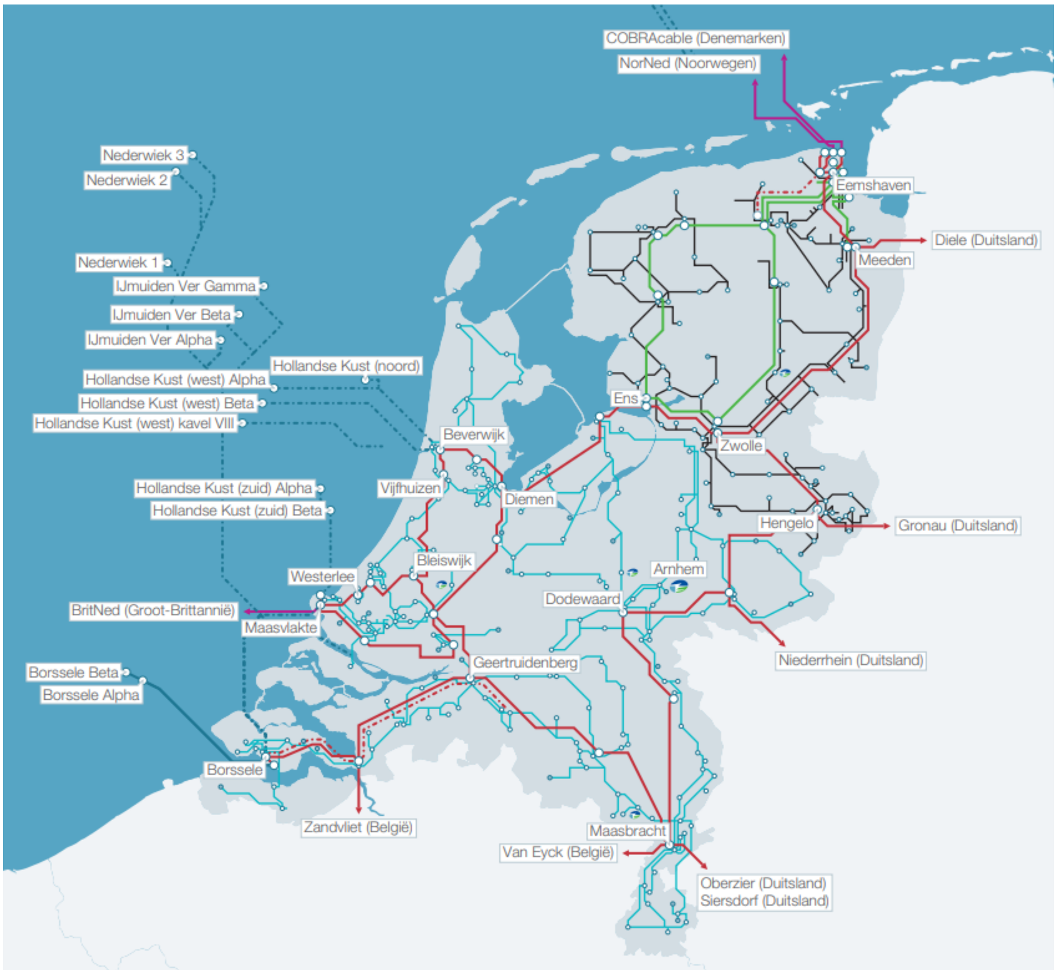

Fig. 2.3.: Map of the transmission grid in the Netherlands. The colour of the lines indicate different voltage levels. The dotted lines are under construction. Arrows indicate cross-border transmission lines. Adapted from [13].

2.1.3 Consumption

The electricity grid currently operates without large scale storage installations (aside from pumped hydro in some countries) [14, 15]. This means that generated power has to be consumed instantly to assure a stable grid operation. The grid infrastructure has to facilitate this instantaneous match in supply and demand by providing sufficient capacity i.e. room for power transmission. Up until recently, generation of electrical power has followed demand by ramping power plant up and down in accordance with a change in demand.

The aggregated electricity demand has a distinct pattern. However, this aggregation consists of countless events of electricity consumption, each with its own pattern. Some events are predictable, such as automated street lighting. Some are hard to predict, such as the use of a laptop charger. As general rule, including a larger number of events in a demand profile increases its predictability. This predictability is important because the total demand profile has to reflected by the generation profile perfectly in order to comply with the match in supply and demand.

With increasing weather dependent generation types such as PV and wind turbines, this becomes a challenge as increasingly little adjustable power supply is available to follow the demand profile. PV and wind are only adjustable by lowering generation through curtailment. A solution to uphold the match of supply and demand with increased shares of RESs lies on the consumption side. A change in demand profile can be realised through Demand Side Management (DSM). DSM is the overarching term for altered electricity consumption behaviour. Currently, some large industrial consumers provide change in demand to support the operation of the electricity grid in return for financial remuneration. Load-shifting is another example of DSM that describes the act of changing the time of electrical power consumption. Load shifting can be done with different goals such as cost reduction, emission reduction or to improve grid performance.

This section explained the physical power flow from generation to consumption. A second, monetary stream flows in the exact opposite direction in order to fund the effort of generating and transmitting electrical power to consumers. The next section will elaborate on the procurement process of electrical power through a range of power markets and the stakeholders that are involved.

2.2 Markets and stakeholders

Generation installations of all types are operated by producers that sell the generated electricity to consumers. The scale of producers range from residential rooftop PV installations producing 1000 Watts peak to multinational utility companies operating a portfolio with capacities of tens of gigawatts. The generated power is sold on electricity markets. Different types of electrical power markets exist depending on the time to delivery of power, ranging from years into the future to seconds ahead. This section presents the most important electricity markets, their operation and involved parties.

2.2.1 Markets

As stated above, power markets can be differentiated by the time to delivery. The market that trades the furthest into the future is conveniently called the future (or forward) market. In the future market, contracts are traded with a specified amount of electricity and specified location and time of delivery. Similarly, Power Purchase Agreements (PPAs) are traded. PPAs are bilateral long term agreements with disclosed power quantities, prices and risks allocation. Closer to the delivery time are the capacities on the day-ahead and intraday market. on these markets, electrical power is traded that is delivered the next day or up to 5 minutes prior to delivery respectively. These three markets are wholesale markets on which large quantities of electrical power are traded. Besides the wholesale markets, where producers, traders, and large consumers trade power, retail markets exists where energy retailers sell electricity (and gas) to individual consumers. On the retail market, electricity is sold to small consumers by retailers and producers through running contracts [16]. These contracts describe the price for which electrical power is delivered, including taxes and transmission costs. The contracts do not specify time of delivery, but deliver power on demand in return for a deposit throughout the contract period. Annually, the precise electricity consumption and paid deposits are settled in an annual statement. The electricity price in retail contracts can be fixed for years in long term contracts, variable per quarter or month, or even dynamic, following the day-ahead market prices. Because of the common indirect pricing mechanisms (fixed and variable), individual consumers are often not aware of the working principles of the wholesale power markets, making it hard to grasp the electricity system characteristics. System knowledge or incentives are needed for change in consumption behaviour, but the indirect retail pricing mechanisms fail to include either.

Different electricity grid areas for which power can be exchanged freely without capacity allocation, are referred to as called bidding zones. European countries typically consist of one or a few bidding zones, e.g. one for the Netherlands (NL) and two for Denmark (DK1 and DK2). Bidding zones show large variations of electricity mixes as the result of regional aspects such as natural resource availability, historical development and political choices. In Germany, lignite provides the majority of electricity. In the Netherlands, natural gas is the predominant source [11]. These varations are the result of a merit order market mechanism. The merit order model, shown in Figure 2.4, is a general explanation of the most widely used dispatch strategy. On the wholesale markets, operators of generation installations place bids specifying for which price they are willing to generate a unit of energy. Together, these bids form a supply curve. These bids will be generally equal to the marginal running cost of specific generation unit. These costs differ per generation type, as shown in Figure **??**. The demand curve is given by the amount of electricity that will be bought related to the market price. Based on the intersection between the demand and supply curves, the market will be cleared, i.e. a price will be set. The generation units with lowest marginal costs will be dispatched at the highest price of the included generators. In the example of Figure 2.4, the electricity generated from wind, PV, nuclear lignite and coal will be sold for the marginal costs of coal fired power plants.

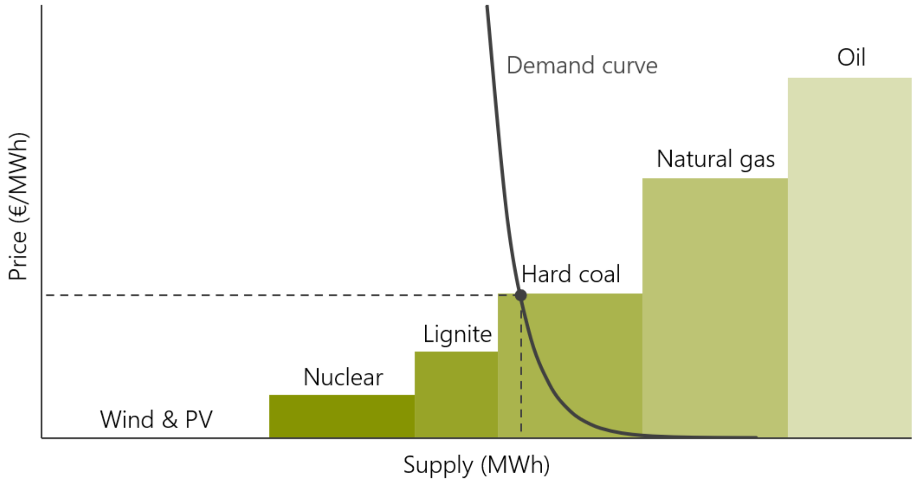

Fig. 2.4.: Illustrative example of the aggregated supply bids and demand curve. The dotted lines show the settled price and supply for this example

Solar and wind generation units are characterised by their low marginal costs. This allows plants of these generation technologies to be dispatched first at times of generation. However, this trend of low-emission technologies being dispatched first does not hold for the entire set of generation types. As a result, the increasing order of marginal running costs does not follow an increasing order of emission intensity [8]. For example, as seen in Figure 2.4, the relatively cheap but emission intensive lignite fired power plants are often dispatched before the relatively expensive, but relatively low-emission, natural gas plants. A hundredfold increase of today's Emission Trading System (ETS) price, Europe's carbon pricing mechanism, would be able to mitigate this situation, but this is not realistic in the near future [8]. Furthermore, power plants with high start-up costs will bid in a small portion of their nominal capacity at a loss-making price to keep the installations running in order to be able to react to market changes. Given these factors, a discrepancy exists between electricity pricing and related emissions [17, 18]. Therefore, electricity consumers are not incentivised by the market to minimise the GHG emission footprint of their electricity use.

In order to ensure stable the match between supply and demand, grid operators make a daily schedule of planned transmission. When a producer or consumer deviates from the program and there is an imbalance of generation and consumption, the frequency will deviate from its nominal value (50 Hz for European grids). On balancing markets, frequency restoration services by fast responding power generation or consumption installations are offered. These are called ancillary services. Four balancing markets are ordered in increasing response time: Frequency Containment Reserve (FCR), Automatic Frequency Restoration Reserve (aFRR), Manual Frequency Restoration Reserve (mFRR) and Restoration Reserve (RR) where the FCR market is able to respond in seconds and the RR market responds after approximately 12.5 minutes. The price paid for these services is collected afterwards from the parties negatively deviating from their planned transmission.

2.2.2 Stakeholders

A large group of stakeholders is involved in the different power markets. The group of producers generating electrical power consists of large industrial producers controlling a portfolio of power plants with a capacity of several gigawatts, small producers generating megawatts of electricity from rest streams, community initiatives with small generation installations and individuals with rooftop PV installations of several kilowatts peak. Similarly, consumers consist of industrial companies that buy electricity directly on the wholesale markets and small consumers that buy their electrical power from retailers. The markets are operated by electricity exchanges. The transmission of power through the transmission and distribution grid is controlled by the government regulated Transmission System Operators (TSOs) and Distribution System Operators (DSOs) respectively. The 39 TSOs active in 35 European countries are represented by the European Network of Transmission System Operators for Electricity (ENTSO-E) [19]. The ENTSO-E publishes data from its members on the Transparency Platform [15]. System operators are responsible for the balance of power generation and consumption. Therefore, they operate the balancing markets and assign balance responsibility to all parties trading volumes of electrical power in the electricity markets. The Balance Responsible Parties (BRPs) have to submit programs of planned transmissions of electrical power to the system operator. As stated in Section 2.2.1, deviation from these programs will result in a fine that covers the cost of acquiring ancillary services such as FCR by the system operator. Governments protect consumers in electricity markets through implementation of policies and set prices for regulated tasks of TSOs and DSOs.

This section gave an introductory overview of the working principles of the electricity grid. The physical electrical power is transmitted to consumers through the electricity grid and a inverse monetary stream flows to the producers of electricity. With the consumption of electricity comes a responsibility of emissions caused by electricity generation. The next section introduces a third and last "flow", the allocation of generation related emissions to consumers.

2.3 Emissions

The introduction of this work started with the fact that 32% of the human-caused GHG emissions are a result of electricity and heat generation [1]. This section explains the relation between GHG emissions and global warming, the origin of electricity related emissions and methods to assign emission responsibility.

2.3.1 Greenhouse gases

"Greenhouse gas emission" is a well-known term, sometimes referred to as "emission" or "carbon emission". In short, GHGs are gases with the potential of absorbing radiative heat. This characteristic causes these gases to capture heat in the atmosphere, resulting in global warming. Besides global warming, other environmental impacts can be analysed in relation to electricity consumption. While the methodology presented in this thesis allows for the analysis of other impacts through the use of impact factors, this thesis focuses on the impact of electricity consumption on global warming. Therefore, the impact factors are referred to as emission factors in this work. The extent to which a gas is able to absorb heat varies per type of gas and is expressed as Global Warming Potential (GWP). The GWP of a gas is expressed as a multiple of the heat that is absorbed by the same mass of carbon dioxide (CO_2). Therefore, the unit of GWP is the gram carbon dioxide equivalent, noted as gCO_2eq. The Intergovernmental Panel on Climate Change (IPCC) determines and publishes the GWP values for different GHGs. Table 2.1, a selection of gases and their respective GWP is shown. The GWP can be interpreted as follows: one kilogram of emitted methane (28 CO_2eq) has the same impact on global warming as 28 kilograms of emitted CO_2 or as 0.106 kilograms of nitrous oxide (265 CO_2eq). In this work, the emissions related to electricity production are expressed as emitted GHGs per unit of electrical energy or gCO_2eq/kWh. This unit expresses the GWP of all GHG emissions related to the generation of one kWh of electrical power as equivalent of the GWP of emitting one gram of carbon dioxide. While the listed GWPs in the assessment report of the IPCC consists of 86 GHGs, most calculations of GHG emissions intensity of electricity only take into account the emissions of CO_2, CH_4 and N_2O, as the quantity of other GHG emissions emitted in the process of electricity generation have a negligible impact on global warming [10].

2.3.2 Electricity related emissions

In an effort order to reduce the GHG emissions related to electricity generation, it is crucial to know their origin. The most obvious source of emissions related to generation of electrical power is the burning of fuels. Emissions as a result of fuel

Gas name	Chemical formula	GWP (100 years) in gCO_2eq
Carbon Dioxide	CO_2	1
Methane	CH_4	28
Nitrous oxide	N_2O	265
Sulfur hexafluoride	SF_6	23500

Tab. 2.1.: Global Warming Potential for a selection of greenhouse gases. IPCC Fifth Assessment Report [20]

incineration are referred to as direct emissions. For example, carbon (C) reacts with oxygen (O_2) to form carbon dioxide (CO_2) and dissipate heat which is converted to electrical power when coal is burned. The burning of biomass also results in direct GHG emissions. However, because the CO_2 captured in the biomass is absorbed by plants from the atmosphere in a negligible time span compared to fossil matter, the absolute direct emissions of electrical power generated from biomass is generally considered to be zero [5]. In its Fifth Assessment Report the IPCC argues for the distinction between temporary and permanent effects on the climate causes by biomass emissions. In this work, this approach and related emission factors are applied. Therefore, the temporary fraction of the direct emissions resulting from the burning of biomass is disregarded.

Apart from direct emissions, more types of electricity generation related GHG emissions exist. Emissions resulting from the construction, transportation, placement, maintenance and dismantlement of generators are indirect emissions. The direct and indirect emissions can be aggregated over the life cycle of a generator, and are therefore referred to as life cycle emissions. Therefore, methods that provide insight in electricity related GHG emissions based on direct emissions only provide an incomplete view of reality. Such an incomplete insight might lead to choices which defeat intended effects. By taking into account life-cycle emissions as opposed to direct emissions only, a more complete overview is created of the environmental impact as result of electricity consumption.

In Figure 2.5, life cycle emission sources of a selection of electrical power generation types are quantified. Methane emissions are part of the fuel production and transport of gas and coal. Furthermore, indirect methane emission make up a large fraction of the total GHG emissions related to hydropower generation as result of degradation of biomass in the water reservoirs. Another cause of emissions in regard to biomass are the CO_2 emissions as result of combustion of regenerative biomass, ecosystem disturbances and changes in surface albedo, i.e. changes in the amount of radiative heat absorbed to the landscape. Emissions from infrastructure and supply chain emissions result from the construction, materials and dismantlement of the power plant itself as well as the energy system infrastructure. Furthermore, the supply chain emissions include secondary material supplies such as solvents and catalysts.

Together, all of the emission categories form the life-cycle emissions of a electrical power supply [10]. Divided by the total amount of power generated over the life-cycle of the installation, the GHG emission intensity of the power can be determined for all generation types.

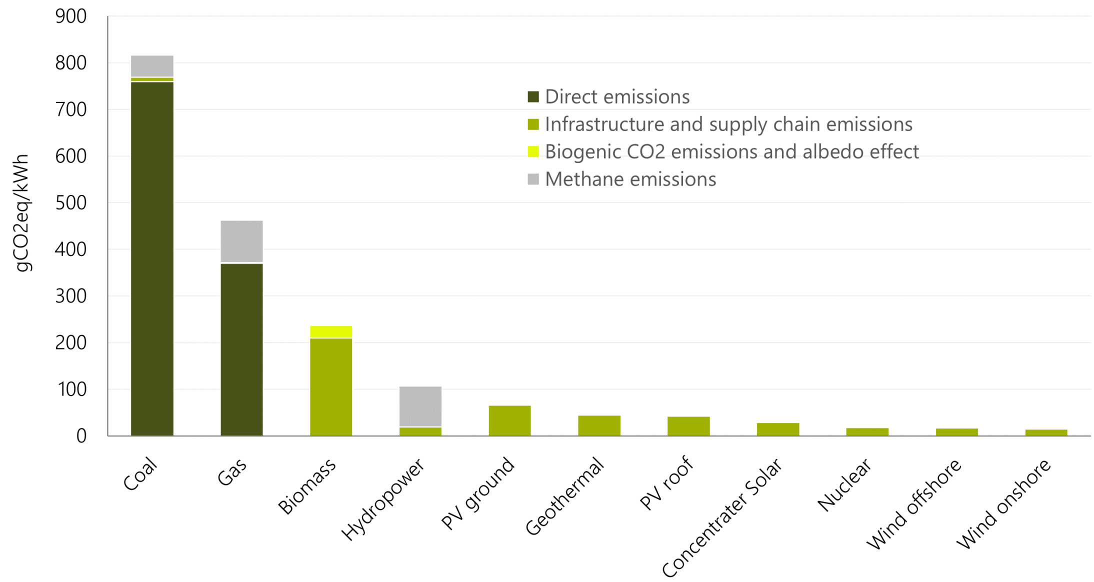

Fig. 2.5.: Types and quantities of life cycle emissions related to the electricity production of different generation types. Adapted from [5]

A Life Cycle Assessment (LCA) is used to quantify a wide range of environmental indicators, e.g. GHG emissions, over the life cycle of an electricity generating installation. The aim of an LCA is to create insight in the environmental profile of a product. In this case, the product is a unit of electrical energy (kWh) resulting from different generation types. By use of a Life Cycle Impact Assessment (LCIA) method, e.g. ReCiPe, environmental impact of electricity can be quantified [21]. The environmental impact can be expressed as single environmental effect (midpoints), e.g. global warming or freshwater eutrophication, or as overarching effects (endpoints) such as damage to human health or resource availability [22]. Table 2.2 shows the generation type specific impact of electricity generation on the midpoint impact categories: global warming, land use, water use, and mineral resources. It is interesting to note the differences between the relative impact of generation types on the different midpoint categories. While from a global warming point of view, electrical power generated by PV installations might be preferable over power from coal fired power plants, the opposite holds when focusing on the depletion of minerals and metals. Midpoints can be converted to endpoints through damage pathways, providing a straightforward interpretation of the environmental impact. However, this conversion increases the uncertainty of the LCIA results. This thesis aims to model the dynamic aspects of the impact of electricity consumption on the global warming midpoint.

Generation type *1 kWh*	Global warming *gCO_2eq*	Land use *points*	Dissipated Water *liters*	Minerals and metals *μg SB eq*
Hard Coal (IGCC)	850	2.4	2.9	520
Natural gas	430	0.2	1.2	240
Hydro	150	2.5	0.37	610
Nuclear	5.1	0.058	2.4	330
PV ground	37	1.9	0.58	4500
PV roof	37	0.86	0.63	7200
Wind onshore	12	0.11	0.18	680
Wind offshore	14	0.11	0.16	980

Tab. 2.2.: Environmental impact of different generation types on midpoint impact categories global warming, land use, water use, and mineral/metal use determined with ReCiPe version 1.13. Adapted from [4].

Multiple renowned studies classify the life cycle GHG emissions of generator types [23, 10, 4]. The inputs are generally characterised as gCO_2eq by weighing the different emissions by their GWP (Table 2.1). Subsequently, the results are characterised to gCO_2eq/kWh which allows for comparison between generator types. Recognised reports by the National Renewable Energy Laboratory (NREL), United Nations Economic Commission for Europe (UNECE) and Intergovernmental Panel on Climate Change (IPCC) provide harmonisations of numerous individual LCAs of global electricity generation related GHG emissions. These emission factors are not specified for Dutch power plants. While LCAs are generally open for interpretation (Appendix B) and results vary depending of the scope, these sources provide a solid basis for estimating the GWP of different generation types (Table 3.3) [23, 10, 4].

2.3.3 Carbon Accounting

With a known generation type composition, related emissions have to be allocated assign responsibility to consumers. Knowing which parties and actions are responsible for specific GHG emissions allows amongst others for fair policy making, better environmental performance determination and well-informed business and consumer decisions [24, 17, 25]. In line with this thought and in order to create a broad incentive for the reduction of GHG emissions, international climate treaties require signing countries to report their emissions annually. As a result, companies and organisations are required to monitor the emissions that result from their activities [26]. This is done through the practice of carbon accounting, which is the process of measuring, quantifying, and reporting greenhouse gas emissions associated with an organisation's activities [27]. It involves identifying and assessing the various sources of carbon emissions, calculating the amount of greenhouse gases released into the atmosphere, and documenting these emissions in a standardised manner.

In 2001, the first edition of the Greenhouse Gas Protocol was published by the World Resources Institute (WRI) and World Business Council for Sustainable Development. The protocol provides a detailed method for organisations to quantify their GHG emissions in a standardised way that allows for comparison. In accordance with the internationally accepted protocol, the emissions of organisations are split into three scopes. In scope 1, the direct GHG emissions emitted by sources controlled or owned by the organisation are accounted for. Scope 2 entails the GHG emissions related to the generation of electricity, steam, heat and cooling that is consumed by the organisation. Scope 3 describes the emissions that are a result of organisation activities where the emissions sources are outside the control of the company e.g. production of purchased materials, use of sold products and outsourced activities [27]. Scope 2, the largest source of GHG emissions for many organisations, is the focus of this thesis. Currently, the standard method of scope 2 carbon accounting is multiplication of annual aggregated electricity consumption (kWh) with an annual GHG emission intensity factor (gCO_2eq/kWh) of the local grid [3, 26]. Many recognised organisations such as the International Energy Agency (IEA), European Environmental Agency (EEA), Intergovernmental Panel on Climate Change (IPCC) and the European Union through the Joint Research Council (JRC) determine this annual GHG intensity factor for a range of countries [28, 29, 30]. For the Dutch electricity mix, the Statistics Netherlands (*Centraal Bureau voor de Statistiek*, CBS) and consultancy bureau CE Delft are the main sources for the annual GHG emission intensity factor [31, 32].

The Average Emission Factor (AEF), expressed in gCO_2eq/kWh, is considered to be the same for every user of the grid, as physical flows of electricity cannot be traced throughout the electricity grid. This means that electricity bought on the power markets is delivered to the grid, not directly to the buyer. Therefore, the generated electrical power is considered to be distributed equally over the loads of all grid connected consumers, i.e. every kW of electrical power is assigned the same average GHG emission intensity.

2.3.4 Guarantees of Origin

Considering the equal distribution of power in the electricity grid, procuring electricity generated by RESs is a complex task. Guarantees of Origin (GOs), referred to as Renewable Energy Certificates (RECs) in the United States, provide a method procuring elelctricity from RESs without direct physical delivery. When a power generating installation produces a MWh of electricity, a GO is issued specifying the origin of the generated electricity. This is illustratively shown in Figure 2.6. The electricity is directly fed to the grid, while the GO can be transferred to a retailer or consumer separately. A GO can be cancelled, meaning that the certificate is entered into a central registry and the attributes of the generated power are allocated to a specified user. The certificates are somewhat geographically and time restricted, e.g. European GOs have to be cancelled (assigned to a consumer) within the EU zone and maximally 18 months after the energy was physically produced.

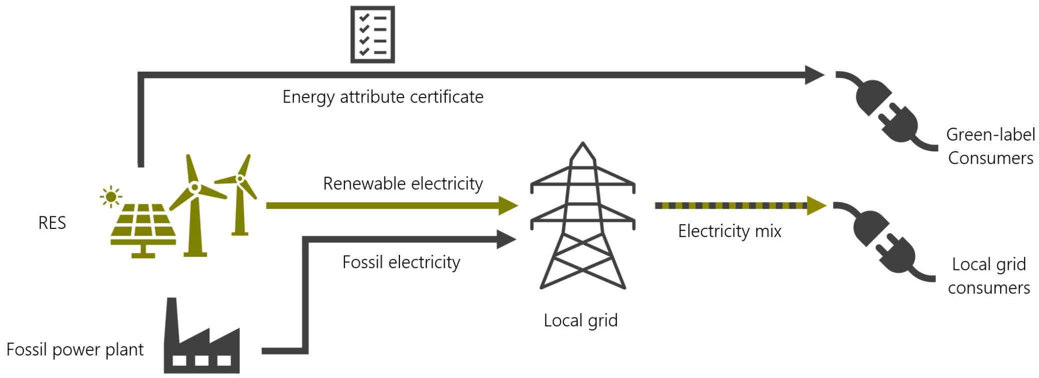

Fig. 2.6.: Overview of separation energy attribute certificate and physical transport of electricity. Adapted from [26].

While the separation of physical delivery and cancelling of GOs provides a method for organisations of buying electricity from renewable sources without realisation of a private physical connection, this separation also disregards the physical characteristics of electricity [33]. For example, a GO belonging to a MWh produced by a Spanish PV installation during the summer can be used by a Dutch company to give a clean label to a MWh of electricity consumption during a winter night. The separation of delivery and GO cancellation in time as well as location provides a false image of the GHG emission intensity of consumed electrical power. This discrepancy between physical transmission of electricity and the issuing of GOs is especially striking in the case of Iceland, where consumers from the European mainland are able to buy and use certificates related to the electricity generation by Icelandic geothermal power plants to label their electricity consumption to be renewable. This clearly shows the flaw of this method of carbon accounting, considering that there is no physical connection between Icelandic and the European grids [34].

The GHG emissions of electricity consumed by both households and multinationals with a certificate backed '100% renewable' label are in practice far from zero (Elaborate in Appendix C). The inverse also holds, consumers without renewable label will inevitably use some power generated by RESs. Their scope 2 actual GHG emissions dependent on the GHG emission intensity of their electricity grid. This method of carbon accounting does not hold because these consumers depend on (1) other consumers to use their renewable electricity in hours of excess of renewable electricity generation and on (2) fossil electricity generation in hours of shortage of renewable electricity generation. To allow a higher penetration of PV panels and wind turbines in the energy mix, a revised carbon accounting method is needed.

While historically the generation could match the consumption continuously, the dynamic generation and grid capacity will determine the allowed consumption in a decarbonised electricity system [14]. In pursuit of realising this system, steering the electricity demand to times of high generation is necessary. DSM is likely to play a significant role in the near future of the electricity system [8]. Forward thinking organisations including system operators, large companies and governmental agencies are calling for a revised version of GOs and PPAs with a stricter geographical and more time granular production-consumption match in order to more accurately reflect the environmental impact of electricity use [33, 35, 36, 37, 38, 26]. Such a revised version of the current GOs are referred to as Granular Certificates (GCs). When a renewable energy certificate has to be cancelled within 15 minutes of production, consumers are forced to change their consumption patterns if they wish to increase the share of their consumption covered by RESs. Large corporations deal with investors, shareholders, clients and consumers that increasingly push for use of low-emission electricity, incentivising the use of GCs. Furthermore, consumption reports of all organisations, progressive or conservative, would reflect their actual carbon footprint of electricity consumption.

2.3.5 Conclusion

The regulatory reform of GOs towards GCs will cost time, which causes deceleration of the energy transition by postponing necessary change in electricity consumption. DSM plays a crucial role in the realisation of electricity generation related GHG emission reduction. However, the currently standard carbon accounting methods do not facilitate DSM for GHG emission reduction. Considering the dynamic electricity mix and therefore the dynamic GHG emission intensity of the grid, methods of carbon accounting based on annual emission intensity factors fail to include insight in temporal effects of renewable electricity production [39, 8, 3]. Without this insight, organisation are not able to spot the potential for scope 2 emission reduction, governments are not able to steer consumption towards hours of peak renewable electricity production, and large and small consumers with a willingness to prevent global warming are not able to adapt consumption patterns to allow progression towards an emission-free electricity system. A dynamic GHG emission intensity factor is needed to progress reduction of GHG emissions before GCs are the new standard of carbon accounting.

Model

3

The previous chapters highlighted the need for and importance of accurate dynamic GHG intensity models. In this chapter, a method of determining the GHG emission intensity factor, also called the Average Emission Factor (AEF), is presented. Existing methodologies from academic literature and methods that appear in publicly available models are analysed. Subsequently, a new methodology of determining the dynamic AEF based on publicly available data is presented. This chapter concludes with an implementation section, in which the model is presented that is used to determine the dynamic AEF.

Throughout this chapter, a methodology for determining the dynamic AEF in near real-time is presented. In this work, near real-time data is defined as the data that is processed directly from the most up-to-date official feed of measurement data. In the case of the Transparency Platform feed, near real-time is a time delay of two hours. Sections 3.1 and 3.4 present an overview of the basic calculation. Sections 3.5 and 3.6 detail two in-depth aspects of the method. In order to provide a clear overview of the variables, Table 3.1 lists the variables that are presented throughout this chapter.

3.1 Average Emission Factor

The general definition of the AEF related to an electricity mix is the quantity of pollutant emissions related to the generation of electricity [40]. The AEF, measured in gCO_2/kWh, is a straightforward and useful metric as every electricity consumption can be directly converted into consumption related emissions. Every bidding zone (from now on called "zone") has a specific and time dependent AEF. This factor describes the average GHG emission intensity of all electricity present in the zone's electricity grid, consisting of domestic generated electricity and electricity imported from other zones. Resulting from the assumption that all electrical power is perfectly mixed throughout the grid (Section 2.3.3), an equal AEF is assigned to consumption and export of electricity. Throughout this chapter, destination zone d will be considered to be the destination zone i.e., the zone for which the AEF is determined. A first definition of a time dependent AEF for destination zone d is given by Equation 3.1. Where H_t represents the total GHG emissions related to generation of electricity in

Variable	Unit	Symbol
Average emission factor	gCO_2eq/kWh	AEF
Generated electricity	MWh	G
Imported electricity	MWh	I
Fraction of power	%	F
GHG emission	$kgCO_2eq$	H
Electrical energy	MWh	E
Time	hour	t
Time window duration	hours	τ
Generation type	-	φ
Set of generation types	-	ϕ
Type specific life-cycle emission factor	gCO_2eq/kWh	ϵ
Destination zone	-	d
zone	-	z
Set of dynamic zones	-	Z
Set of static zones	-	S
Province	-	p
Included provinces	-	P
Global horizontal irradiation	W/m^2	γ
Energy conversion efficiency	%	η
Installed nominal capacity	MWp	C
Mechanical power	MW	MP
Air density	kg/m^3	ρ
Rotor area	m^2	A
Wind velocity	m/s	υ
Height	m	H
Helmann coefficient	-	α
Availability factor	%	AF
Threshold	-	T

Tab. 3.1.: Overview of the variables and related units and symbol used in Chapter 3

$kgCO_2eq$ at time t. $G_{d,t}$ is the domestic electricity generation (MWh) of zone d for time window t. $I_{d,t}$ is the electricity (MWh) imported to zone d during time window t.

$$AEF_{d,t} = \frac{H_t}{G_{d,t} + I_{d,t}} \tag{3.1}$$

In practice, it is not possible to measure the GHG emissions of the numerous power generators in (near) real-time. Furthermore, as discussed in Section 2.3.2, a significant part of the life cycle emissions related to the generation of electricity is indirect, sometimes emitted years before the power delivery and on the other side of the globe. Therefore, an indirect approach is necessary to determine the near real-time GHG emissions related to electricity use. The most suitable approach is the use of near real-time generation data in combination with generation type specific emission factors (EFs). Power generation is measured in real-time and European system operators are required to publish this data in near real-time, typically with a two hour delay [41]. This power generation data is categorised into generation types, which allows for the use of generation type specific emission factors. As elaborated in Section 2.3.2, the generation type specific life cycle EF describes the GHG emissions (gCO_2eq) that can be allocated to one kWh of electricity generated by a generation unit of a certain type. The AEF can be expressed as function of generation divided into types and their respective EFs, as shown in Equation 3.2, where $G_{\varphi,t}$ is the total electricity generation (domestic and import) in MWh by a specific generation type φ, e.g. coal fired power plants, for time window t. ϵ_φ is the life cycle emission factor in $gCO2_2eq/kWh$. These factors are listed in Table 3.3 in Section 3.7.

$$AEF_{d,t} = \sum_{\varphi \in \phi} \frac{G_{\varphi,t}}{G_{d,t} + I_{d,t}} \cdot \epsilon_\varphi \tag{3.2}$$

Before further depth is added to the method of determining the dynamic AEF, the basic definition of the AEF based on generation type EFs as given in 3.2, is used to analyse existing methods in reference. The following section summarises work related to this thesis and its respective methodologies. Besides methods from academic work, publicly available models are introduced and analysed.

3.2 Related Work

Research into dynamic grid emission factors has gained momentum over the last decade as a result of growing volatility of electricity mixes with increased penetration of intermittent RESs as well as the growing practice of carbon accounting. These two perspectives developed into three fields of research into dynamic grid emission factors can be distinguished. First, general research is aimed at developing a methodologies that determine the dynamic GHG emission intensity of an electricity grid. Second, as argued in Section 2.3.4, DSM is needed for the progression towards a decarbonised electricity supply. Therefore, emission factors are needed to provide insight that facilitates DSM. In this context, research is conducted to find the qualitative curve of GHG emission intensity. Third, most electricity use cases do not have a constant electrical power consumption, which results in a discrepancy between dynamic and static carbon accounting methods. For example, the dynamic scope 2 GHG emissions of an electric stove are different from those of a washing machine as a result of different times of consumption, while their annual consumption, and therefore their static scope 2 carbon footprint, might be equal. Therefore, dynamic emission factors are necessary to allow for dynamic scope 2 carbon accounting.

The main differences between DSM and carbon accounting in approaches for determining the dynamic GHG emission intensity of the grid are time windows and choice for AEF or Marginal Emission Factor (MEF). In (scope 2) carbon accounting, a GHG emission is allocated to historical consumption of electricity. Therefore, this approach requires insight in historical dynamic AEFs. DSM requires forecasted emission factors to adapt the timing of loads to future scenarios. For DSM, the AEF as well as the MEF can be used. The MEF describes the GHG emissions related to the change in demand. This is equal to the emission intensity of the marginal generator, i.e. the generator on the intersection of the demand and supply curve (Figure 2.4). The MEF is more complex to determine and validate than the AEF, as it involves modelling a hypothetical scenario parallel to the real scenario i.e. determining how much emissions are avoided by change consumption requires expressing two scenarios of which one can be realised [42]. An elaborate comparison is made by [43, 36]. In this thesis, only the AEF is expressed as basis for emission intensity calculation, as it is more precise, reliable and it realistically reflects the individual impact on the GHG emission reduction. The difference in intentions of DSM and carbon accounting emphasise the profile of the emission intensity and its quantity respectively.

A part of the research related to dynamic emission factors focuses on the creation dynamic GHG emission factors with the aim to facilitate carbon accounting. [44] investigates the geographical and temporal emission footprints and environmental pollution as result of inter-state electricity transmission in the United States. This data can be used for state-wide carbon accounting. A specific field of research looks into the impact of dynamic GHG intensities of the electricity grid on the environmental performance of buildings. [45] includes dynamic GHG emission intensities in evaluating the environmental performance of energy efficient buildings. [39] looks into the bias of static emission factors compared to dynamic emission factors in carbon accounting of residential, commercial, industrial and agricultural facilities which are also quantified by [46].

The large majority of studies that develop dynamic GHG emission factors aim to provide insight for DSM. A popular approach is using dynamic emission factors for the quantification of reduction potential and related costs of DSM [47, 17, 48, 49, 8, 50, 51]. Some studies model the dynamic emission intensity to investigate DSM potential of specific appliances such as heat pumps [25, 52]. Prediction of GHG emission intensities for DSM is developed by [53] and [54]. Some studies model the dynamic GHG intensity for insight in energy transition scenarios far into the future [55, 7, 56]. Fundamental studies that develop a method of determining the dynamic

GHG emission intensity without specific application. For example, studies that specifically look into the effect of cross border transmissions in modelling dynamic emission factors [24, 3, 57, 58]. Other research focuses on the emission reduction by RES implementation to the grid [59, 60, 61, 62].

As result of these studies and private research, multiple dynamic GHG intensity models have been developed for commercial or public use. Examples of implemented models that commercially or publicly aim to provide GHG intensity data are Electricity Maps [63], CO2 Monitor [64], Elmada [8], WattTime [65], Carbonara [66], CarbonIntensity [67], Nowtricity [68] and Eco2mix [69]. The models that include the Netherlands in their reported data are Electricity Maps, WattTime, Elmada, Nowtricity and CO2 Monitor. WattTime and Nowtricity provide limited insights in their methodology. Furthermore, WattTime expresses the GHG emission intensity in a relative percentage of 'cleanness' compared to other electricity grids. Therefore, these models are not included in further comparison.

All of the models that focus on European zones make use of ENTSO-E Transparency Platform data to model the dynamic GHG emission intensity. This data is considered to be accurate, as it is provided by TSOs in accordance with EU law [41]. However, TenneT, the Dutch TSO, notes the following: "The publication represents the generation identifiable per fuel type, if not identifiable the data is published as "others" or not published. Data on Solar is mostly not available". This note is crucial in the development of an accurate model that determines the GHG emission intensity of the Dutch electricity mix based on data from the Transparency Platform. Using this data exclusively to determine the GHG intensity of the Dutch electricity grid therefore provides a inaccurate image of reality.

This missing data is handled in various ways by the existing studies and models that cover the Netherlands. The academic studies that calculate the dynamic GHG emission intensity for the Netherlands show no method of filling the gap of missing PV and onshore wind data [24, 50, 8]. The models shows a similar incompleteness: Elmada regards the ENTSO-E data as complete. This results in a model that disregards the significant installed capacity of most Dutch onshore wind turbines and all non-utility PV installations. Electricity Maps uses multiple sources to model the generation per type in the Netherlands, but fails to include weather data for the PV installations. This results in a standardised sinusoidal electricity generation by PV panels, regardless of the daily weather conditions, which is elaborated in Section 4.2.3. CO2 Monitor developed a model that determines the dynamic generation of PV and onshore wind turbines in the Netherlands. However, unlike the Elmada and Electricity Maps, CO2 Monitor only includes domestic production, disregarding the import of electricity.

Therefore, no open methodology or model exists for determining the dynamic GHG emission intensity of the Dutch electricity mix including all generation installations, weather data and imported power. In conclusion, the three open models covering the Netherlands have a specific focus, but all lack a key characteristic of determining the dynamic GHG intensity of the Dutch electricity mix. In the following sections, a methodology for determining the GHG emission intensity covering all key aspects of the electricity mix and a related model is presented.

3.3 Method requirements

As stated in the previous section, this thesis presents a new methodology and derived model for calculation of the GHG emission intensity of the Dutch electricity mix. In order to satisfy the research goal of creating a valid model, the method has to fulfil certain requirements. The need for a public method is emphasised in the introduction. Therefore, the methodology needs to be completely based on public data and the methodology as well as the model must be published to allow for open discussion and improvement.

The dynamic aspect of the method is the main driver for this work, and should be precise enough to capture diurnal profiles. A time interval τ of one hour was chosen to reflect the dynamic intraday aspects of the AEF in line with the highest time granularity provided on the Transparency Platform for all relevant datasets. Note that as result of this choice generated power (MW) and generated electrical energy (MWh) are equal in value. Throughout this chapter, electricity generation is expressed in MWh.

Decentral electricity sources like PV panels and onshore wind turbines form a growing share of the electricity mix. Collecting real-time generation data from decentralised sources is complex as real-time generation of these sources is not centrally registered. As previously mentioned (Section 3.2), the official generation data for the Netherlands provided by the ENTSO-E is missing decentralised electricity generation, specifically onshore wind turbines and non-utility PV installations. Because there is no (near) real-time generation data available in the Netherlands, the generated power of these sources have to be estimated. The method of estimation needs to provide insight in the actual electricity mix including all domestic generation types. Therefore, non-ENTSO-E data sources have to be incorporated to determine the GHG intensity of the grid.

The Dutch electricity mix consists of more than the domestic generation of electricity. The European electricity grid is integrated and electrical power is traded on an international level. Different countries make use of various generation types (Section 2.2.1). Therefore, the method needs to determine the quantity as well as the composition of imported electricity from other zones. Furthermore, a clear approach is needed for the selection of included zones.

Finally, the model should provide near real-time as well as historical data. Near real-time data publishing is the first step towards a prediction functionality which will allow for load planning and DSM. Currently, the ENTSO-E Transparency platform publishes data related to electricity generation and transmission with a 2 hour delay. Historical data can be used to improve carbon accounting by incorporating dynamic aspects. The data can be used to calculate carbon footprints related to historical electricity consumption.

Some possible requirements are not incorporated into the presented work, but could be part of future versions. These include, but are not limited to: prediction functions, smaller time granularity (e.g. 15 min interval), functions for footprint or load-shift impact calculation, marginal intensity factors or a public online information dashboard. This is elaborated in Section 6.

3.4 Methodology overview

Equation 3.3 shows the general equation for determining the time dependent AEF for destination zone d as introduced in Section 3.1. $G_{\varphi,t}$ is the total electricity generation (domestic and import) by generation type φ. This is described in Equation 3.4 as the product of $G_{\varphi,z,t}$, the domestic electricity generation by type φ in zone z and $F_{z,t}$, the fraction of domestic electricity from zone z in the mix of destination zone d, summed over all included zones. The total domestic generation of destination zone d and its total imported electricity are defined in Equation 3.5.

$$AEF_{d,t} = \sum_{\varphi \in \phi} \frac{G_{\varphi,t}}{G_{d,t} + I_{d,t}} \cdot \epsilon_{\varphi} \tag{3.3}$$

$$\text{with} \qquad G_{\varphi,t} = \sum_{z \in Z} G_{\varphi,z,t} \cdot F_{z,t} \tag{3.4}$$

$$\text{and} \qquad G_{d,t} = \sum_{\varphi \in \phi} G_{\varphi,d,t} \qquad \text{and} \qquad I_{d,t} = \sum_{z \in Z} I_{z \to d,t} \tag{3.5}$$

Z is a set of all included dynamic zones, elaborated in Section 3.6. Φ is a set of the included types of generation, shown in Table 3.3 in Section 3.7, are based on the production types reported on the ENTSO-E Transparency Platform [15].

The variables that need to be determined in order to calculate the AEF are the zone specific generation mixes $G_{\varphi,z,t}$, the cross border electricity transmissions to the destination zone $I_{z\rightarrow d,t}$, fractions of generation mixes from different zones in the electricity mix of the destination zone $F_{z,t}$, and the generation type specific life cycle emission factors ϵ_{φ}.

$G_{\varphi,z,t}$ and $I_{z\rightarrow d,t}$ are available in near real-time on the ENTSO-E Transparency platform [15]. As discussed in Section 3.2 the electricity generated by PV installations, $G_{pv,NL,t}$, and onshore wind turbines, $G_{on.wind,NL,t}$ in the Netherlands is not published. A method to estimate the electricity generation of these sources $G_{pv,NL,t}$ and $G_{on.wind,NL,t}$ based on installed capacities and weather data is presented in Section 3.5. The fractions of generation imported from other zones to the destination zone, $F_{z,t}$, can be derived from the cross border electricity transmissions between all of the included zones, $I_{z1\rightarrow z2,t}$ (electricity transmission from zone $z1$ to $z2$), which is elaborated in Section 3.6.

3.5 Methodology decentralised generation

In the Netherlands, there is no official near real-time data source for decentralised electricity production. To fill this data gap in order to provide a complete overview of the Dutch electricity mix, this generation has to be estimated. This section presents a method of estimating the near real-time generation of PV installations and onshore wind turbines in the Netherlands based on nominal capacities and weather data.

3.5.1 PV

The electricity generation of PV panels is linearly dependent on the Global Horizontal Irradiation (GHI), which is the irradiation power that a horizontal surface on Earth receives from the sun in W/m^2 [70]. This means that the power output of a PV system can be expressed as function of the global irradiation. All PV panels and PV installations are given a rated power in kilowatt peak (kWp) to quantify their nominal capacity. This rated power determined under standard test conditions. The rated power is the power generated at a GHI of 1000 W/m^2 according to the IEC 61538 standard test conditions. The percentage of the rated power that a PV panel delivers is thus equal to the current GHI (γ_t) divided by 1000 (γ_{stc}). Therefore, the time dependent PV generation (MWh) for zone z, $G_{pv,z,t}$, is given by Equation 3.6. Where the constant γ_{stc} is the GHI of 1000 W/m^2 used as standard test condition.

$$G_{pv,z,t} = \frac{\gamma_{z,t}}{\gamma_{stc}} \cdot C_{pv,z,t} \cdot \eta \cdot \tau \tag{3.6}$$

Where τ is the time window in hours. η is the system efficiency, accounting for losses of the PV installation between the panel output and the grid connection, such as losses from sub optimal PV tilt angles, degradation and power conversion. These losses are different for every individual PV system, but an estimation of 16.4% is made in calibration with the annual Dutch PV generation as published by the CBS. $\gamma_{z,t}$ is the GHI in W/m^2 at time t. The Royal Dutch Meteorological Institute (*Koninklijk Nederlands Meteorologisch Instituut*, KNMI) publishes the GHI every 10 minutes for 34 weather stations in the Netherlands [71].

The installed nominal capacity (rated power), C_{pv} in MW, is based on data published by the CBS. The CBS collects data from Energy Data Services Netherlands (EDSN) where all PV installation owners are required to register their installation and additional data from the tax authorities where owners of PV installations file their installations for subsidies [72]. The CBS publishes the capacities of PV installations per region and type [73](new)[74](old). The data distinguishes three types: small installations with a nominal capacity up to 15 kWp, large (>15 kWp) roof mounted installations and large (>15 kWp) field installations. From this point forward, roof and field mounted PV installations are modelled separately due to the difference in their respective life cycle emission factors. It is assumed that the small installations are all roof-mounted. The installed nominal capacity is time dependent, as more PV panels are being installed over the years. In order to reflect this time dependent increase of installed nominal capacity, the installed capacity over time is estimated using a linear interpolation of the annual data that is published by the CBS. This linear interpolation implies the assumption that capacity is added evenly over time between the annual data points. The last available data-point published by the CBS is used as static capacity. This means that currently, no estimation is made for the increase in installed nominal capacity since the latest data point provided by the CBS.

Both the weather data and the nominal capacity data are published regionally, this allows for the estimation of regional generation instead of national generation. This increases the accuracy of the estimation as the generation data will account for regional weather effects e.g. clouds in the south of the country. The twelve provinces of the Netherlands were chosen as regions of calculation. The installed nominal PV capacity $C_{pv,t}$, is published per province. The weather data is published per weather

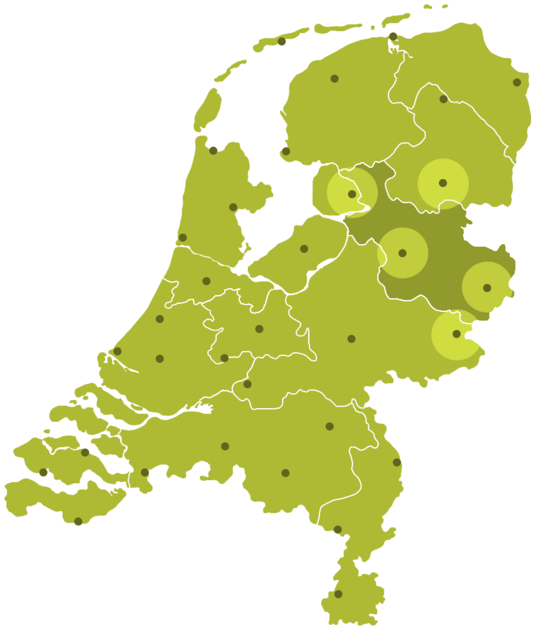

Fig. 3.1.: Overview of 33 automatic weather stations in the Netherlands. The province of Overijssel and the weather stations of which data is averaged for Overijssel are highlighted.

station and has to be converted to reflect the province average weather. This is determined by taking average data of the weather stations which locations reflect the shape of the province sufficiently, as shown in Figure 3.1. The calculation of PV generation on province level is shown in Equation 3.7. The power generation by field and roof installations are calculated separately indicated by $pvfi$ (shown in Equation 3.7) and $pvro$ respectively.

$$G_{pvfi,NL,t} = \sum_{p \in P} \frac{\gamma_{p,t}}{\gamma_{stc}} \cdot C_{pvfi,p,t} \cdot \eta \cdot \tau \tag{3.7}$$

γ_{stc} and $\gamma_{p,t}$ are the GHI under standard test conditions (1000) and the average GHI of the province-specific set of weather stations respectively. $C_{pvfi,p,t}$ is the aggregated nominal capacity of field installations in province p at time t.

3.5.2 Wind

Similar to the estimation of PV generation, the electricity generation of wind turbines can be determined by weather data and the installed nominal capacity. The same dataset that provides the GHI, also provides the wind velocity that is measured by the KNMI at the same stations.

To determine the generation of electricity from the wind velocity, a few intermediate steps are necessary. First the mechanical power of the wind is determined. This is the power that the turbine will convert into electrical power. The mechanical power, MP_{wind} (in MW), harnessed in the wind is given by Equation 3.8 [75].

$$MP_{wind} = \frac{1}{2}\rho A \upsilon^3 \cdot \frac{1}{1000000} \tag{3.8}$$

Where ρ is the density of air in kg/m^3. A is the rotor area perpendicular to the wind in m^2 and υ is the wind velocity in m/s. The fraction $\frac{1}{1000000}$ is added to the convert Watts to MW.

Equation 3.8 determines the power that a wind turbine converts into electricity based on the wind velocity. However, it should be noted that the velocity should be taken at the hub height of the wind turbine. The wind velocities are measured by the KNMI at a height of 10m above the surface [76]. Wind speeds vary for different heights, therefore the measured value has to be corrected for height. The wind profile power low, or wind gradient law, given in Equation 3.9 gives the conversion for wind speeds at different heights [75].

$$\upsilon = \upsilon_0 \left(\frac{H}{H_0}\right)^{\alpha} \tag{3.9}$$

Where υ is the velocity of the wind at height H (m) in m/s. υ_0 is the velocity of the wind at height H_0 (m) in m/s. α is the Helmann coefficient which describes geographical factors such as the location, terrain characteristics and atmospheric properties. In short, wind velocity is height dependent and the presence of obstacles on land, e.g. buildings and trees, determine the rate at which the wind velocity increases per meter height. The Helmann coefficient, α, also referred to as the surface roughness coefficient, is location specific. Combining Equation 3.8 and 3.9 gives Equation 3.10.

$$MP_{turbine,t} = \frac{1}{2}\rho A_{turbine} \left(\upsilon_{0,t} \left(\frac{H_{hub}}{H_0}\right)^{\alpha}\right)^3 \cdot \frac{1}{1000000} \tag{3.10}$$

Equation 3.10 gives the mechanical power harnessed in the wind of a specific area. This mechanical power is converted into electricity by a wind turbine. According to Betz' law, published by Albert Betz in 1919, the power that can be extracted by an ideal wind turbine is limited to $\frac{16}{27}$ or 59.3% (Betz' limit) of the mechanical power of the wind [77]. This law is a result of the conservation of flow and mass. If all the power of the wind is converted and the wind speed would be zero behind the rotor, incoming wind cannot continue to flow through the rotor. Modern wind turbines are able to operate around 80% of the Betz' limit converting 47% of the wind power into mechanical power on the generator axis.

The conversion of wind power into electrical power is subject to losses such as wake effects, electrical efficiencies, curtailment, Balance of Plant (BoP) power consumption and turbine availability [78]. The turbine availability expressed as availability factor, AF, describing what percentage of time the wind turbine is available for power production, and when the system is down e.g. due to maintenance or repairs [78]. Similar to PV panels, wind turbines have a specified nominal capacity. This is the electrical power that the turbine is able to generate in abundant wind power conditions. The minimal wind speed at which the nominal power generation is reached is called the rated velocity, shown in Figure 3.2. During windstill times, the turbines are not able to generate any power. The minimal wind speed at which the turbine is able to generate electrical power is called the cut-in velocity. During storms or extreme gusts of wind, the turbine is shut down to prevent damages by continued operation. The wind speed at this turbine limit is called the cut-out velocity. The CBS publishes data collected from TSOs and DSOs regarding installed onshore wind turbine capacities, total rotor area and annual power production. This data is available per province with an annual time interval.

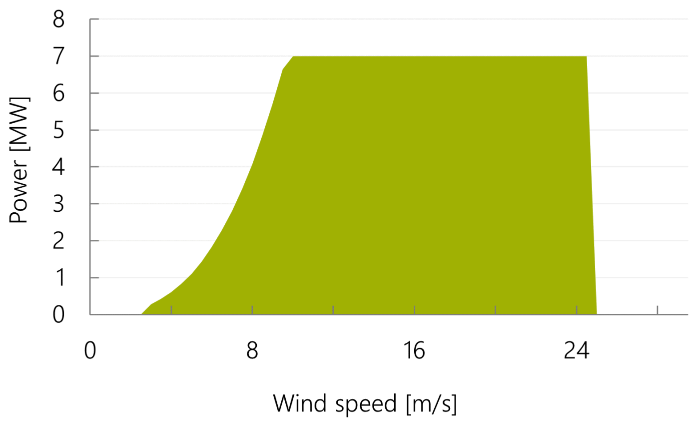

Fig. 3.2.: Power generation of a 7MW wind turbine with a rotor diameter of 170m at varying wind speeds (hub height). Cut-in velocity is 3.5 m/s, rated velocity is 10 m/s, cut-out velocity is 25 m/s, air density is 1.25 kg/m^3. Adapted from [79].

The electricity generation of a wind turbine $G_{wind,t}$ (MWh) is given in Equation 3.11. AF is the availability factor. η is the efficiency of conversion from wind power to electrical power, including all named losses. An efficiency of 28% was found in calibration with annual generation data by the CBS, comparable to 30% found in literature [80]. τ is the time window length in hours. $C_{wind,p,t}$ is the nominal capacity of onshore wind turbines in province p at time t. Similar to the installed PV capacity, both the installed onshore wind capacity and the rotor diameter are modelled by linearly interpolating the annual data points from the CBS. This is done to incorporate addition of new turbines, assumed to be added evenly throughout the year. Similar to the modelling of PV generation, the latest annual data point is used as current value. This means, again, that currently no estimation is made for the increase in installed nominal capacity since the latest data point provided by the CBS. $v_{p,t}$, v_{cut-in}, v_{rated} and $v_{cut-out}$ are the provincial wind velocity at time t, the cut-in velocity, the rated velocity and the cut-out velocity respectively, all in m/s at hub height.

$$G_{wind,p,t} = \begin{cases} 0 & \text{for } v_{p,t} < v_{cut-in} \\ AF * \eta \cdot MP_{wind,p,t} \cdot \tau & \text{for } v_{cut-in} \leq v_{p,t} < v_{rated} \\ C_{wind,p,t} & \text{for } v_{rated} \leq v_{p,t} < v_{cut-out} \\ 0 & \text{for } v_{p,t} \geq v_{cut-out} \end{cases} \tag{3.11}$$

The domestic electricity generation by onshore wind turbine is given by the sum of provincial generation, as shown in Equation 3.12. Where d is the destination zone and P is the set of all provinces.

$$G_{wind,d,t} = \sum_{p \in P} G_{wind,p,t} \tag{3.12}$$

Table 3.2 gives an overview of the default parameters used in the estimation of hourly generation by onshore wind turbines in the Netherlands.

parameter	value	source
average hub height	119 m	[81]
surface roughness coefficient	0.2	[82, 83]
average air density at hub height	1.246 kg/m^3	[84]
overall turbine efficiency	0.30	CBS calibrated
availability factor	0.97	[85]

Tab. 3.2.: Wind model parameters, input values and sources

3.5.3 Energy storage

Energy Storage Systems (ESSs) of different types, e.g. lithium ion batteries and hydrogen, will be increasingly added to the grid to help match generation of electrical power with its demand. Charging an ESS, like consumption of electrical power, does not affect the AEF (Section 3.1). However, discharging the ESS delivers power to the grid which should be taken into account when determining the dynamic

GHG emission intensity. Limited by data availability (ENTSO-E does not publish near real-time data on ESSs), ESSs can not be taken into account in current AEF calculations. Nonetheless, the following section presents a method of incorporating ESSs in future calculations.

Like generating installation, the ESS has to be produced, installed, maintained and eventually disassembled, processes that entail indirect emissions. When charging, the dynamic AEF changes, creating a unique electricity mix for the electricity stored in the ESS. This means that a discharging ESS has its own emission factor that has to be included in the modelling. Different types of ESSs have varying conversion efficiencies (also called round-trip efficiencies), meaning that energy is 'consumed' in the process of storing. If the purpose of an ESS is to shift the delivery of power over time, the GHG emission factors related to this consumption can be regarded as direct emissions from operation. Therefore, these direct emissions should be included in the calculation of the emission factor of stored electricity. The ESS life cycle emission factors, dynamic AEF during charging, round trip efficiency and emission intensity of initial charge lead to the formula for ESS emission factor given in Equation 3.13.

$$\epsilon_{ess,t'} = \frac{E^0 \cdot \epsilon^0_{ess}}{E^0 + \sum_{t=1}^{t'} E_t} + \frac{\sum_{t=1}^{t'} E_t \cdot (AEF_{d,t} + \epsilon_\varphi)}{\left(E^0 + \sum_{t=1}^{t'} E_t\right) \cdot \eta_\varphi} \tag{3.13}$$

Where ϵ_{ess} is the emission factor of the electricity fed to the grid by an ESS in gCO_2eq/kWh. $t = 1$ until t' represents the charging period. E^0 and ϵ^0 are the initial charge (MWh) and related emission intensity (gCO_2eq/kWh) at the beginning of the charge period. E_t is the charged energy at time window t in MWh. $AEF_{d,t}$ is the GHG emission intensity of the grid in zone d at time window t in gCO_2eq/kWh. ϵ_φ and η_φ are the life cycle emission intensity and round trip efficiency of the ESS of technology type φ in gCO_2eq/kWh and % respectively.

3.6 Interconnection

Power is transmitted to an electricity grid by domestic generators and imported via interconnections. In order to determine the composition of power in an electricity mix, the composition of both domestic generation and imported power must be known. The data of the Transparency Platform completed with additional data for PV and onshore wind (Section (3.5) provide a complete composition of domestic generation. This section details the methodology for determining the generation type composition of the electrical power in destination zone d, including both domestic generation and imported power.

The generation type composition of imported power can be determined by taking into account the electricity mixes of all included zones. Unlike the domestic generation, the generation types of the imported power fractions is initially not known. The initial import mixes, as obtained from the Transparency Platform, consist of a part domestic generation, $F_{z,dom}$, and various fractions of imported power, $F_{z1 \rightarrow z2}$ (power transmission from zone $z1$ to $z2$). The generation type composition of imported power can be derived from the electricity mixes of zones from which power is imported. This derivation, elaborated throughout this section, consists of two aspects: (1) selection of dynamically included zones and (2) repetitive replacement of import fractions by the respective electricity mixes. These aspects are elaborated in Section 3.6.1 and 3.6.2 respectively.

3.6.1 Zone selection

The quantity and composition of cross-border transmissions are dynamic of nature. Electricity can be transmitted to zones, but also through zones. For example, if the Belgian electricity mix consists for 10% of power imported from France and the Dutch electricity mix consists for 15% of power imported from Belgium, the Dutch electricity mix consists for $10\% \cdot 15\% = 1.5\%$ of imported power from France. This power flows through Belgium, but ends up in the Dutch electricity mix. In this scenario, the composition of French power should therefore be known when determining the composition of the Dutch electricity mix. Calculating the electricity mix of destination zone d thus requires information about all zones connected (through cross-border transmission) directly or indirectly to destination zone d.

The number of included zones has to be limited because of two reasons. Because reliable data is only publicly available for a selection of zones and to limit complexity of interaction cycles. In order to limit the amount of zones included in the calculation, a static ring of zones is introduced. The static ring of zones is a selection of zones for which a static composition of generation types is assumed. A static emission factor is assigned to the zones within the static ring e.g. 79 gCO_2eq/kWh for French electricity in 2020 [86]. In this assumption, the imported power from a static zones can be included as domestic production with a fixed emission factor. An illustrative example of a static ring of zones is shown in Figure 3.3 where a static GHG emission factor is assigned to the French power delivered to the Belgium grid. Therefore, the French power imported to Belgium is modelled as part of the domestic generation of Belgium.

The assumption of a static ring of zones, provides a simplified view of reality. Therefore, a conscious decision should be made where the dynamic inclusion of zones is capped with the static ring of zones. The static zones are preferably

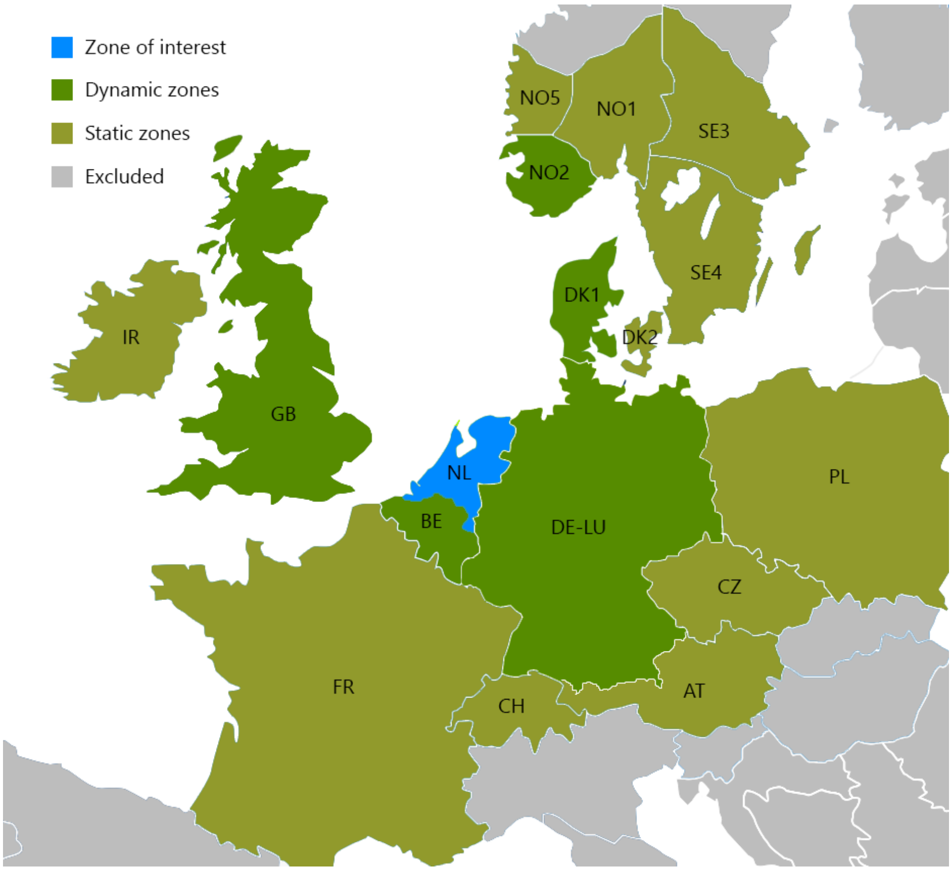

Fig. 3.3.: Illustrative example of the selection of included dynamic zones with regard to a zone of interest for which the AEF is calculated. The dynamic region is surrounded by a static ring of zones. Bidding zone map adapted from [87].

characterised by a low cross-border capacity on the border with the dynamically included zones. This would limit the quantitative discrepancy between the assumed static and real dynamic scenario. Logically, inclusion of many zones will lead to a more realistic emission factor compared to the inclusion of a small number of zones. The discrepancy is limited, as most electricity in the mix is generated domestically. In 2017, 98.4% of the consumed electricity in the Netherlands was domestically generated [88]. Although the import fractions become larger due to increasing interconnection capacities, the share of secondary imports in the electricity remains small. In the supplementary materials, an overview matrix is given of all physical cross-border connections of all bidding zones in Europe. This matrix can be used to automatically select a static ring of zones based on a selection of dynamic zones.

3.6.2 Import iteration

The composition of imported power can be determined by replacing imported fractions by their respective electricity mixes. To illustrate this, consider an example where the Dutch electricity mix consists of 85% offshore wind and 15% imported power from Belgium, and the Belgian mix consists of 50% PV and 50% offshore wind. In this case, the Belgian import fraction in the Dutch electricity mix can be replaced by its elements, resulting in a Dutch electricity mix of 92.5% offshore wind and 7.5% PV. Only when the electricity mix of destination zone d is composed completely of known generation types, the AEF can be determined.

Interconnection loops can arise when exported power is fed back to the same exporting zone. These loops can be formed directly over multiple connections across the same border, or through a route over many zones. These interconnection loops increase the complexity of replacing the imported fractions with their respective electricity mixes. The next section presents a methodology for this replacement.

When replacing the fraction imported power from zone z in electricity mix d, the domestic generation as well as the import fractions of zone z are added to the electricity mix of zone d. In this way, direct import as well as indirect power flows, i.e. those that flow through a third country, are attributed to the electricity mix of destination zone d. The repetition of this replacement is shown in Algorithm 1. Through this addition, the known generation type composition of the electricity mix of destination zone d increases by every replacement, while unknown generation type composition of import fractions decreases. The sum of domestic generation fractions with known generation type composition will approach 100%.

Algorithm 1 Import iteration algorithm for replacing the import fractions $F_{z1 \rightarrow z2}$ with domestic generation fractions F_z in the electricity mix of destination zone d.

function FRACTION ITERATION(T, Z, d, F)
    {Initialisation}
    for $z \in Z$ **do**
        $F_z^{(0)} \leftarrow 0$
    end for
    $n \leftarrow 1$
    {Iterative process}
    while $\sum_{z \in Z} F_z < T$ **do**
        for $z \in Z$ **do**
            $F_z^{(n)} = F_z^{(n-1)} + F_{z \rightarrow d}^{(n-1)} \cdot F_{z,dom}$
            for $k \in Z \setminus \{z\}$ **do**
                $F_{k \rightarrow d}^{(n)} = F_{k \rightarrow d}^{(n-1)} + F_{z \rightarrow d}^{(n-1)} \cdot F_{k \rightarrow z}^{(0)}$
            end for
            $F_{z \rightarrow d}^{(n)} = 0$
        end for
        $n \leftarrow n + 1$
    end while
end function

Input variables for the function are threshold T, selection of dynamic zones Z, destination zone d and F, a matrix containing the initial electricity mixes of all included dynamic zones. $F_{z \to d}$ is the fraction of the electricity mix of zone d that is imported from zone z. F_z is the fraction domestic generation of zone z in the electricity mix of zone d. For example, when the Dutch electricity mix is determined, F_{BE} is the fraction of the Dutch electricity mix that is domestically generated in Belgium. As the electricity mix of destination zone d initially consists of domestic production in zone d and import fractions, all F_z values are initialised as zero. $F_{z,dom}$ is the fraction of the electricity mix of zone z that is domestically generated in zone z. A criteria of convergence, threshold T, is introduced to assume this fraction of known generation type composition to be 1 when this fraction exceeds the threshold e.g. $T = 0.9999$. When the criteria of convergence is reached, the remaining import fractions making up $(1 - T)$ part of the electricity mix of destination zone d, can be assumed to be negligible. This assumption results in an electricity mix for destination zone d expressed as domestic generation fractions. The generation type composition of these domestic fractions is known, therefore, the generation type composition of the total electricity mix is known. This electricity mix is used as input for the general AEF Equation (3.3).

In conclusion, due the interconnected nature of the European electricity grid, it is important to consider the quantities and compositions of imported power when calculating the GHG emission intensity. A conscious selection of zones must be made to incorporate realistic cross-border transmission effects while limiting the scope of calculation. The import fractions contained in the electricity mix can be iteratively converted into domestic generation fractions with known compositions.

3.7 ODECT

Using the methodological approach introduced in the previous sections, the Open Dynamic Electricity Composition Tracker (ODECT) is developed. With ODECT, the GHG emission intensity of the Dutch electricity mix is calculated as well as the related power generation and emissions mixes. An overview of ODECT is shown in Figure 3.4. From five data sources, the hourly average emission factor is determined for a given period. The results are be analysed in Chapter 4.

The data used by ODECT consists exclusively of public sources. The foundation of the data input is the ENTSO-E Transparency Platform. On this platform, European TSOs publish their measured capacities on an hourly or quarter-hourly basis. Main inputs for ODECT are the 'Actual Generation per Production Type' and 'Cross-Border Physical Flows' datasets. Data is collected via requests to the Transparency Platform restful API. Current Great Britain's generation data is not available on the Transparency Platform due to Brexit. Therefore, this data is gathered from the data website of National Grid ESO, the TSO of Great Britain. Furthermore, as mentioned earlier in this chapter, the ENTSO-E datasets regarding actual generation presented on the Transparency Platform are incomplete for at least onshore wind and PV in the Netherlands. In order to fill these gaps in the data, these sources are modelled separately according to the methods presented in Section 3.5 based on weather data from the KNMI collected via the KNMI Developer Portal API and capacity data gathered from CBS.

In order to determine the AEF, ODECT uses generation type specific emission factors. Differentiating the generation types into more specific categories increases the accuracy of the model but also increases the required data. For example, the emission factors for the category 'coal fired power plants' contains less specific information than those for the category 'Polish pulverised coal fired power plants built in 1950-1960'. In the process of choosing a differntiation level, the completeness, reliability and availability of data for all categories is essential. This consideration led to the categories and emission factors shown in Table 3.3 for which reliable and complete data is available in near real-time.

Generation types for which emission factors are not covered by renowned institutes are waste and both "other renewable" and "other non-renewable". The emissions related to incineration of municipal solid waste is extremely dependent on the composition of waste and therefore complex to estimate [89]. Because of the similar processes and the increasing trend of recycling waste materials, the emission factor of biomass is assigned to energy from waste (230 gCO_2eq/kWh). To the category "other non-renewable", the weighted average of the Dutch non-renewable electricity sources (76% gas, 23% coal and 2% oils) is assigned [90]. Similarly, the weighted average of Dutch renewable sources (46% wind, 29% PV, 25% biomass) is assigned to the category "other renewable" [90].

ODECT, represented schematically in Figure 3.4, calculated the dynamic GHG intensity of the Dutch electricity grid from the presented data sources and data flows. The green databases represent online information sources from which data is extracted automatically (green arrows) or has been extracted and incorporated manually (blue arrow). The user specifies a time window in the main script. The data requests containing the time frame given by the user are represented as orange arrows. The light green boxes represent the model components. The blue databases represent locally stored data intended to minimise run-time of the model. When the script is executed, the time window request is send to the first "internal" level of the model, which checks if the local database contains generation data within the requested time window. This prevents the model from requesting data from APIs at every execution, a time-consuming step. If the data is not available locally, the request is forwarded to the next layer of the model: three parser scripts. Each script is made to

Generation type	Emission factor	Source
φ	ϵ_{type}	-
-	gCO_2/kWh	-
Biomass	230	[5]
Lignite	1137	[91]
Coal gas	838	[23]
Natural Gas	490	[5]
Coal	820	[5]
Oil	840	[23]
Shale	758	[23]
Peat	1100	[92]
Geothermal	38	[5]
Hydro power	24	[5]
Marine	17	[5]
Nuclear	12	[5]
Solar roof	41	[5]
Solar field	48	[5]
Waste	230	eq. to biomass
Wind offshore	12	[5]
Wind onshore	11	[5]
Other non-renewable	571	w.avg. fos. types
Other renewable	76	w.avg. ren. types

Tab. 3.3.: Generation type specific life cycle emission factors.

collect data from a specific API and process the collected data into a usable format. The formatted data is fed back to the Function script which calculates the emissions and emission intensities for the hours within the user prompted time window. Subsequently, the local databases are updated to limit the time consumption when running the model repeatedly for (parts of) the same time window.

M stands for electricity mix consisting of a list of generation types and generated electricity (MWh) for a specific time window. I is the electricity import from a specific country to the Dutch grid in MWh. V and IRR are the province specific wind velocity and solar irradiation in m/s and W/m^2 respectively. CAP is the province specific nominal (or peak) capacities in MW for onshore wind and PV. ROT is the province specific rotor area of onshore wind turbines in m^2. GEN is a list of generated electricity of specific types in MWh. EM is a list of emissions of specific types and in mtCO_2eq. AEF is the main output of the model, the average emission factor, describing the GHG emission intensity of the Dutch electricity mix in gCO_2eq/kWh.

The complete calculation without locally stored data takes approximately 32 seconds per requested day consisting of 24 hourly GHG emission intensity calculations. In comparison, calculating the same day with generation data from the local database takes around 10% of this time averaging 3.2 seconds. The complete code of the model, which is developed in the Python programming language, as well as its

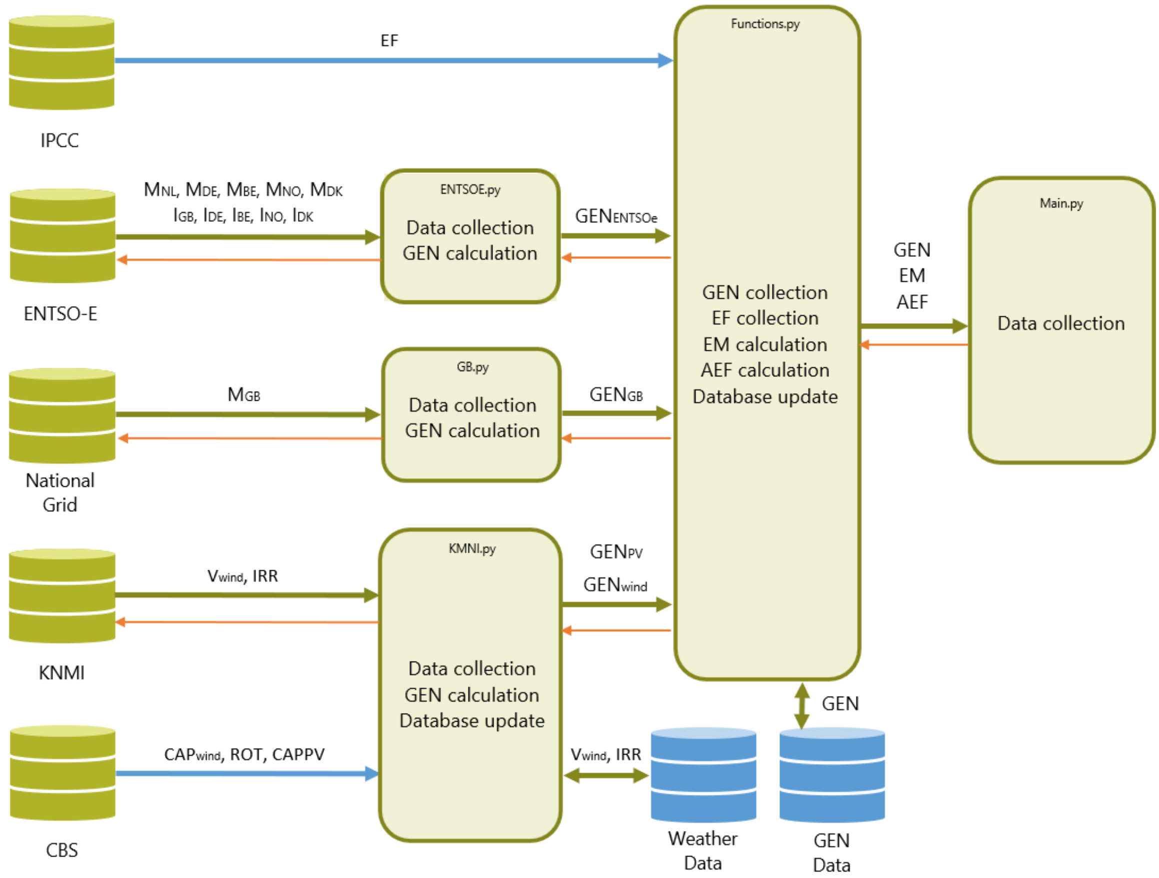

Fig. 3.4.: Schematic overview of dynamic AEF calculation model ODECT.

results (1-1-2016 until 1-4-2023) are publicly available as part of the supplementary materials [93].

The data sources combined in ODECT provide a complete view of the quantity and composition of power in the Dutch electricity mix, with the exception of indirect import. The scope and resources of this thesis did not allow incorporation of all methodological aspects of import iteration and ESSs into the current version of ODECT. Import iteration (Section 3.6) was simplified. Only the direct power imports from neighbouring zones BE, DE-LU, DK1, NO2 and GB are included. Furthermore, due to lack of public data, the effects of energy storage in ESS are not included.

Results

4

4.1 Overview

The ODECT model accumulated and processed data for the period 1-1-2016 until 1-4-2023. Figure 4.1 presents the hourly GHG emission intensity generated by ODECT. Two characteristics of the AEF signal stand out. First, the GHG intensity of the electricity in the Dutch grid declines over the assessed period. This is a direct effect of the increasing installed capacity of renewable energy sources such as wind and PV and phasing out of the most GHG emission intensive generation types. The second notable characteristic of the AEF signal is the increasing volatility over time. The period of early 2016 until the first quarter of 2019 present a time of relatively low volatility with values staying roughly within the range of 400 to 600 gCO_2eq/kWh. From 2019 on, the AEF has become more volatile as result of higher share of electricity supply with intermittent character.

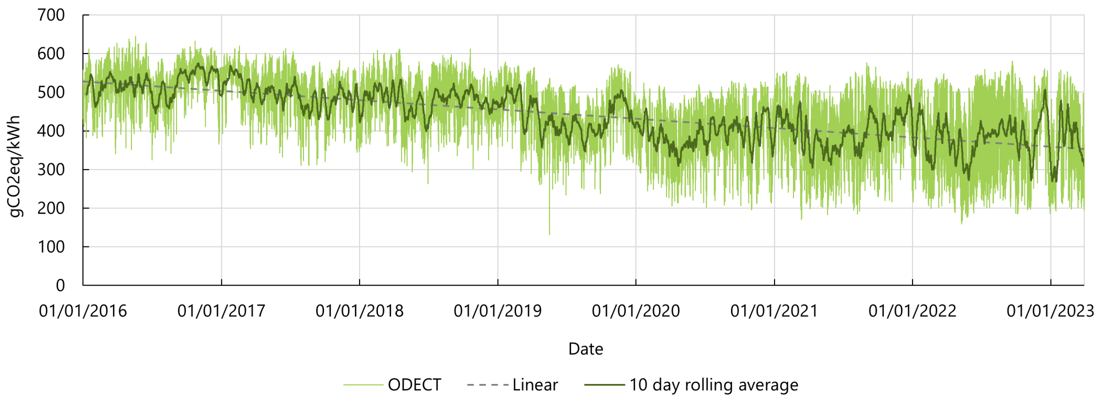

Fig. 4.1.: ODECT AEF over the period of 1-1-2016 until 1-4-2023 in light green. For quick analysis, a 10 day rolling average (dark green) and linear trendline (grey) are shown.

These two effects are also visible in Figure 4.2, where the AEF is displayed per hour of day for the years 2016 until 2022. In 2016, the average daily profile ranges from 497 gCO_2eq/kWh at noon to 539 gCO_2eq/kWh in the evening, a range of 42 gCO_2eq/kWh. In 2022, the average daily profile ranges from 302 gCO_2eq/kWh at noon to 437 gCO_2eq/kWh in the evening, a range of 135 gCO_2eq/kWh, 321% of the range in 2016. These values are representative of the change in the electricity system, and clearly reflect the trends of GHG intensity decline and growing volatility.

Interesting to note is the resemblance of the "duck curve" by the daily GHG intensity curve as result of increasing PV capacity.

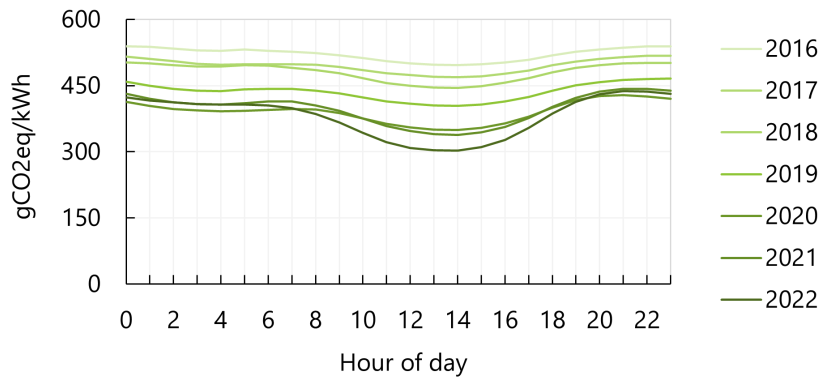

Fig. 4.2.: ODECT average daily intensity profiles for the years 2016 until 2022.

The AEF is directly dependent on the electricity mix i.e., the composition of generation types. Figure 4.3 shows the shares of annual power generation by generation type. This includes domestic as well as imported power. Natural gas is the predominant source of power for the Netherlands followed by coal, onshore wind and roof mounted PV. The unaccounted other non-renewable category also provides a significant share of the annual power generation. The share of power provided by coal and natural gas decreased from 58.4% in 2016 to 43.6% in 2022. From 2016, the initial phase out of coal can be clearly seen up until a turning point in 2020 where the gas prices started to rise, re-incentivising power from coal [94]. Where the share of power generated by lignite shows a gradual decline, power from waste increases. Furthermore, the total share of power generated by RESs grows, but the share of hydropower decreases. The share of nuclear power is relatively stable over the analysed period.

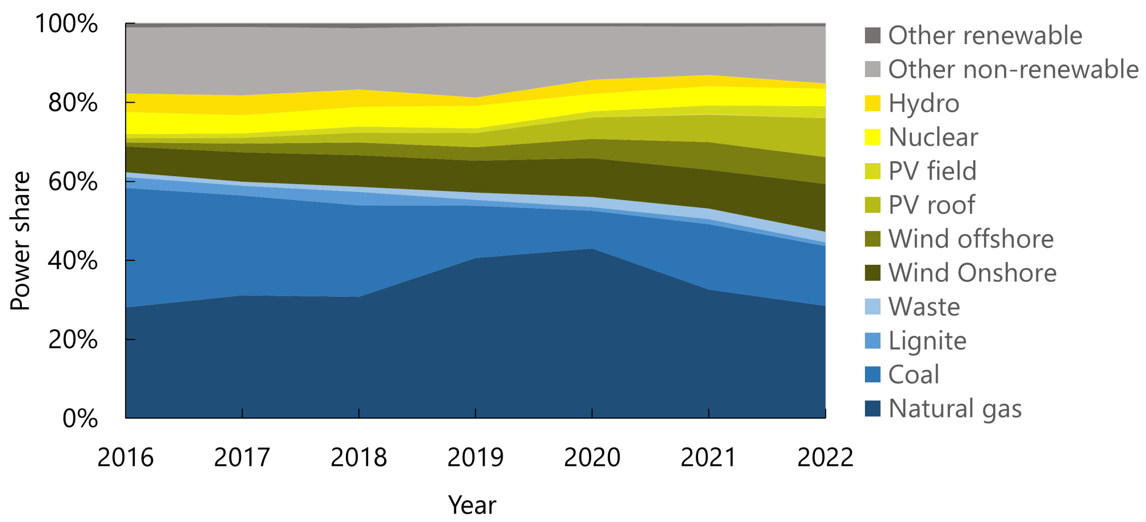

Fig. 4.3.: ODECT calculated shares of annual power generation (domestic and import) in the Netherlands per generation type.

In Figure 4.4, the generation type composition of these emissions is displayed. Coal and gas are the main contributors to the Dutch electricity related emissions. Furthermore, what is interesting to note are the emission contributions from lignite and renewable energy sources. The most emission intensive source with 1137 gCO_2eq/kWh, lignite, contributes significantly to the Dutch emission composition [91]. Power from lignite is imported excelusively from Germany. In 2018, the lignite incineration accounted for 8.1% of all electricity related emissions of the Netherlands. Since 2018, the power provided to the Dutch electricity mix by lignite has decreased each year. In 2022, lignite accounted for 2.7% of the emission of the Dutch electricity mix. As the result of increasing penetration of RESs, the share life cycle emissions related to the generation by RESs in the emission composition of the electricity mix has grown steadily from 1.1% of emissions in 2016 to 2.7% by 2022. This means that in 2022, the GHG emissions related to the 52 TWh from RESs were equal to the GHG emissions related to the 1 TWh from lignite.

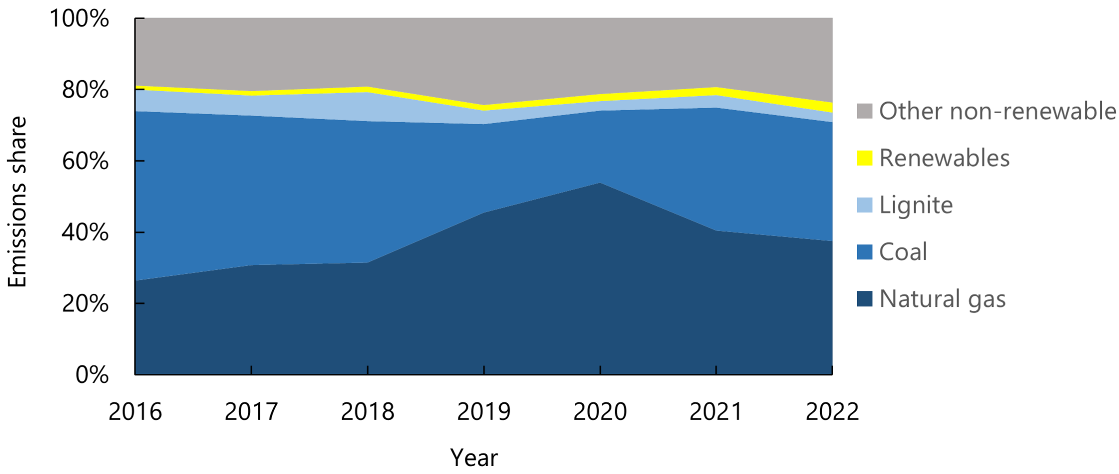

Fig. 4.4.: ODECT calculated shares of annual emissions related to generation of power (domestic and import) in the Netherlands per generation type.

This section provided an introductory overview of the ODECT results. The dynamic AEF shows a gradual decrease and growing volatility over the analysed period. The share of generation by RESs is growing and the shares of natural gas and coal are prone to fluctuations in the geopolitical landscape. Prior to further analysis of the results. The quality of the ODECT results are assessed. The next section analyses the validity of the data by comparing it to similar methods as well as real life measurements.

4.2 Validation

In this section, the validity of ODECT is assessed. In order to check the validity of ODECT and its results, it is compared to recognised public methods of expressing the GHG emission intensity of the Dutch electricity mix. Without ground truth of a measured dynamic AEF, renowned annual methods provide an indication of realistic results. A sensitivity analysis in the form of a confidence interval is conducted regarding the uncertain components of the model. Furthermore, the estimated generation by PV and onshore wind turbines are compared to annually published data. In the case of onshore wind, the data resulting from ODECT is compared to measured hourly data of a real wind park.

4.2.1 Annual AEF

The AEF results are annualised to compare it to related sources. Renowned methods by the CBS [95], EEA [28], IPCC [30], JRC [29] and dynamic models Electricity Maps [63] and CO2 Monitor [64] are included in the comparison. Figure 4.5 shows the publicly available AEFs resulting from the aforementioned methods over a period of 22 years. The differences of the seven models displayed in Figure 4.5 are the result of different approaches to model data gaps in official data sources. Furthermore, as discussed above, the methods define varying scopes in calculating the AEF. For example, some models include cross-border transmissions while others do not, the same holds for emission allocation for combined heat and power systems and distributed electricity generation. The following section dissects these components in order to analyse there respective approach and impact.

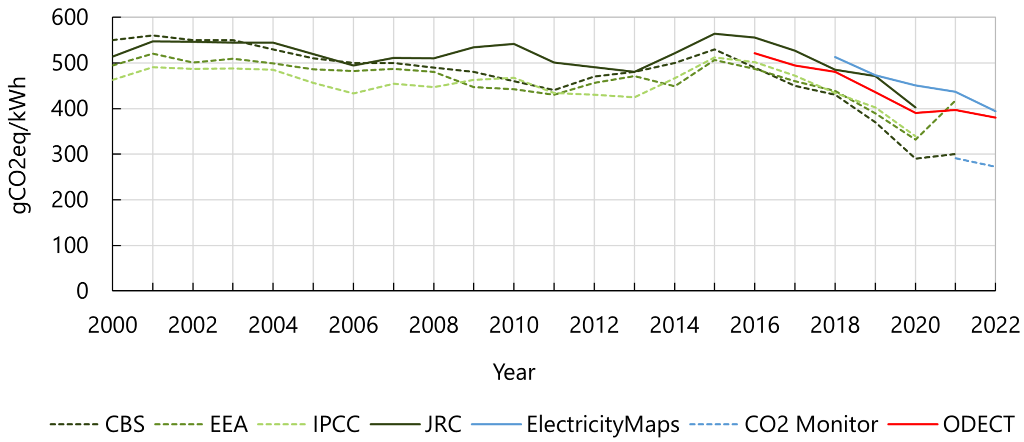

Fig. 4.5.: Comparison annual methods of calculating the GHG intensity of the Dutch electricity mix.

First, a discrepancy is noted between the methods based on direct emissions (CBS, EEA, IPCC and CO2 Monitor) and life cycle emission (JRC, Electricity Maps and ODECT). Only direct emissions from fossil power plant operation are included. A similar methodology is used by the European Environmental Agency (EEA) [28] and the Intergovernmental Panel on Climate Change (IPCC) [30]. In these methods, life cycle emissions are also disregarded. The CBS disregards life cycle emissions due to the perceived complexity of calculation [95]. However, many studies have already investigated the life cycle emissions of different generation sources [4, 10]. The data resulting from these studies can be used as input for determining the AEF. Furthermore, the CBS reasons for the exclusion of indirect emissions with the fact that over 95% of the emissions of fossil power plants are direct emissions [95]. While this was true in 2012, the assumption of negligible upstream and downstream emissions becomes less realistic over time considering the relatively large indirect emissions of renewable generation sources as compared to the indirect emissions of fossil fuels (as shown in Figure 2.5). The energy system at the time of the CBS methodology development consisted of considerably less renewable energy sources. Disregarding the indirect emissions will result in an increasingly large underestimation of GHG intensity. When, instead of only direct emission factors, life cycle emission factors are applied to the CBS methodology for all fossil and renewable generation types for the year 2019, the GHG emission intensity becomes 432 gCO_2eq/kWh instead of the original 369 gCO_2eq/kWh, an increase of 17% [32].

The EEA method does not include emissions resulting from combustion of biomass [96]. While the ODECT method presented in this thesis also disregards the direct emissions of biomass incineration, the indirect emissions e.g. as result of albedo effect, are significant and should not be disregarded. The only recognised source of annual emission factors that makes use of life cycle emission factors is the European Commission's Joint Research Centre (JRC). The JRC publishes annual GHG emission intensity factors for the Dutch electricity mix [29]. ODECT is based on life cycle emission factors as well. This explains the relatively close alignment of the JRC, Electricity Maps and ODECT methods. The average difference between ODECT and the JRC model, the methodologically most similar method, is 13 gCO_2eq/kWh over the range of overlapping years.

The methodology of the CBS and CO2 Monitor stand out on the aspect of imported power [95, 64]. In both methodologies, imported power is disregarded. This provides unrealistic image of the GHG emission intensity of the power in the Dutch grid, as imported power makes up a significant fraction of the electricity mix. The relatively higher volatility of the CBS method can be explained by the fact that the mix of imported electrical power is disregarded in this method.

Overall, ODECT data lies well within the bounds of existing annual AEF methods. Limited transparency about the used methodologies and data sources of the existing models does not allow for a detailed comparison of methodologies. The methodologically comparable method from JRC aligns the closest with ODECT of all compared methods. Therefore, the accuracy of the average ODECT AEF is on par with renowned models.

4.2.2 Uncategorised generation

One of these uncertain components is the generation data that is labelled as 'other'. ENTSO-e, publisher of the official European TSO data, gives no description of the generation types contained in the 'other' category. While TSOs of other countries, such as RTE of France, specify the generation types in the 'other' category, Tennet does not do so for the Netherlands. This results in an inevitable assumption of the generation type composition of the 'other' category to be made. The category is split into two groups: other-renewable and other non-renewable. The other-renewable group consists of renewable electricity sources not contained in the renewable categories. While this category exists within the ENTSO-e dataset, the data feed is left empty by Tennet. Therefore, other-renewable very limited impact on the AEF of the Dutch electricity mix. The non-renewable variant of the 'other' category makes up a significant 14.7% of the electricity mix in the period 2016 until April 2023.

Because the composition of sub-types in this category is unknown, a general emission factor is given to the non-renewable 'other' generation. An emission factor of 571 gCO_2eq/kWh, the weighted average of all non-renewable technologies in the Dutch electricity mix, is assigned to the category (Section 3.7). Similarly (based on European weighted average), Electricity Maps assigns a emission factor of 700 gCO_2eq/kWh to this category. In order to analyse the sensitivity of this parameter, the model was executed with a emission factor 10% higher and lower than the assumed 571 gCO_2eq/kWh, 514 and 628 gCO_2eq/kWh respectively. Figure 4.6 shows the results of this 20% confidence interval in the years 2016 and 2022. As can be seen in the figure, the effect of the relatively large deviations on the GHG emission factor for the 'Other' category is limited. The largest interval between the two levels occur during the afternoon peak in 2022 where the 'Other' category contributes relatively more to the electricity mix. Generally, a 1% change in the emission factors of the category leads to a change in GHG intensity of between 0.8 and 1.3 gCO_2eq/kWh. With respect to the daily volatility of the GHG intensity, in Figure 4.6 illustrated by a daily profile, the impact of this uncertain model parameter on the certainty of calculation is limited.

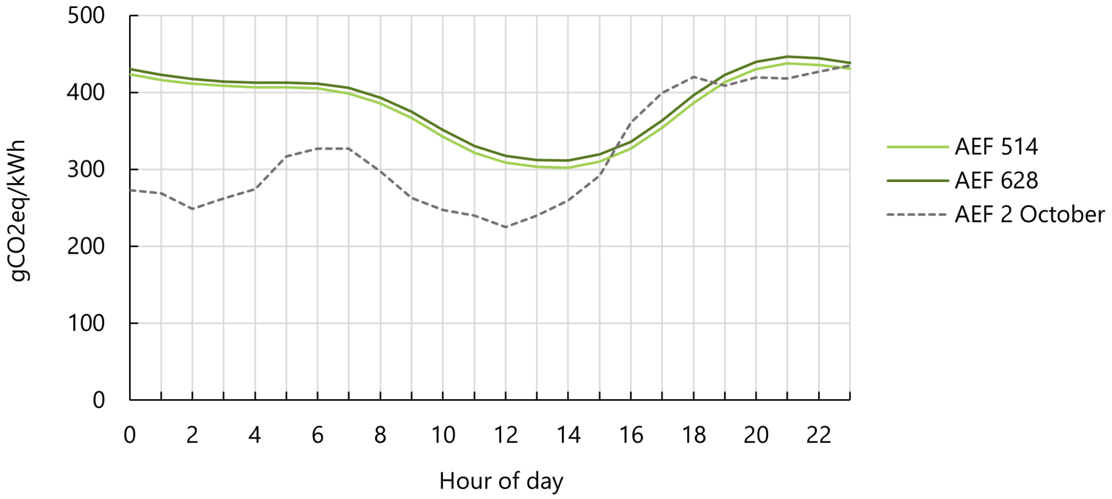

Fig. 4.6.: Sensitivity analysis of the emission factor of the generation category 'Other non-renewable' in ODECT. Line 'AEF 514' refers to the average emission factor in 2022 with a GHG emission factor of 514 gCO_2eq/kWh for the category 'Other'. In similar notation 'AEF 628' is shown. For volatility reference, the AEF is shown for 2 October 2022.

4.2.3 PV generation

Another ENTSO-e data-gap induced uncertainty is the generation by onshore decentralised electricity sources in the form of PV installations and onshore wind turbines. The electrical power generated by these sources is modelled based on weather data. The electricity generated by PV panels is modelled as function of the province average global irradiation based on KNMI data and the installed PV capacity per province from CBS data. To obtain the electrical power generation from the irradiation value, a loss factor is included. In calibration with annual CBS data, the efficiency of the conversion from irradiation to electricity is set to 83.6%, implying that 16.4% of the irradiation energy is lost in the conversion process. A loss of 14% is used as default by industry standard PV models [97]. Taking a confidence interval of -3% up to +3% with respect to the referenced 16.4% would result in a similar variation in generation, as the generation is directly related to the system efficiency. A 3% increase would lead to a 3% larger PV generation. With a maximum share (2023 Q1) of PV in the electricity mix of 28.5%, the share of PV would increase by 0.86%. With a life cycle emission factor of 41 gCO_2eq/kWh for roof mounted PV installations and 48 gCO_2eq/kWh for field installations, the change in emission intensity as result of the change in PV system efficiency would be negligible. Therefore, the uncertainty of PV system efficiency does not limit the accuracy of the GHG intensity calculation.

The performance of the PV part of the model cannot be directly measured as there is no official national data of dynamic PV generation in the Netherlands. Therefore, it is compared to annual PV generation data, shown in Figure 4.7, and to dynamic weather data, shown in Figure 4.8. The generation of electricity by PV installations is annually reported by the CBS which collects data from TSO Tennet, DSOs, Central Registration of System Elements (*Centrale Registratie van Systeemelementen*, CERES) and the Tax Administration. Figure 4.7 shows that the modelled PV generation matches the CBS reported generation very well on an annual level. The largest deviation occurs in 2018 where the model underestimates generation by 2.0%.

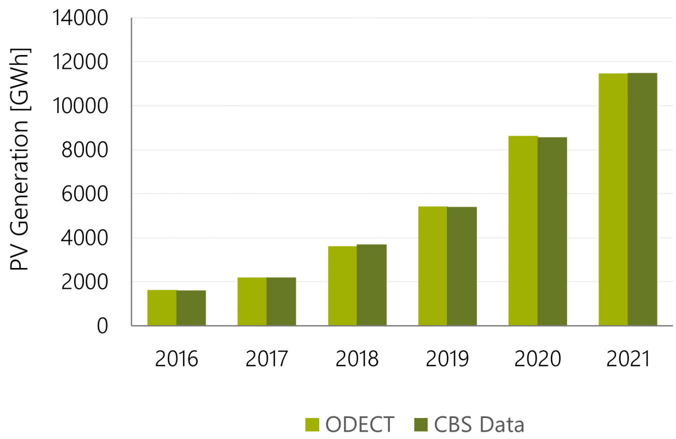

Fig. 4.7.: Comparison of ODECT calculated annual generation of electricity by PV installations in the Netherlands with annually reported CBS data [74].

Inspecting the hourly PV generation curve for a week in Figure 4.8, the similarity with irradiation is shown. However, subtle differences can be spotted between the total PV generation and the irradiation. This is a result of the differences in installed capacities and local weather per province taken into account in the model, while the figure shows the country average global irradiation. When the generation curve is compared to the data determined by Electricity Maps (EM) it becomes clear that the EM data is unrelated to the weather. The PV generation curve determined by EM seems to follow a relatively constant sinusoidal curve based on clear sky irradiation of winter months.

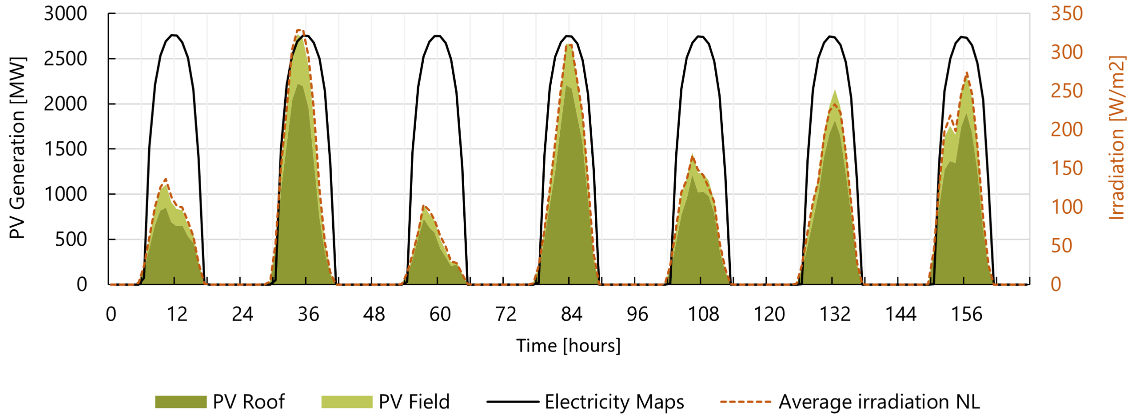

Fig. 4.8.: ODECT modelled PV generation, Electricity Maps [63] PV generation and country average global irradiation (KNMI) for the first week of October 2020. The ODECT differentiates between installations on roofs and fields.

Figure 4.9 shows that the real generation by PV installations is much higher than the EM model determines for the large part of the year. During the winter months, EM consequently overestimates the share of PV in the electricity mix. Annually, this general assumption made by Electricity Maps results in a large underestimation of PV generated power. For 2022, the CBS reported 11494 GWh of PV production while Electricity Maps modelled 9760 GWh, a deviation of 15%. In comparison, ODECT resulted in 11471 GWh of PV generated electricity for 2022, a deviating 0.2% from the reported data. Only the difference in PV generation leads to deviations of the dynamic AEF up to 141 gCO_2eq/kWh, as large as 37% of its average value. With large companies such as Google relying on the methodology of Electricity Maps [35], this could lead to choices based on bad knowledge with unintended effects. For example, shifting loads to datacenters in other countries while trying to reduce the carbon footprint could result in an increase of the real carbon footprint when the actual PV generation is not modelled accurately.

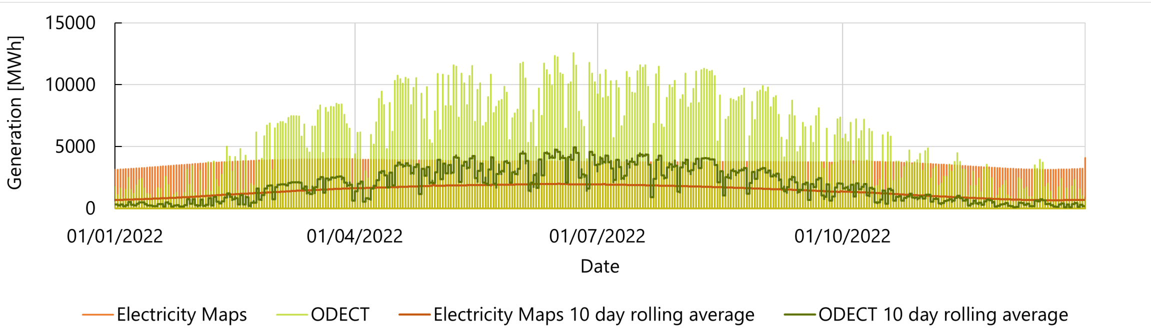

Fig. 4.9.: Generation of electricity by PV installations in the Netherlands as modelled by ODECT and Electricity Maps [63]

4.2.4 Onshore wind

Similar to PV generation, the generation of electricity by onshore wind turbines is only reported partially by the ENTSO-e transparency platform. Using wind data from the KNMI and capacity data from CBS, the generation is modelled per province and subsequently aggregated. Similar to the generation by PV installations, CBS annually reports the electricity generated by onshore wind turbines with collected data from DSOs, certificate issuer CertiQ and the Netherlands Enterprise Agency (*Rijksdienst voor Ondernemend Nederland*, RVO). Figure 4.10 shows the comparison between the modelled wind generation and the reported real generation. The model follows the trend of annual production closely, with the largest deviations in 2016 and 2022 with an overestimation of 3.8% and an underestimation of 3.1% respectively.

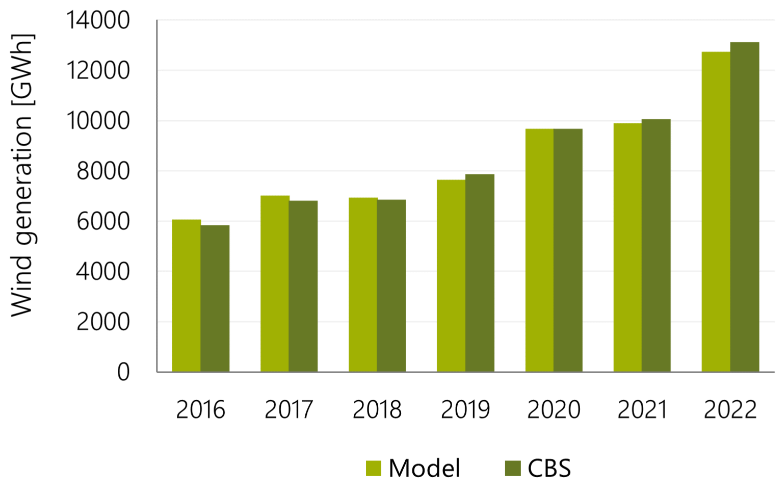

Fig. 4.10.: Comparison of ODECT modelled annual generation of electricity by onshore wind turbines in the Netherlands with annually reported CBS data.

Considering the dynamic nature of the GHG intensity calculation, more emphasis should be placed on performance of the model on a finer time scale than on the annual comparison. In order to analyse the dynamic performance of the model, a comparison is made between the modelled onshore wind electricity generation and physically measured quarter-hourly generation data from Dutch wind park Krammer. Krammer is the largest community build wind park of the Netherlands, realised by Zeeuwind and Deltawind. The park is located in the former estuary Grevelingen in the province Zeeland. Wind park Krammer consists of 34 Enercon E-115 turbines with a combined nominal capacity of 102 MW. The turbines are characterised by a rotor diameter of 115.7 meters and a hub height of 122 meters. The model parameters are adapted to the nominal capacity, rotor area and hub height of the park in order to reproduce the electricity generation based on KNMI wind data. The modelled generation can be compared to the real generation on hourly basis covering the year 2022. Figure 4.11 shows the comparison for a week in March and Figure

4.12 shows the comparison for weekly aggregated energy production throughout 2022. Figure 4.11 shows the dynamic performance of the model. The model is able to track the real electricity generation with an absolute average deviation of 15.4%. On weekly basis, shown in Figure 4.12, a similar comparison can be seen. Here the absolute deviation is 16.2% on average. These deviations are a result of different factors. First and foremost, the wind speeds are not measured at the turbine hubs, but 10 meters above ground in weather stations Wilhelminadorp, Woensdrecht and Vlissingen. These speeds are averaged and converted to hub height with a surface roughness coefficient. This limits accurate approximation of complex and a locally volatile wind speeds. Furthermore, the generation of electricity is not always a product of wind speeds as the wind park is subject to curtailments. Specifically, wind park Krammer is curtailed in three cases: detection of birds or bats, detection of ice or in the case of negative prices on the imbalance markets. These characteristics are impossible to model from the available data as these cases are site specific. Birds, bats and ice occur locally and thresholds for negative imbalance prices differ per operator. Other wind parks are located near residents, forcing curtailment to limit hours of shadow flickering.

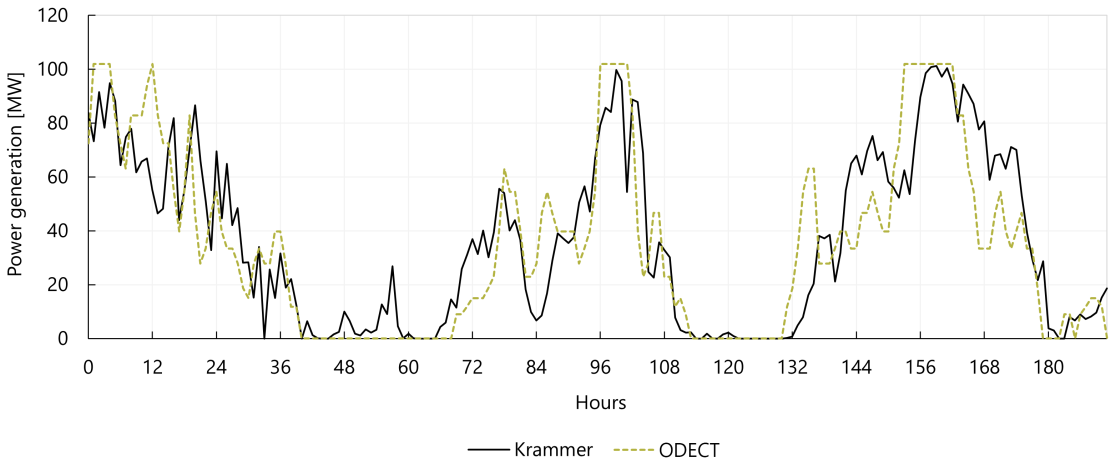

Fig. 4.11.: Comparison of modelled electricity generation and measured data from wind park Krammer for a week in March 2022.

The section above illustrates the performance of ODECT compared with data of one wind park. The model overestimates as much as it underestimates. Out of 8760 hours that were analysis the model overestimated the generation for 4300 hours (49%) and underestimated it for 3917 hours (45%). During the remaining 543 hours, the model was exactly right. Furthermore, the average (not absolute) deviation is negligible with 2%. This balance of deviations is beneficial when modelling a large multitude of wind parks on national scale. Local variations in wind speeds and curtailments will cancel out when large number of turbines are covered. Therefore, the performance of the wind model will be better on a national scale than it is modelling wind park Krammer.

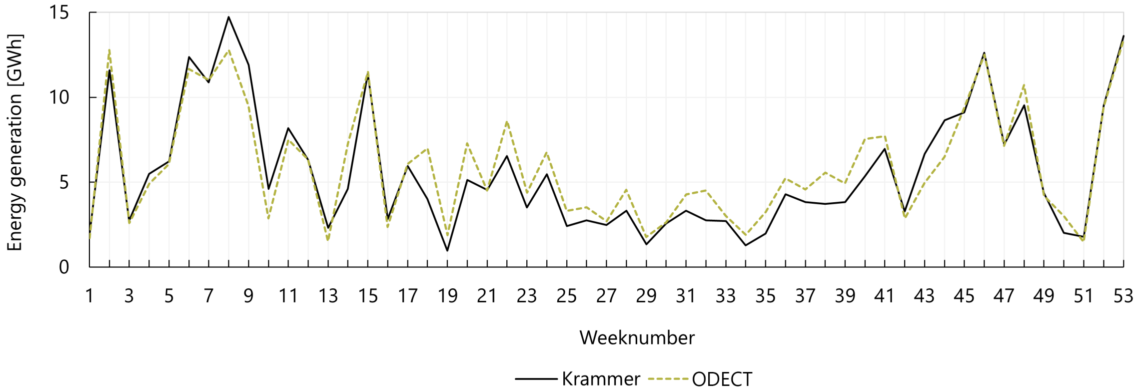

Fig. 4.12.: Comparison of modelled energy generation and measured data from wind park Krammer for all weeks in 2022.

4.2.5 Conclusion

Section 4.2 compared the results of the ODECT model to existing data in order to assess its accuracy. Renowned annual AEF models, annual measured generation data and hourly measurements of a Dutch wind park were included in this comparison. Furthermore, a sensitivity analysis was conducted regarding model uncertainties. Overall, as far as it can be proven without ground truth, ODECT shows accurate results. In some aspects, ODECT created data with considerably higher accuracy than renowned models. This is especially the case for PV generation estimation as compared to Electricity Maps. Furthermore, inclusion of electricity imports and life cycle emissions provide a AEF which reflects the impact of electricity consumption in a more complete manner than the models that exclude these aspects.

4.3 In-depth analysis

The validation of the model allows for deeper analysis of the results. After deep data analysis, three interesting aspects of the GHG intensity identified. First, the electricity mix is changing in profile and composition. Second, the potential of load shifting for emission reduction is growing due to the increasing volatility in the GHG emissions intensity of the electricity mix. Third, the large potential for emission reduction by changing the merit order to the merit order of emissions. This section will highlight each of these aspects, reason why they occur and explore their effects.

4.3.1 Composition

The composition of the electricity mix changes continuously. Figure 4.13 shows the monthy average composition of the Dutch electricity mix for the assessed time period. First and foremost, a rise in generation by RESs is seen over the years. Where in 2016, RESs accounted for around 20% of the generated power, 2022 shows a RES share of around 35%. Taking a closer look at the share of PV, the steep increase of capacity can be seen by the growing generation shares during the summer months. A similar increase of installed nominal capacity can be seen for both of the wind energy shares.

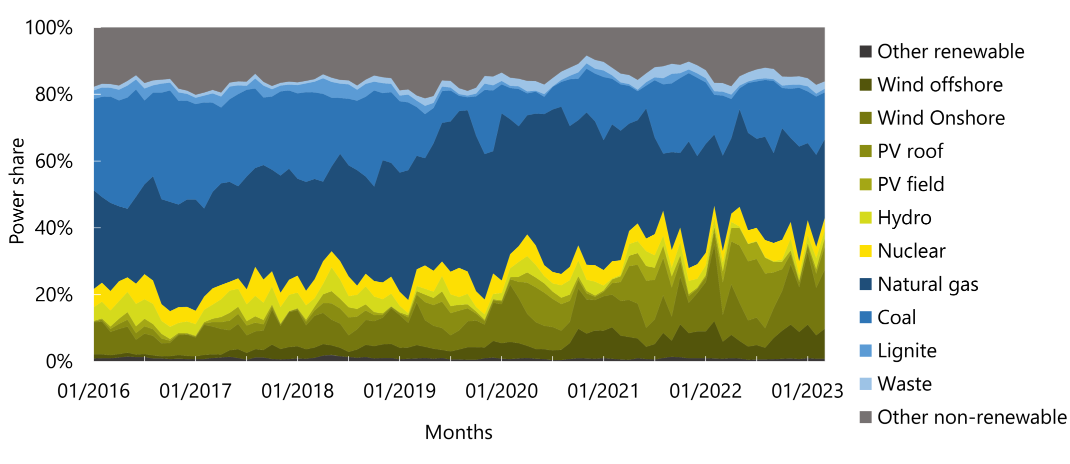

Fig. 4.13.: ODECT monthly average generation type composition of the Dutch electricity mix.

Figure 4.14 shows the average generation type composition of power for every hour of the day in 2022. The dominant shape is a result of the power generated by PV installations. In this figure, the difference in intermittency characteristics of PV and wind are illustrated clearly. Compared to the PV curve, wind energy provides power evenly distributed throughout the day. Most interesting to note is visibility of the dispatch characteristics of adjustable power sources. Power from waste provides an almost constant share of the power mix, followed by relatively stable sources nuclear and coal. Natural gas however, shows a large variation in power share throughout the day. This is a result of both the ramp rate characteristics and merit order effect. Natural gas is quickly ramped up or down based on the availability of RESs with low marginal costs while some power generated from "must-run" sources such as coal and nuclear is sold on the power markets for a loss, just to keep the installations running and standing by for dispatch.

The same variable power share effect is can be seen in Figure 4.15, where the GHG emission composition of the Dutch electricity mix is shown per hour of day in 2022. The main sources of emissions throughout the day are natural gas and coal. Here,

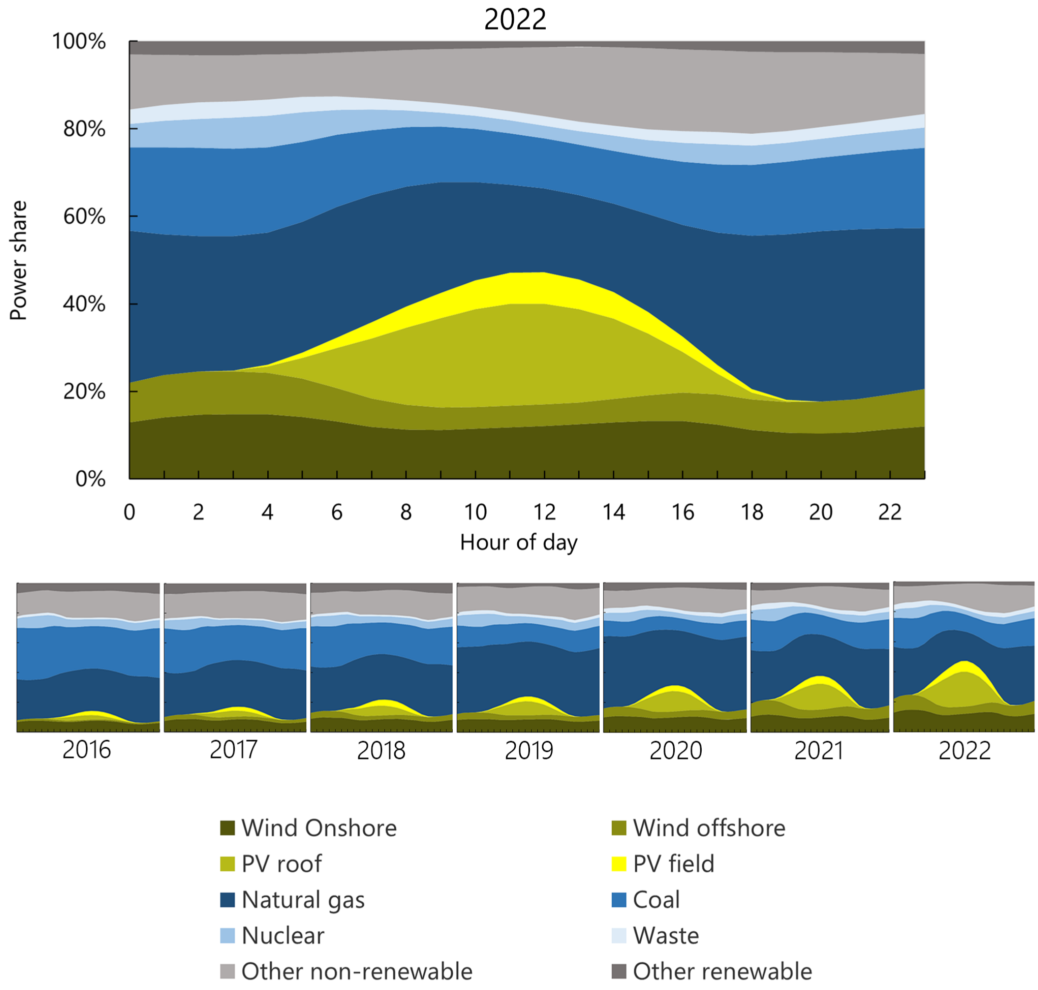

Fig. 4.14.: ODECT annual average composition of the Dutch electricity mix for the hour of day in 2016 until 2022.

the variability of dispatch is illustrated for natural gas compared to the more stable emission share of coal. The life cycle emission of PV installations are notably present. Where in Figure 4.13, the share of power from lignite is relatively invisible for the last years, this fraction is prominently present in the emission mix shown in Figure 4.15. This is a result of the high generation type specific emission factor of lignite compared to other sources of electricity. The odd curve of emission share of "other non-renewable power" can possibly result from small natural gas fired installations that are used to peak-fire at times of relatively high weather dependent power supply, e.g. to mitigate drops in power supply by clouds that pass over PV installations.

Renowned methodologies for the GHG emission intensity of the Dutch electricity mix, the CBS and CO2 Monitor method, do not include the dynamic import of electricity and the composition of imports. Therefore, it is interesting to analyse the effects of excluding this part of the electricity mix and its insights that might be overlooked.

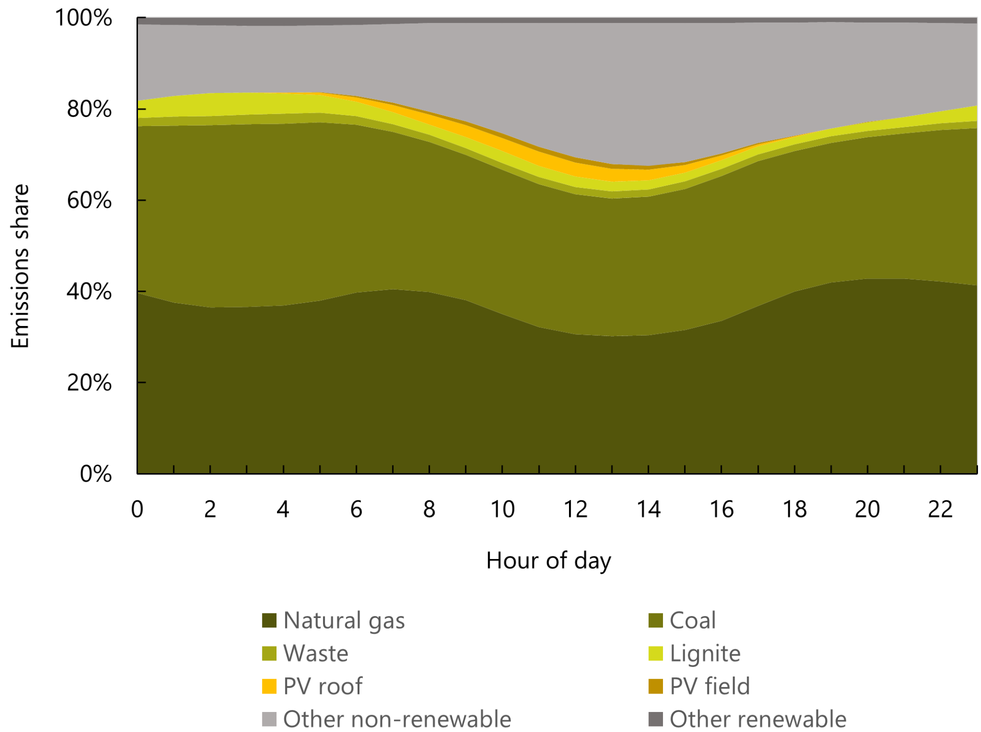

Fig. 4.15.: ODECT GHG emission composition per hour of day in 2022.

In Figure 4.3, the share of imported power is shown for the time period 2016 until 2022 as well as the average import shares per hour of day in 2022. In the left graph, a steady decrease is shown for the annually imported power share. While the renewable share of domestic power generation increases rapidly for the Netherlands, the renewable fraction of the imported power remains relatively constant. The cause for this effect is shown in the right graph. The share of imported power is high at times of low generation by RESs. Still the imported power consists of large shares of renewable power from wind, hydro, biomass and nuclear power plants. This makes that currently, importing power as alternative to domestic generation decreases the GHG emission intensity of the Dutch electricity mix. However, the fact that power is imported particularly during times of low PV production results in a steady fossil fraction within the imported power.

Figure 4.17 shows the evolution of the average imported power share per hour of day of the Dutch electricity mix for the years 2016 and 2022. In blue, the relatively horizontal line can be seen, the imports in 2016 fluctuated minimally around 20% throughout the day. Extreme values in 2016 were broadly limited to 3% to 40%. In 2022, a different curve can be seen. The average import share throughout the day dropped, with the except of the night and early morning hours. The upper bound

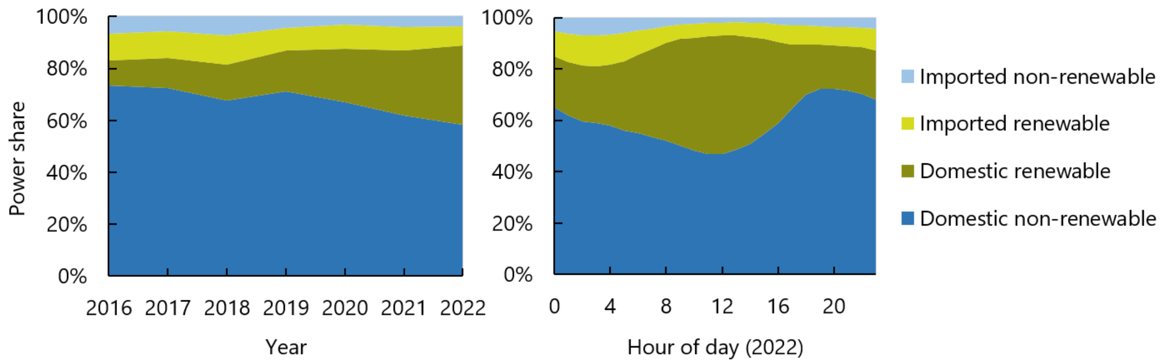

Fig. 4.16.: ODECT composition of domestic and imported power, separated in non-renewable and renewable sources.

of extreme values shows the same change with higher magnitude where imports in the night hours increased and the imports around noon decreased. In this way, the cross border connections are used as adjustable power supply to provide power during "Dunkelflaute", times of low generation by weather dependent RESs PV and wind. As said, this is currently positive effect as zones neighbouring the Netherlands contain large capacities of constant RESs, e.g. hydro in Norway and nuclear in France, but this not a given, as seen in the nuclear phase out in Germany [98]. However, during dunkelflaute, the neighbouring zones will have a relatively high GHG emission intensity resulting from lower generation by their weather dependent generation installations. Therefore, the constant fossil fraction in power imported at nighttime should be taken into account when planning the domestic electricity supply of future. While this fraction is relatively small compared to the fossil share of domestic generation, it will become relatively bigger as fossil domestic generation is phased out. By assigning the domestic GHG emission intensity to imported power, the CBS currently overestimates the emissions related to electricity consumption. However, following the trends seen in Figure 4.16, this assumption will lead to a underestimation of emissions. In 2022, the fossil share of imported power accounted for 8.0% of the electricity related emissions, and therefore of the GHG emission intensity, on average. Using methods that exclude imported power will result in a growing blind spot for international carbon dependency.

4.3.2 Volatility increase

The GHG emission intensity of the electricity mix varies continuously. This is a result of a broad range of factors. Human behaviour causes a constantly changing demand. The weather causes fluctuations in weather dependent generators. Physical installations break down. Geopolitical situations cause price fluctuations, such as increasing gas prices due to Russia invading Ukraine. Or, as seen in the previous section, a flock of birds cause wind turbines to shut off. All of these factor have an

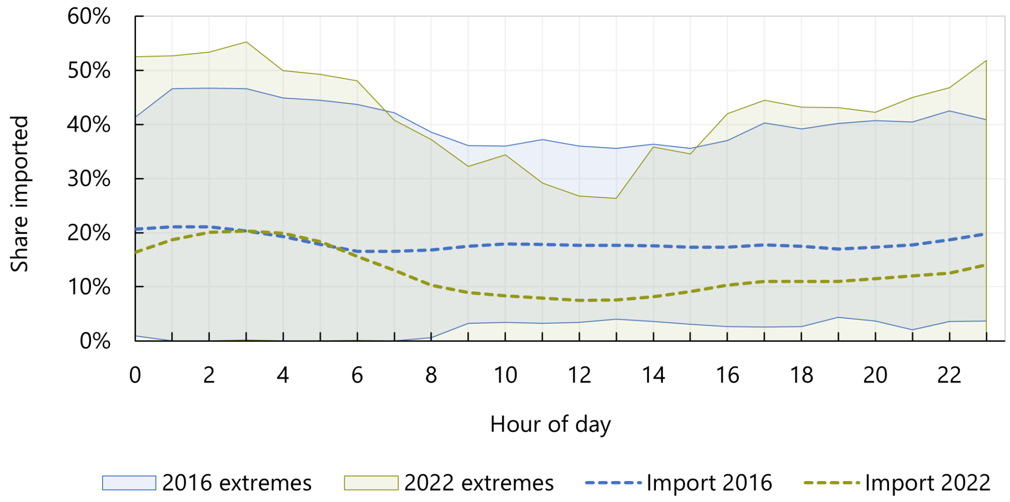

Fig. 4.17.: ODECT average and extreme values for the share of imported power per hour of day for 2016 and 2022.

impact on the value and profile of the GHG emission intensity. As seen in Section 4.1, the volatility of the AEF shows an upwards trend from 2016 up until April 2023. This section elaborates on the characteristics of this growth in volatility as well as its potential for DSM.

The change in hourly profile between 2016 and 2022 is shows in Figure 4.18 where the average GHG intensity per hour of day is shown for January and July for 2016 and 2022. The figure shows the relatively stable GHG intensity over the day in 2016 for both January and July. In 2022, the profile has changed drastically in range and seasonal variation. The January profile of 2022 shows a less stable profile than January 2016, and a large increase of the range between the extreme values. This range can be attributed from hours of optimal wind production (low AEF) to hours of predominant coal and lignite generation (high AEF). The July curve of 2022 shows a clear representation of the "duck curve" with a large PV cause dip around noon. While the extreme values of July 2022 increased in reference to 2016, the bandwidth remains narrow compared to the January 2022 curve. Furthermore, Figures 4.19 and 4.20 show the annual development of the hourly AEF curves for January and July respectively. In these figures, the downwards trend as well as the increased volatility are clearly visible. Interesting is the development of the AEF during the summer night hours. While the other hours show a clear decline in AEF over the year, the night hours of July show no significant change (compared to the previous year) in 2017, 2020 and 2021 and even show a significant increase in 2018 and 2022. This is the result of changing marginal power plants which change predominantly as result of changes in marginal prices, e.g. rising gas costs making coal the marginal power plant for some periods in 2021 and 2022.

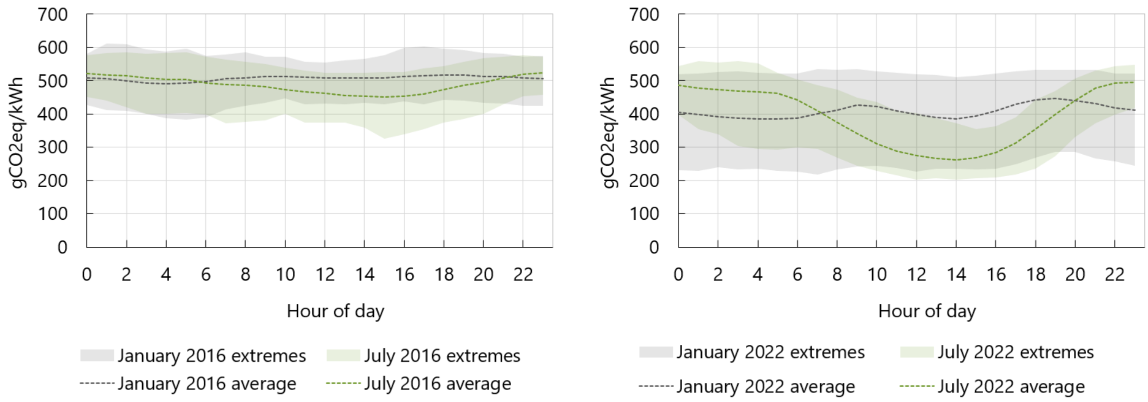

Fig. 4.18.: Hourly profile of the GHG emission intensity of the Dutch electricity mix in January and July of 2016 and 2022.

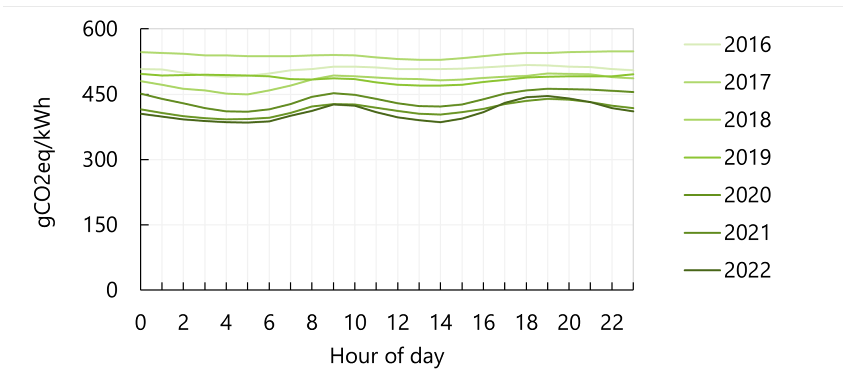

Fig. 4.19.: ODECT January AEF per hour of day for 2016 until 2022.

Coming back to the upwards trend in the intraday volatility, the GHG intensity of the electricity mix will vary increasingly within the day. This trends leads to two important conclusions. Thee first conclusion is the need for standard dynamic reporting of the GHG intensity of the electricity mix increases. By annually reporting the GHG intensity, these growing dynamic fluctuations remain invisible in carbon accounting and postpones incentives for electricity consumers and policy makers to prepare for an increasingly intermittent green electricity supply. For example, not knowing the growing fluctuations in emission intensity, consumers are left unable to adapt to the rhythm of the weather dependent electricity supply, slowing down the energy transition towards an emission-free electricity system. In short, dynamic effects of the electricity mix should be reflected in the price and carbon footprint of electricity consumption.

This brings forward the second conclusion regarding the growing volatility. The difference in GHG intensity within a day is equal to the potential carbon reduction by shifting electricity demand in time. Therefore, a growing intraday volatility is equal to a growing potential for load shifting for emission minimisation. Figure 4.21 shows the difference between the daily high and low point in the emission intensity.

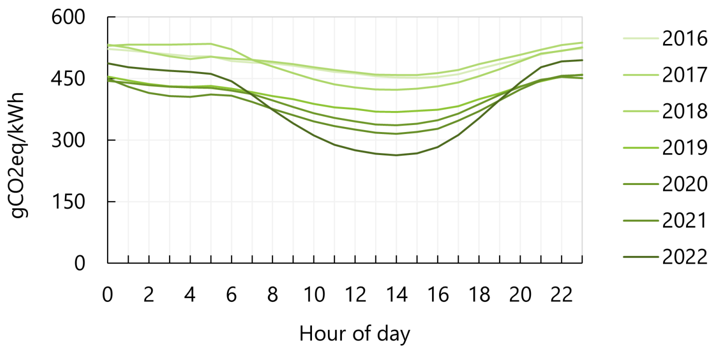

Fig. 4.20.: ODECT July average AEF per hour of day for 2016 until 2022.

This is the intraday volatility of the curve. In the 30 day rolling average an upwards trend as well as a seasonal pattern can be seen. These characteristics are a direct result of increasing penetration of intermittent power generators such as wind and PV in the electricity mix. In the beginning of 2016, shifting 1 kWh of demand within the day could potentially reduce the carbon footprint of that kWh with 65 gCO_2eq. By April 2023, this potential has grown to 175 gCO_2eq/kWh. In 6 years load shifting has become 2.7 times as effective in reducing emissions. During summer months, this potential is even higher, with reduction up to 330 gCO_2eq/kWh in July 2022.

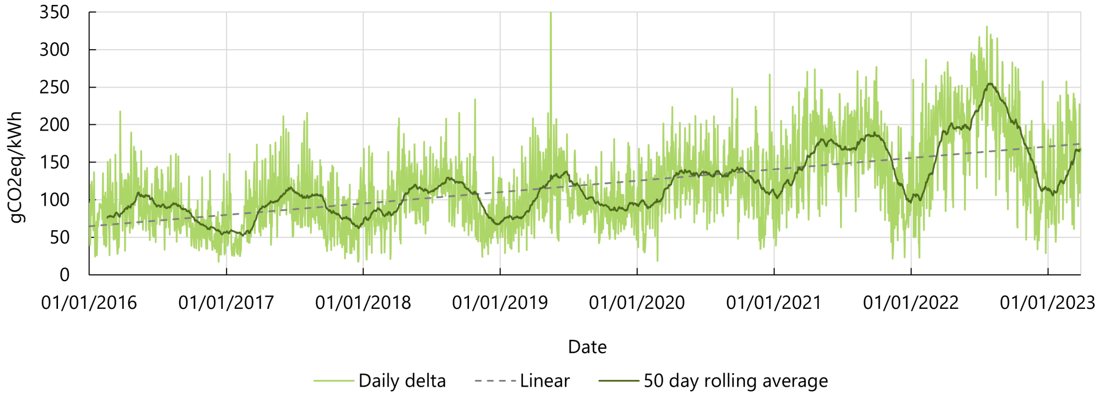

Fig. 4.21.: Daily difference between maximum and minimum GHG intensity of the Dutch electricity mix. Added for clarity are a 30 day rolling average and a linear trend.

In order to put this knowledge discrepancy between annual AEF methods and dynamic AEF methods into context, the carbon accounting of an theoretical household is determined with a static and a dynamic GHG intensity. Figure 4.22 shows the comparison between the two methods with regards to the reduction of GHG emissions by shifting a load in time. A light dotted line is added to show a load shift of 0.545 kW, the energy required to run an eco-program on a B-label washing machine. The load is shifted from peak hour 18.00 to off-peak hour 12.00. Interesting to note is that the static load shifting curve does not change in area compared to the non-load shifting curve i.e. the drop in the afternoon equal in area to the rise at noon. Therefore, the total emissions of the day remain the same under the static method. This is logical as the GHG emission intensity is assumed to be constant (static) throughout the year. The dynamic method shows a different result, where the afternoon drop in emissions as result of load shifting is significantly larger than the rise in emissions at noon. Using the dynamic approach an emission reduction of 2% or 67 gCO_2eq is realised by shifting the load, where the static approach states no difference in emissions between the base scenario and the scenario with the load shift. Given the increasing potential for load shifting to reduce GHG emissions, the use of static GHG intensities for carbon accounting causes a growing blind spot for emission reduction.

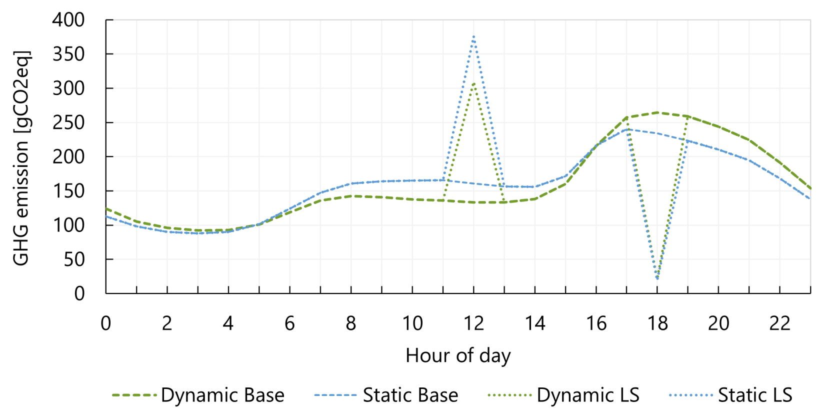

Fig. 4.22.: Average emissions per hour of day for a household with average electricity profile (MFFBAS) and an annual demand of 3500 kWh. Compared are methods of calculating hourly emissions with a dynamic (hourly) or static (annual) GHG intensity factor. Furthermore, a load shift of 0.545 kW from 18.00 to 12.00 o clock is presented (light dotted lines, LS).

4.3.3 Merit order

A conscious choice should be made regarding the adjustable power that is activated during times of low renewable energy supply. The existing merit order in European markets does not always reflect the order of emission intensity i.e. the most economic generation type is not always the most sustainable generation type. The merit order dilemma of emissions, as also described by Fletschutz [8], therefore plays a role in the adjustable interconnection effect.

In order to quantify the impact of this merit order dilemma of emissions, the example of lignite imports is taken. In the Netherlands, the installed capacity of natural gas fired power plants is published by the CBS. Theoretically, not taking into account economics and physical imports of commodities, every MWh of imported electrical power generated by German lignite could be replaced by a MWh of natural gas generated electricity as long as there is unused capacity of gas fired power plants. This illustrates a situation where the environmentally friendlier natural gas fired power plants are given priority over the emission intensity lignite fired power plants. As result of type specific emission intensity factors, every MWh of lignite generated power that is replaced by a MWh generated by a gas power plant will reduce emissions by 647 kg CO_2eq.

Figure 4.23 shows the relation of imported lignite power and unused gas fired power plant capacity for every hour of 1-1-2016 until 1-4-2022. The large potential for GHG reduction by giving priority to gas in the merit order can be noted. The diagonal line shows the balance of imported lignite power and unused gas capacity, where dot on the right side of the line represents a import value of lignite that could theoretically completely be replaced by electrical power generated by domestic gas fired power plants. If in 2021 the imports of power from lignite would be replaced by power from gas within the physical capacity of the installations, an emission reduction of 0.77 megatons of CO_2eq could be realised. To put this figure into perspective, this is 3.3% of the total electricity related emissions of the Netherlands in 2021 [99]. In order to realise these kind of emission reduction in the electricity system, either the ETS price has to increase significantly to naturally change the merit order or market reform is needed where the merit order is based on emission intensity.

Fig. 4.23.: Imported power generated from German lignite and time related unused capacity of domestic natural gas fired power plants for every hour from 1-1-2016 until 1-4-2023. For every data point below the 1:1 line, all the imported lignite power can be replaced by remaining unused capacity of gas fired power plants.

5 Conclusion

The goal of this thesis is to find a methodology for the calculation of the GHG emission intensity of the Dutch electricity mix by answering the main research question:

> How can the dynamic GHG emission intensity of the Dutch electricity mix be modelled using publicly available data sources?

This research question was answered through the analysis of the (1) functioning of the electricity grid, (2) comparison of existing methods, and (3) development of a methodology and model. Subsequently, (4) the performance of the model was analysed by comparison to widely recognised annual GHG emission intensity models as well as physically measured data.

> 1. How is the production and consumption of electrical power organised?

The electrical power consumption (Section 2.1.3) has to match its production in order to ensure the stable operation of the grid (Section 2.1.2). Demand side management will become increasingly important in facilitating this match of supply and demand as result of increasing volatility and capacity of power generation. The supply by many generation types (Section 2.1.1) is matched to the demand through power markets based on economic merit which is different than environmental merit (Section 2.2). The impact of electricity consumption on global warming (Section 2.3) is analysed. Life cycle emissions should be considered for a complete view of the global warming potential. Carbon accounting aims to assign emissions resulting from electricity consumption (scope 2) to consumers, but current methods fail to include the physical system boundaries of the electricity grid. The temporal and local matching of demand and supply are not covered by Guarantees of Origin. Therefore, the progression towards a low-carbon electricity supply stagnates because consumers do not see the possibility or necessity of adapting their consumption to the generation profiles of renewable energy sources.

> 2. How are dynamic GHG emission intensity factors calculated by existing methods and models?

In the comparison of existing academic and commercial methodologies a broad range of depth and focus is found. Most methods rely on general assumptions, e.g. not taking into account electricity imports or modelling PV production as weather independent sinus wave. Some methods are precise, but rely on data that is only available long after the time for which the GHG emission intensity is calculated. No open model or methodology exists that determines the GHG emission intensity of the Dutch electricity mix including all generation installations and imported power.

> 3. How can the GHG emission intensity of the electricity mix be determined from publicly available data?

In this work, a methodology (Section 3.4) is presented that determines the GHG emission intensity for an electricity grid. The methodology presented makes use of multiple public data sources to determine the GHG emissions intensity in near real-time. Decentral weather dependent generation types of which near real-time generation is not available in public databases are modelled based on weather data (Section 3.5). A method of including energy storage is presented although no data is currently available for modelling this aspect of the electricity mix. A key factor included in determining the emission intensity of the electricity mix is the quantity and composition of imported power composition of imported power which can be calculated iteratively (Section 3.6). Based on the presented methodology, the Open Dynamic Electricity Composition Tracker (ODECT) is developed (Section 3.7).

> 4. What is the validity of the developed methodology?

The ODECT results are compared to renowned methods publish the GHG emission intensity of the Dutch electricity grid annually (Section 4.2.1). The method most similar to ODECT is that of the JRC, which shows good alignment with an average difference of 13 gCO_2eq/kWh. Overall, ODECT gives reliable insight on annual time frame compared to recognised methods. A sensitivity analysis of the uncategorised generation shows that change in the assigned emission intensity of the 'other' categories has negligible influence on the total GHG emission intensity compared to its daily volatility (Section 4.2.2). The modelled generation of PV installations and onshore wind turbines is validated using measured generation data from CBS (Sections 4.2.3 and 4.2.4). The modelled PV generation shows a maximum annual deviation of 2.0% for the years 2016 until 2021. The modelled onshore wind generation shows a maximum deviation of 3.8% for the year 2016 until 2022. Furthermore, the modelled onshore wind generation is validated with measured hourly generation data from wind park Krammer over the year 2022 (Section 4.2.4). ODECT shows an average absolute deviation of 15.4% compared to the measured generation data from Krammer. The model is considered to be more accurate when taking into account more wind parks over a larger region, as local variations in weather cannot be derived from nearby weather stations and turbine specific curtailment, e.g. from bird detection, cannot be modelled.

5.1 Key takeaways

In the analysis of these results, two key findings are presented.

First, a standard open access methodology is needed to progress towards a low-carbon electricity supply. Many methods of determining the GHG emission intensity are developed with different scopes and depths. Instead of many individual models, researchers, innovators, policy makers, consumers and producers will benefit from one reliable and consistent source of information about the dynamic environmental impact of electricity consumption. A standard, open access methodology that covers the dynamic composition of the electricity mix and accurate life cycle environmental impact factors could provide validated insights and facilitate the progress towards a low-carbon electricity supply. A complete electricity mix including decentral domestic generation as well as cross-border transmissions should be considered in this methodology. This information could be published on official channels such as the Transparency Platform of the ENTSO-E, open market data page of the EEX group or governmental websites. The openness of methodology is crucial to allow for open discussion and levelled carbon footprint comparison. Finally, open access to historical and predicted data provides a solid basis for a broad range of research and innovations.

Second, by not taking into account the dynamic aspects of the electricity grid, large potentials for GHG emission reduction are overlooked. The results presented in this work indicate significant volatility in the GHG emission intensity of the Dutch electricity mix. By relying on static annual carbon accounting methods, the impact of consumption timing on electricity related GHG emissions remain invisible. Therefore, opportunities for emission reductions through DSM are overlooked. Furthermore, current carbon accounting methods lead consumers to believe that their electricity consumption consists of 100% renewable energy which leads to the false conviction that they are independent of fossil sources of electricity. Dynamic emission allocation and related pricing will provide a economical and moral incentive for change in consumption behaviour. Another potential for emission reduction exists in the merit order operation of the power markets. As prime example, emission intensive lignite power plants are dispatched at times when relatively low-emission natural gas plants are standing by. Market reform and increased ETS prices have the potential of significantly reducing the GHG emissions related to the generation of electricity without impacting the reliability of power supply.

5.2 Significance

This work forms a stepping stone towards an accurate public and recognised GHG emission intensity indicator. Such an information source can be used by electricity retailers to inform consumers about their carbon footprint, by a wide range of load-shifting initiatives to realise emission reductions, and by governmental bodies and other organisations to analyse accountable (scope 2) emitters.

In the development of ODECT and its methodology, many existing methods of calculating the dynamic GHG emission intensity of electricity grids were analysed (Section 3.2). In this analysis, assumptions and approaches were found that strongly limit the accuracy of the model. Examples of these assumptions, presented in Section 3.2, consist of exclusion of weather data (Electricity Maps), imported power (CO2 Monitor) and decentral RESs (Elmada). This thesis presents an open methodology that includes these components. Therefore, the existing models can use this work to improve and reflect upon their models.

In fact, some of this improvement has already taken place during writing. CO2 Monitor added information to their website elaborating on the used methodology upon correspondence about this thesis. Where the initial given information was scarce, CO2 Monitor now details their included data sources, model boundaries and emission factors. This is a prime example of how critical analysis can improve the insight provided by existing models. In similar fashion, organisations behind existing models providing insights about the dynamic emission intensity of electricity grids should use this thesis to improve the quality of their models. For example, Electricity Maps could implement the modelling of PV generation based on KNMI and CBS data to increase the accuracy of their model. In this way, better insight is provided to a large number of consumers, which is key in the progression towards a sustainable electricity system.

6 Recommendations

The presented work provides a comprehensive view of the real composition and GHG emission intensity of the Dutch electricity mix. While the model takes into account a range of factors and multiple extensive datasets, some influential aspects of the electricity mix are disregarded. The most relevant example is the incorporation of more neighbouring zones and inclusion of a static outer layer of zones. While this is included in the theoretical methodology, derived model ODECT only takes into account the imported power from direct neighbouring zones. In order to provide a complete and increased realistic view of the composition of the electricity mix, the generation and cross-border transmission of more zones should be taken into account, as described methodologically in Section 3.6. An analysis of the degree of interconnection between European zones could help to weigh the balance between completeness of included zones and complexity of the model. As result of this analysis, a region of included zones can be determined with an outer ring of static zones for which the electricity composition is assumed to be constant or dynamically based on a function of time.

The addition of energy storage becomes more imminent as larger storage systems are added to the electricity mix. Real-time operation data of grid scale Energy Storage Systems (ESSs) is needed to include storage in ODECT. Currently, generation and consumption of pumped hydro is included on the Transparency Platform, ESSs could be included in the same way. Another aspect that can be predicted to increase the performance of ODECT is the installed nominal capacity of PV and onshore wind. By predicting what is installed since the last published data by the CBS, a precise time dependent nominal capacity estimation, and therefore precise time dependent generation estimation can be achieved.

The 'other' category in the generation data of ENTSO-e forms another data gap in the current model. Research can be conducted in order to find the precise consistency of this category for the different included countries. This information can be used to attribute the power contained in the 'other' category to the defined generation types. Alternatively, limited information about the composition of this special category can be used to express an educated guess of the emission factor of 'other'. Similarly, the composition of waste that is incinerated to generate electrical power could be analysed to specify a more accurate life cycle emission factor to electricity from waste.

A third incomplete feat of the model can be found in the modelling of decentral sources in the form of PV installations and onshore wind turbines. As result of local events, these sources are occasionally curtailed. For example, when there is an abundance of electricity production in the local grid, the voltage will rise. In order to protect physical installations, inverters turn off, i.e. curtail, PV installations when the measured voltage passes a threshold. The same reasoning holds for wind turbines as well as the mentioned curtailment reasons in the Krammer section of Chapter 4: bird detection, ice formation, shadow flickering and negative imbalance prices. A future version of the presented model could take into account some of these curtailment occurrences such as ice and shadow formation based on weather data and inclusion of imbalance prices. For very local, not centrally registered events such as flocks of birds and voltage violations, it seems unlikely that these can be modelled based on public data. Another factor of the decentral wind generation is the effect of surface roughness on the height conversion of wind speeds. ODECT could be improved by investigating the surface roughness coefficient for the different provinces of the Netherlands in order to model their respective electricity generation by onshore wind turbines more accurately. Real-time public generation data of decentral sources could provide an overarching solution to the uncertainty of modelling this data gap. Similarly ENTSO-e should consider to start reporting the consumption and generation data of the increasing share of large ESSs besides hydro (which is already reported) in order to allow for a more precise calculation of the electricity mix.

Further general improvement of the model can be achieved by incorporation of targeted emission factors for generation types. The presented model makes use of a globally determined set of emission factors by the IPCC. More accuracy can be found in usage of country specific emission factors. In some cases, the information about the direct emissions of electricity production is already available as part of the Union Registry of emissions which accounts for all allowances under the European Emission Trading System (ETS). Depending on the zone and data availability, these plant specific emissions can be derived [100]. In an ideal situation, publishing of plant specific emissions can be regulated in order to provide reliable and precise information about the electricity mix and its related GHG emissions. Another consideration in determining the type specific emission factors are the allocation of emissions to the production of heat. When heat is considered to be a usable product, the emissions of combined heat and power production should be divided over the electricity and the heat. This is elaborated in Appendix B.

Self consumption forms a complex factor of modelling the average emission intensity of the electricity grid. Self consumption exists behind the meter, invisible to the public (operated) grid. When modelling share of PV in the electricity mix, it is based on weather characteristics. The local electricity consumption of the PV installation owner is unknown. Therefore, it is unknown what fraction of the PV generated power is delivered to the grid. A modern grid connection typically consists of three phases. As result of connecting practices, it is possible that the PV installation is connected to a different phase than the consuming appliances. In this case, consumers are physically not be able to consume the power they generate, even though the timing and location of production and consumption might align. This leads to the conclusion that the scope of grid must be considered to range from the generator to the consuming appliances. If the grid would be defined as the infrastructure between the generator and the meter, a method of modelling behind-the-meter generation has to be developed.

ODECT is developed to model the dynamic generation type composition of electrical power. In the future, the energy sector is destined to become an interconnected multi-domain system, where carriers of energy are interchanged to fit different purposes such as transport or heat generation. Energy carrier with a fixed connection between demand and supply, either with or without monitored storage, can be modelled by ODECT. For example, an emission intensity can be assigned to the heat generated as product of coal fired power plants similar to electricity. Besides heat, hydrogen and gas which are fed to a grid can be tracked in terms of emission intensity. When the conversion of energy carriers is modelled considering conversion efficiency and life cycle emissions of conversion installations, ODECT can be broadened to cover the emission intensity of a multi-domain system. In this context, the heat, hydrogen, gas and electricity used by a consumer can be translated into the environmental impact of generating these sources of energy.

Improvement of the performance and usefulness of ODECT can be realised by implementing a prediction function, a footprint and DSM calculation tool, marginal emission factors and a smaller time interval. Furthermore, a public dashboard could improve the general accessibility of the insights. These functions can be implemented to improve usefulness for a targeted user group.

Bibliography

[1]World Resources Institute. *Climate Watch Historical GHG Emissions*. https://www.climatewatchdata.org/ghg-emissions. Accessed: December 14, 2022. 2015 (cit. on pp. 1, 13).

[2]RIVM Emissiregistratie CBS. *Uitstoot broeikasgassen naar sector*. https://www.cbs.nl/nl-nl/dossier/dossier-broeikasgassen/welke-sectoren-stoten-broeikasgassen-uit-. Accessed: December 9, 2022. 2015 (cit. on p. 1).

[3]Didier Vuarnoz and Thomas Jusselme. „Temporal variations in the primary energy use and greenhouse gas emissions of electricity provided by the Swiss grid“. In: *Energy* 161 (2018), pp. 573–582 (cit. on pp. 1, 2, 17, 19, 25).

[4]United Nations Economic Commission for Europe. *Carbon Neutrality in the UNECE Region: Integrated Life-cycle Assessment of Electricity Sources*. 2022 (cit. on pp. 1, 16, 47).

[5]IPCC. *Contribution of Working Group III to the Fifth Assessment Report of the Intergovernmental Panel on Climate Change*. 2014 (cit. on pp. 1, 14, 15, 40).

[6]IEA. *Coal-Fired Electricity*. https://www.iea.org/reports/coal-fired-electricity. 2022 (cit. on p. 1).

[7]Nils Seckinger and Peter Radgen. „Dynamic prospective average and marginal GHG emission factors—scenario-based method for the german power system until 2050“. In: *Energies* 14.9 (2021) (cit. on pp. 1, 24).

[8]Markus Fleschutz, Markus Bohlayer, Marco Braun, Gregor Henze, and Michael D. Murphy. „The effect of price-based demand response on carbon emissions in European electricity markets: The importance of adequate carbon prices“. In: *Applied Energy* 295 (2021), p. 117040 (cit. on pp. 2, 11, 19, 24, 25, 62).

[9]NEA. *Uranium 2020: Resources, Production and Demand*. https://www.oecd-nea.org/jcms/pl_52718/uranium-2020-resources-production-and-demand. Accessed: 4 July, 2023. 2020 (cit. on p. 5).

[10]IPCC. *Contribution of Working Group III to the Fifth Assessment Report of the Intergovernmental Panel on Climate Change*. 2014 (cit. on pp. 6, 13, 15, 16, 47).

[11]International Energy Agency. *Electricity Information 2022 edition*. https://www.iea.org/data-and-statistics/data-product/electricity-information. Accessed: February 13, 2023. 2022 (cit. on pp. 6, 10).

[12]Peter van Oirsouw. *Netten voor distributie van elektriciteit*. 2012 (cit. on p. 7).

[13]TenneT TSO. *Netkaarten*. https://www.tennet.eu/nl/grid/netkaarten. 2023 (cit. on p. 8).

[14]Ben Voorhorst. *Landelijk Actieprogramma Netcongestie*. https://www.rijksoverheid.nl/binaries/rijksoverheid/documenten/rapporten/2022/12/21/landelijk-actieprogramma-netcongestie/landelijk-actieprogramma-netcongestie.pdf. Accessed: December 22, 2022. 2022 (cit. on pp. 8, 19).

[15]ENTSO-E. *ENTSO-E Transparency Platform*. https://transparency.entsoe.eu/. Accessed: 4 July, 2023 (cit. on pp. 8, 12, 28).

[16]ACM. *De Energiemarkt*. https://www.acm.nl/nl/onderwerpen/energie/de-energiemarkt/de-energiemarkt. Accessed: 4 July, 2023 (cit. on p. 10).

[17]Pia Stoll, Nils Brandt, and Lars Nordström. „Including dynamic CO2 intensity with demand response". In: *Energy Policy* 65 (2014), pp. 490–500 (cit. on pp. 11, 16, 24).

[18]Gerwin Hoogsteen, Aditya Pappu, Bahman Ahmadi, et al. „On the Effects of Active Energy Community Participation in the Energy System". In: *2022 IEEE PES Innovative Smart Grid Technologies Conference Europe (ISGT-Europe)*. IEEE, Nov. 2022, pp. 1–5 (cit. on p. 11).

[19]ENTSO-E. *Official mandates*. https://www.entsoe.eu/about/inside-entsoe/official-mandates/. Accessed: 4 July, 2023 (cit. on p. 12).

[20]IPCC. *Contribution of Working Group I to the Fifth Assessment Report of the Intergovernmental Panel on Climate Change*. 2013 (cit. on p. 14).

[21]Mark A J Huijbregts, Zoran J N Steinmann, Pieter M F Elshout, et al. „ReCiPe2016: a harmonised life cycle impact assessment method at midpoint and endpoint level". In: *Int. J. Life Cycle Assess.* 22.2 (Feb. 2017), pp. 138–147 (cit. on p. 15).

[22]RIVM. *LCIA: the ReCiPe model*. https://www.rivm.nl/en/life-cycle-assessment-lca/recipe. 2018 (cit. on p. 15).

[23]Scott Nicholson and Garvin Heath. *Life cycle emissions factors for electricity generation technologies*. report: https://www.nrel.gov/docs/fy21osti/80580.pdf, dataset: https://data.nrel.gov/submissions/171. 2021 (cit. on pp. 16, 40).

[24]John Clauß, S Stinner, Christian Solli, et al. „A generic methodology to evaluate hourly average CO2eq. intensities of the electricity mix to deploy the energy flexibility potential of Norwegian buildings". In: Dec. 2018 (cit. on pp. 16, 25).

[25]Paolo Valdiserri, Vincenzo Ballerini, and Eugenia Rossi di Schio. „Interpolating functions for CO2 emission factors in dynamic simulations: The special case of a heat pump". In: *Sustainable Energy Technologies and Assessments* 53 (2022), p. 102725 (cit. on pp. 16, 24).

[26]Mary Sotos. „GHG Protocol; Scope 2 Guidance". In: World Resources Institute, 2015. Chap. 1 (cit. on pp. 16–19).

[27]World Resources Institute and World Business Council for Sustainable Development. „The Greenhouse Gas Protocol". In: WBCSD, 2004. Chap. 4 (cit. on pp. 16, 17).

[28]EEA. *Greenhouse gas emission intensity of electricity generation*. https://www.eea.europa.eu/data-and-maps/daviz/co2-emission-intensity-13/#tab-chart_3. Accessed: 2 May, 2023 (cit. on pp. 17, 46, 47).

[29]Lo Vullo, Muntean, Duerr, Kona, and Bertoldi. *GHG Emission Factors for Electricity Consumption*. https://data.jrc.ec.europa.eu/dataset/919df040-0252-4e4e-ad82-c054896e1641. Sheet: EU$_LCA_GHG.Accessed: 2May, 2023$. 2020 (cit. on pp. 17, 46, 47).

[30]Lo Vullo, Muntean, Duerr, Kona, and Bertoldi. *GHG Emission Factors for Electricity Consumption*. https://data.jrc.ec.europa.eu/dataset/919df040-0252-4e4e-ad82-c054896e1641. Sheet: EU$_IPCC_GHG.Accessed: 2May, 2023$. 2020 (cit. on pp. 17, 46, 47).

[31] CBS. *Rendementen, CO2-emissie elektriciteitsproductie, 2021*. https://www.cbs.nl/nl-nl/maatwerk/2023/06/rendementen-co2-emissie-elektriciteitsproductie-2021. Accessed: 2 May, 2023. 2023 (cit. on p. 17).

[32] CE Delft. *Ketenemissies elektriciteit*. https://www.co2emissiefactoren.nl/wp-content/uploads/2022/01/23-CE-Delft-Ketenemissies-elektriciteit-2022.pdf. 2022 (cit. on pp. 17, 47).

[33] LDES Council and McKinsey & Company. *A path towards full grid decarbonization with 24/7 clean Power Purchase Agreements*. https://www.mckinsey.com/industries/electric-power-and-natural-gas/our-insights/decarbonizing-the-grid-with-24-7-clean-power-purchase-agreements. Accessed: December 14, 2022. 2022 (cit. on pp. 18, 19).

[34] AIB. *AIB Member Countries/Regions*. https://www.aib-net.org/facts/aib-member-countries-regions. 2023 (cit. on p. 18).

[35] Google. *Moving toward 24x7 carbon-free energy at Google data centers*. https://www.gstatic.com/gumdrop/sustainability/24x7-carbon-free-energy-data-centers.pdf. Accessed: February 13, 2023. 2018 (cit. on pp. 19, 51).

[36] WattTime Tomorrow. *A vision for how ambitious organisations can accurately measure electricity emissions to take genuine action*. https://www.watttime.org/app/uploads/2021/08/GHG-Frameworks-WhitePaper-Tomorrow-WattTime-202108.pdf. Accessed: February 13, 2023. 2021 (cit. on pp. 19, 24).

[37] ENTSO-E. *Views on a Future-Proof Market Design for Guarantees of Origin*. https://eepublicdownloads.blob.core.windows.net/public-cdn-container/clean-documents/Publications/Position%20papers%20and%20reports/2022/entso-e_pp_guarantees_of_origin_220715%20for%20publication.pdf. Accessed: December 22, 2022. 2022 (cit. on p. 19).

[38] International Energy Agency. *Advancing Decarbonisation through Clean Electricity Procurement*. https://www.iea.org/reports/advancing-decarbonisation-through-clean-electricity-procurement. Accessed: December 14, 2022. 2022 (cit. on p. 19).

[39] Gregory J. Miller, Kevin Novan, and Alan Jenn. „Hourly accounting of carbon emissions from electricity consumption“. In: *Environmental Research Letters* 17.4 (2022) (cit. on pp. 19, 24).

[40] EPA. *Basic Information of Air Emissions Factors and Quantification*. https://www.epa.gov/air-emissions-factors-and-quantification/basic-information-air-emissions-factors-and-quantification. Accessed: 26 June, 2023. 2023 (cit. on p. 21).

[41] Council of European Union. *Commission Regulation (EU) No 543/2013 of 14 June 2013 on submission and publication of data in electricity markets*. https://eur-lex.europa.eu/eli/reg/2013/543/oj. Accessed: 18 April, 2023. 2013 (cit. on pp. 23, 25).

[42] A.D. Hawkes. „Estimating marginal CO2 emissions rates for national electricity systems“. In: *Energy Policy* 38.10 (2010). The socio-economic transition towards a hydrogen economy - findings from European research, with regular papers, pp. 5977–5987 (cit. on p. 24).

[43] Anika Regett, Felix Böing, Joehen Conrad, Steffen Fattler, and Constanze Kranner. „Emission Assessment of Electricity: Mix vs. Marginal Power Plant Method“. In: *2018 15th International Conference on the European Energy Market (EEM)*. 2018, pp. 1–5 (cit. on p. 24).

[44] Jacques A. de Chalendar, John Taggart, and Sally M. Benson. „Tracking emissions in the US electricity system“. In: *Proceedings of the National Academy of Sciences* 116.51 (2019), pp. 25497–25502 (cit. on p. 24).

[45] Charlotte Roux, Patrick Schalbart, and Bruno Peuportier. „Accounting for temporal variation of electricity production and consumption in the LCA of an energy-efficient house“. In: *Journal of Cleaner Production* 113 (2016), pp. 532–540 (cit. on p. 24).

[46] A. Sahebalam, Chen Ding, Gary Michor, Greg Doucette, and Marjan Ahadi. „Hourly Live GHG Calculation and Forecasting“. In: *2018 IEEE Canadian Conference on Electrical Computer Engineering (CCECE)*. 2018, pp. 1–6 (cit. on p. 24).

[47] Maria Kopsakangas-Savolainen, Maija K. Mattinen, Kaisa Manninen, and Ari Nissinen. „Hourly-based greenhouse gas emissions of electricity – cases demonstrating possibilities for households and companies to decrease their emissions“. In: *Journal of Cleaner Production* 153 (2017), pp. 384–396 (cit. on p. 24).

[48] Daniel L. Summerbell, Diana Khripko, Claire Barlow, and Jens Hesselbach. „Cost and carbon reductions from industrial demand-side management: Study of potential savings at a cement plant“. In: *Applied Energy* 197 (2017), pp. 100–113 (cit. on p. 24).

[49] Nils Baumgärtner, Roman Delorme, Maike Hennen, and André Bardow. „Design of low-carbon utility systems: Exploiting time-dependent grid emissions for climate-friendly demand-side management“. In: *Applied Energy* 247 (2019), pp. 755–765 (cit. on p. 24).

[50] Ingrid Munné-Collado, Fabio Maria Aprà, Pol Olivella-Rosell, and Roberto Villafáfila-Robles. „The Potential Role of Flexibility During Peak Hours on Greenhouse Gas Emissions: A Life Cycle Assessment of Five Targeted National Electricity Grid Mixes“. In: *Energies* 12.23 (Nov. 2019), p. 4443 (cit. on pp. 24, 25).

[51] Maarten Messagie, Jan Mertens, Luis Oliveira, et al. „The hourly life cycle carbon footprint of electricity generation in Belgium, bringing a temporal resolution in life cycle assessment“. In: *Applied Energy* 134 (2014), pp. 469–476 (cit. on p. 24).

[52] Thibault Q. Péan, Jaume Salom, Joana Ortiz, and Adrià de Besòs. „Environmental and Economic Impact of Demand Response Strategies for Energy Flexible Buildings“. In: 2018 (cit. on p. 24).

[53] Kenneth Leerbeck, Peder Bacher, Rune Grønborg Junker, et al. „Short-term forecasting of CO2 emission intensity in power grids by machine learning“. In: *Applied Energy* 277 (2020), p. 115527 (cit. on p. 24).

[54] Ana Carolina Riekstin, Antoine Langevin, Thomas Dandres, Ghyslain Gagnon, and Mohamed Cheriet. „Time Series-Based GHG Emissions Prediction for Smart Homes“. In: *IEEE Transactions on Sustainable Computing* 5.1 (2020), pp. 134–146 (cit. on p. 24).

[55] R. Bettle, C.H. Pout, and E.R. Hitchin. „Interactions between electricity-saving measures and carbon emissions from power generation in England and Wales“. In: *Energy Policy* 34.18 (2006), pp. 3434–3446 (cit. on p. 24).

[56]Felix Boing and Anika Regett. „Hourly CO2 Emission Factors and Marginal Costs of Energy Carriers in Future Multi-Energy Systems“. In: *Energies* 12.12 (June 2019), p. 2260 (cit. on p. 24).

[57]Pareschi, Giacomo, Georges, Gil, and Boulouchos, Konstantinos. „Assessment of the Marginal Emission Factor associated with Electric Vehicle Charging“. In: (2017) (cit. on p. 25).

[58]Bo Tranberg, Olivier Corradi, Bruno Lajoie, et al. „Real-time carbon accounting method for the European electricity markets“. In: *Energy Strategy Reviews* 26 (2019), p. 100367 (cit. on p. 25).

[59]R. Camilla Thomson, Gareth P. Harrison, and John P. Chick. „Marginal greenhouse gas emissions displacement of wind power in Great Britain“. In: *Energy Policy* 101 (2017), pp. 201–210 (cit. on p. 25).

[60]Joseph Wheatley. „Quantifying CO2 savings from wind power“. In: *Energy Policy* 63 (2013), pp. 89–96 (cit. on p. 25).

[61]Jun Kono, York Ostermeyer, and Holger Wallbaum. „The trends of hourly carbon emission factors in Germany and investigation on relevant consumption patterns for its application“. In: *The International Journal of Life Cycle Assessment* 22.10 (Feb. 2017), pp. 1493–1501 (cit. on p. 25).

[62]Imran Khan, Michael W. Jack, and Janet Stephenson. „Analysis of greenhouse gas emissions in electricity systems using time-varying carbon intensity“. In: *Journal of Cleaner Production* 184 (2018), pp. 1091–1101 (cit. on p. 25).

[63]ElectricityMaps. https://app.electricitymaps.com/map. Accessed 14 February, 2023 (cit. on pp. 25, 46, 51).

[64]NetAnders. *CO2 Monitor*. https://co2monitor.nl/. Accessed: April 18, 2023 (cit. on pp. 25, 46, 47).

[65]WattTime. *The power to choose clean energy*. https://www.watttime.org/. Accessed: April 18, 2023 (cit. on p. 25).

[66]Singularity. *Carbonara by Singularity*. https://carbonara.singularity.energy/app/home. Accessed: April 18, 2023 (cit. on p. 25).

[67]National Grid ESO. *Carbon Intensity*. https://www.carbonintensity.org.uk/. Accessed: April 18, 2023 (cit. on p. 25).

[68]Nowtricity. *Nowtricity*. https://www.nowtricity.com/. Accessed: April 18, 2023 (cit. on p. 25).

[69]RTE France. *Eco2mix*. https://www.rte-france.com/eco2mix. Accessed: April 18, 2023 (cit. on p. 25).

[70]N. Hamrouni, M. Jraidi, and A. Cherif. „Solar radiation and ambient temperature effects on the performances of a PV pumping system“. In: *Revue des Energies Renouvelables* 11.1 (2008), pp. 95–106 (cit. on p. 28).

[71]KNMI. *Actual synoptic observations KNMI the Netherlands per 10 minutes*. https://dataplatform.knmi.nl/dataset/actuele10mindataknmistations-2. Accessed: 18 April, 2023. 2023 (cit. on p. 29).

[72] CBS. *Hernieuwbare Energie in Nederland 2020 - Zonne-energie*. https://www.cbs.nl/nl-nl/longread/aanvullende-statistische-diensten/2021/hernieuwbare-energie-in-nederland-2020/5-zonne-energie. Accessed: 18 April, 2023. 2021 (cit. on p. 29).

[73] CBS. *Zonnestroom, vermogen en vermogensklasse, bedrijven en woningen, regio*. https://opendata.cbs.nl/#/CBS/nl/dataset/85005NED/table. Accessed: 18 April, 2023. 2022 (cit. on p. 29).

[74] CBS. *Zonnestroom, vermogen bedrijven en woningen, regio (indeling 2019)*. https://opendata.cbs.nl/#/CBS/nl/dataset/84783NED/table. Accessed: 18 April, 2023. 2021 (cit. on pp. 29, 50).

[75] „Introduction: Modern Wind Energy and its Origins“. In: *Wind Energy Explained*. 2009. Chap. 2, pp. 23–87 (cit. on p. 31).

[76] KNMI. *Windmetingen*. https://www.knmi.nl/kennis-en-datacentrum/uitleg/windmetingen. Accessed: 27 June, 2023 (cit. on p. 31).

[77] „Aerodynamics of Wind Turbines“. In: *Wind Energy Explained*. 2009. Chap. 3, pp. 91–153 (cit. on p. 31).

[78] DNV. *Definitions of Availability Terms for the Wind Industry*. 2017 (cit. on p. 32).

[79] Md Rasel Sarkar, Sabariah Julai, Chong Wen Tong, et al. „Hybrid Pitch Angle Controller Approaches for Stable Wind Turbine Power under Variable Wind Speed“. In: *Energies* 13 (2020) (cit. on p. 32).

[80] EPA. *Renewable Energy Fact Sheet: Wind Turbines*. 2013 (cit. on p. 32).

[81] WindStats. *Ontwikkeling Afmetingen*. https://windstats.nl/statistieken. Accessed 12 April, 2023 (cit. on p. 33).

[82] Andrew Stepek and Ine L. Wijnant. *Interpolating wind speed normals from the sparse Dutch network to a high resolution grid using local roughness from land use maps*. https://cdn.knmi.nl/knmi/pdf/bibliotheek/knmipubTR/TR321.pdf. Accessed: 27 June, 2023 (cit. on p. 33).

[83] Francisco Bañuelos-Ruedas, César Angeles-Camacho, and Sebastián Rios-Marcuello. „Methodologies Used in the Extrapolation of Wind Speed Data at Different Heights and Its Impact in the Wind Energy Resource Assessment in a Region“. In: *Wind Farm*. 2011. Chap. 4 (cit. on p. 33).

[84] Engineering Toolbox. *Air - Density, Specific Weight and Thermal Expansion Coefficient vs. Temperature and Pressure*. https://www.engineeringtoolbox.com/air-density-specific-weight-d_600.html. Accessed 13 April, 2023 (cit. on p. 33).

[85] Yanhui Feng and Peter Tavner. *Introduction to Wind Turbines and their Reliability Availability*. https://www.ewea.org/ewec2010/fileadmin/ewec2010_files/documents/side_events/Reliability_PJT.pdf. Accessed: 27 June, 2023 (cit. on p. 33).

[86] Joana Bastos, Eleonora Lo Vullo, Marilena Muntean, et al. *GHG Emission Factors for Electricity Consumption*. http://data.europa.eu/89h/919df040-0252-4e4e-ad82-c054896e1641. 2020 (cit. on p. 35).

[87] PSE. *Integrated Annual Report 2017 edition*. https://raport2016.pse.pl/en/. 2017 (cit. on p. 36).

[88] ENTSOe. *Electricity in Europe 2017*. https://eepublicdownloads.entsoe.eu/clean-documents/Publications/Statistics/electricity_in_europe/entso-e_electricity_in_europe_2017_web.pdf (cit. on p. 36).

[89] Nana Yaw Amponsah, Mads Troldborg, Bethany Kington, Inge Aalders, and Rupert Lloyd Hough. „Greenhouse gas emissions from renewable energy sources: A review of lifecycle considerations". In: *Renewable and Sustainable Energy Reviews* 39 (2014), pp. 461–475 (cit. on p. 39).

[90] CBS. *Aandeel hernieuwbare elektriciteit met 20 procent gestegen in 2022*. https://www.cbs.nl/nl-nl/nieuws/2023/10/aandeel-hernieuwbare-elektriciteit-met-20-procent-gestegen-in-2022. Accessed: 27 June, 2023 (cit. on p. 39).

[91] Umweltbundesamt. *Entwicklung der spezifischen Treibhausgas-Emissionen des deutschen Strommix in den Jahren 1990 - 2022*. https://www.umweltbundesamt.de/sites/default/files/medien/11740/publikationen/2023_05_23_climate_change_20-2023_strommix.pdf. 2023 (cit. on pp. 40, 45).

[92] United States Geological Survey. *What are the types of coal?* https://www.usgs.gov/faqs/what-are-types-coal. Accessed 2 March, 2023 (cit. on pp. 40, 89).

[93] Bas Jansen. *ODECT: Open Dynamic Electricity Composition Tracker*. https://github.com/utwente-energy/odect. 2023 (cit. on pp. 41, 87).

[94] CBS. *Elektriciteitsproductie uit kolen bijna verdubbeld*. https://www.cbs.nl/nl-nl/nieuws/2021/49/elektriciteitsproductie-uit-kolen-bijna-verdubbeld. Accessed: 1 July, 2023 (cit. on p. 44).

[95] Mirjam Harmelink, Lex Bosselaar, Joost Gerdes, et al. *Berekening van de CO2-emissies het primair fossiel energiegebruik en het rendement van elektriciteit in Nederland*. 2012 (cit. on pp. 46, 47).

[96] Ember Climate. *European Electricity Review 2022: Methodology*. https://ember-climate.org/app/uploads/2022/02/EER-Methodology.pdf. Accessed: 2 May, 2023. 2022 (cit. on p. 47).

[97] Thomas Huld, Richard Müller, and Attilio Gambardella. „A new solar radiation database for estimating PV performance in Europe and Africa". In: *Solar Energy* 86.6 (2012), pp. 1803–1815 (cit. on pp. 49, 101).

[98] Reuters. *As Germany ends nuclear era, activist says there is still more to do*. https://www.reuters.com/world/europe/germany-ends-nuclear-era-activist-says-still-more-do-2023-04-15/. Accessed: 4 July, 2023 (cit. on p. 58).

[99] CBS. *Uitstoot broeikasgassen naar sector*. https://www.cbs.nl/nl-nl/dossier/dossier-broeikasgassen/welke-sectoren-stoten-broeikasgassen-uit-. Accessed: 18 May, 2023. 2022 (cit. on p. 63).

[100] Jan Frederick Unnewehr, Anke Weidlich, Leonhard Gfüllner, and Mirko Schäfer. „Open-data based carbon emission intensity signals for electricity generation in European countries – top down vs. bottom up approach". In: *Cleaner Energy Systems* 3 (2022), p. 100018 (cit. on p. 70).

[101] E.J. Finnemore and J.B. Franzini. *Fluid Mechanics With Engineering Applications*. McGraw-Hill Education, 2001 (cit. on p. 89).

[102] Theodore Wildi. *Electrical machines, drives and power systems: Pearson new international edition*. Pearson Higher Ed, 2013 (cit. on p. 89).

[103] Pavel Fott. „Carbon emission factors of coal and lignite: analysis of Czech coal data and comparison to European values". In: *Environmental Science Policy* 2.3 (1999), pp. 347–354 (cit. on p. 89).

[104] National Research Council. „Coal: Research and Development to Support National Energy Policy". In: 2007. Chap. Appendix E: Coal Mining and Processing Methods (cit. on p. 89).

[105] Paul Breeze. „Chapter 3 - Coal-fired Power Plants". In: *Power Generation Technologies (Second Edition)*. Ed. by Paul Breeze. Second Edition. Boston: Newnes, 2014, pp. 29–65 (cit. on p. 89).

[106] Ruud Meij and Henk te Winkel. „The emissions of heavy metals and persistent organic pollutants from modern coal-fired power stations". In: *Atmospheric Environment* 41.40 (2007), pp. 9262–9272 (cit. on pp. 89, 90).

[107] Paul Breeze. „Chapter 4 - Natural Gas-Fired Gas Turbine and Combined Cycle Power Plants". In: *Power Generation Technologies (Second Edition)*. Second Edition. Boston: Newnes, 2014 (cit. on p. 90).

[108] Soon Kiat Yee, Jovica V. Milanovic, and F. Michael Hughes. „Overview and Comparative Analysis of Gas Turbine Models for System Stability Studies". In: *IEEE Transactions on Power Systems* 23.1 (2008), pp. 108–118 (cit. on p. 90).

[109] Paul Breeze. „Chapter 5 - Piston Engine-Based Power Plants". In: *Power Generation Technologies (Second Edition)*. Second Edition. Boston: Newnes, 2014 (cit. on p. 91).

[110] Giacomo Luciani Manfred Hafner. „Chapter 6 - Power Generation from Coal, Oil, Gas, and Biofuels". In: *The Palgrave Handbook of International Energy Economics*. palgrave Macmillan Cham, 2022 (cit. on p. 91).

[111] Paul Breeze. „Chapter 15 - Biomass-Based Power Generation". In: *Power Generation Technologies (Second Edition)*. Second Edition. Boston: Newnes, 2014 (cit. on p. 91).

[112] U.S. Environmental Protection Agency Combined Heat and Power Partnership. „Catalog of CHP Technologies". In: Sept. 2017 (cit. on p. 91).

[113] Paul Breeze. „Chapter 16 - Power From Waste". In: *Power Generation Technologies (Second Edition)*. Second Edition. Boston: Newnes, 2014 (cit. on p. 91).

[114] Twence. *Emissies naar lucht van afvalverbranding*. `https://www.twence.nl/over-ons/veiligheid`. Accessed 6 March, 2023 (cit. on p. 92).

[115] G F Hewitt and John G Collier. *Introduction to nuclear power*. Series in chemical and mechanical engineering. Boca Raton, FL: CRC Press, June 2000 (cit. on p. 92).

[116] Paul Breeze. „Chapter 17 - Nuclear Power". In: *Power Generation Technologies (Second Edition)*. Second Edition. Boston: Newnes, 2014 (cit. on p. 92).

[117] NASA. *Earth. Our home planet*. `https://solarsystem.nasa.gov/planets/earth/in-depth/`. Accessed 6 March, 2023 (cit. on p. 93).

[118] Paul Breeze. „Chapter 12 - Geothermal Power". In: *Power Generation Technologies (Second Edition)*. Second Edition. Boston: Newnes, 2014 (cit. on pp. 93, 94).

[119] Adele Manzella. „General Introduction to Geothermal Energy“. In: *Geothermal Energy and Society*. Ed. by Adele Manzella, Agnes Allansdottir, and Anna Pellizzone. Springer International Publishing, 2019, pp. 1–18 (cit. on p. 93).

[120] K. Vignarooban, Xinhai Xu, A. Arvay, K. Hsu, and A.M. Kannan. „Heat transfer fluids for concentrating solar power systems – A review“. In: *Applied Energy* 146 (2015), pp. 383–396 (cit. on p. 94).

[121] K. Lovegrove and W. Stein Csiro. „1 - Introduction to concentrating solar power (CSP) technology“. In: *Concentrating Solar Power Technology*. Ed. by Keith Lovegrove and Wes Stein. Woodhead Publishing Series in Energy. Woodhead Publishing, 2012, pp. 3–15 (cit. on p. 94).

[122] Paul Breeze. „Chapter 13 - Solar Power“. In: *Power Generation Technologies (Second Edition)*. Second Edition. Boston: Newnes, 2014 (cit. on pp. 94, 95).

[123] Mark Mehos, Craig Turchi, Judith Vidal, et al. „Concentrating Solar Power Gen3 Demonstration Roadmap“. In: (Jan. 2017) (cit. on p. 94).

[124] A. Reinders, Pierre Verlinden, Wilfried van Sark, and Alexandre Freundlich. *Photovoltaic Solar Energy: from Fundamentals to Applications*. Jan. 2017 (cit. on p. 95).

[125] „Introduction: Modern Wind Energy and its Origins“. In: *Wind Energy Explained*. 2009. Chap. 1, pp. 1–22 (cit. on p. 96).

[126] Lucy Y. Pao and Kathryn E. Johnson. „Control of Wind Turbines“. In: *IEEE Control Systems Magazine* 31.2 (2011), pp. 44–62 (cit. on p. 96).

[127] Vattenfall. *Hollandse Kust Zuid*. `https://vattenfall-hollandsekust.nl/en/blog/2019/11/27/turbines/`. Accessed 21 February, 2023 (cit. on p. 97).

[128] Paul Breeze. „Chapter 8 - Hydropower“. In: *Power Generation Technologies (Second Edition)*. Second Edition. Boston: Newnes, 2014 (cit. on p. 97).

[129] EU Joint Research Centre. *Ocean Energy - Technology Development Report 2020*. 2021 (cit. on p. 97).

[130] Paul Breeze. „Chapter 14 - Marine Power Generation Technologies“. In: *Power Generation Technologies (Second Edition)*. Second Edition. Boston: Newnes, 2014 (cit. on p. 97).

[131] Energy Industrial Strategy Department for Business. *UK government announces biggest investment into Britain’s tidal power*. `https://www.gov.uk/government/news/uk-government-announces-biggest-investment-into-britains-tidal-power`. Accessed 22 February, 2023 (cit. on p. 97).

[132] Bojan Stojkovski. *Russia wants to build the world’s most powerful tidal power plant in Kamchatka*. `https://www.renewable.news/innovation-technology/russia-wants-to-build-the-worlds-most-powerful-tidal-power-plant-in-kamchatka/`. Accessed 22 February, 2023 (cit. on p. 97).

[133] EDF. *The Rance tidal power plant*. `https://www.edf.fr/usine-maremotrice-rance/presentation`. Accessed 22 February, 2023 (cit. on p. 97).

[134] Korea Water Resources Corporation. *Sihwa tidal power plant*. `https://www.kwater.or.kr/eng/tech/sub01/sub02/patentPage.do?s_mid=1207`. Accessed 22 February, 2023 (cit. on p. 97).

[135] Basavaraj Patil, Bhookya devojee, Preeti Hj, and Majeed Pasha. „Advances in Renewable Energy Technologies“. In: Apr. 2020, pp. 85–99 (cit. on p. 98).

[136] MFFBAS. https://www.mffbas.nl/documenten/. Accessed 15 Dec. 2022 (cit. on p. 101).

[137] Stefan Pfenninger and Iain Staffell. *Renewables.ninja*. https://renewables.ninja. Accessed 15 Dec. 2022 (cit. on p. 101).

List of Figures

List of Tables

Supplementary materials

Supplementary materials related to this thesis consisting of ODECT code and resulting databases can be found online at [93].

Generation Types

A

A.1 Turbines and generators

Before elaborating the different sources of electricity, it is worth taking a look at two fundamental components that occur in all methods of electricity generation with the exception of PV panels, namely turbines and generators. A turbine is a mechanical device that converts kinetic energy contained in a fluid into mechanical energy in the form of a turning shaft. Examples are gas, steam, wind and water turbines. The basic working principle of a turbine consists of a flowing volume of fluid which is passed through a tube. Within this tube, a rotor is mounted to convert the kinetic energy (inpulse turbines) or pressure (reaction turbines) of the fluid into rotational mechanical power by changing the direction of the flow. This mechanical power can be converted into electricity by use of generator [101]. A generator is a device that transforms mechanical energy into electrical energy. The three-phase synchronous generator is the largest source of the electricity consumed today. This machine consists of a stationary part, the stator, and a rotating part, the rotor. Most often, the rotor contains a magnetic field which induces an electrical current in the armature windings of the stator when the rotor is turning [102].

A.2 Coal

As can be seen in Fig 2.1, coal is the largest source of electricity worldwide. Before electricity can be generated, the coal is extracted from the earth by surface mining, removing the top soil to expose to coal layer, or underground mining. The type (rank) of coal depends on its stage of the so-called 'coalification' process which starts with plant matter and turns into peat, lignite, subbituminous, bituminous and lastly anthracite [92]. The different types of coal vary in chemical composition. This results in a difference in installation design and GHG emissions [103]. Before it is burned, the coal is processed (crushed, sized and cleaned) to optimise efficiency in the power plant [104]. Electricity from coal is predominantly generated in pulverised coal-fired boilers [105, 106]. This method makes use of pulverised coal powder that burns easier and more efficient compared to burning of larger coal particles. The powder is fed to a boiler where it is burned. The resulting heat is used to convert water to steam. The pressure of the steam is subsequently convert in mechanical power by a turbine which is convert to electrical power by a generator. To a lesser extent, Coal Gasification Combined Cycle (CGCC) installations are used to generate electricity from coal, this technique is similar to the combined cycle gas turbine which will be discussed in the next section [106].

A.3 Natural gas

Gas turbines are able to process a wide range of gases with minimal adaptation. The majority of gas fired power plants use natural gas as fuel [107]. Gas fired power plants can be categorised as Open-Cycle Gas Turbine (OCGT) or Combined Cycle Gas Turbine (CCGT). Furthermore, natural gas is burned in reciprocating engines, this is elaborated in the next section. Both OCGTs and CCGTs operate with the principles of the Brayton cycle. This cycle consists of four processes: compression, heat addition, expansion, heat extraction. First, as shown in Fig A.1, air is drawn in and compressed to high pressure. Secondly, fuel is added to the high pressure air flow and burned which leads to a volume increase. Finally, the the gas mixture flows out through the turbine which starts turning with the use of blades and the gas is released to the environment [108, 107]. A CCGT makes use of a Rankine cycle complementary to the Brayton cycle, using the heat as rest-product of the Brayton cycle as input for a second (steam) turbine. OCGTs have the advantage of providing high flexibility i.e. quick response to demand peaks. CCGTs have a higher overall efficiency due to the reuse of heat and thus provides the more economical solution [107].

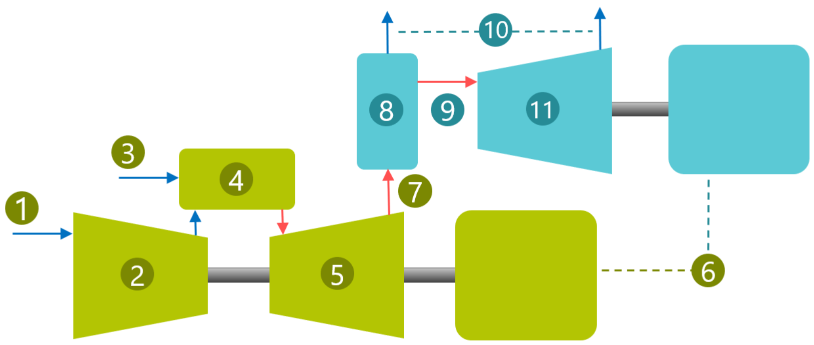

Fig. A.1.: Schematic representation of a gas turbine. The green section (1-5) shows the open cycle gas turbine. In case of a combined cycle gas turbine, the blue section (6-10) is added. (1) Air intake, (2) air compressor, (3) gas intake, (4) combustion chamber, (5) gas turbine, (6) generator, (7) heat exhaust, (8) heat recovery, (9) steam intake, (10) air outlet, (11) steam turbine. Adapted from [107].

A.4 Oil

Aside from their use in vehicles, reciprocating (piston) engines are also used to generate electricity. The uses ranges from small diesel fired generators design for emergency power supply to large plants for base load power generation. Usable fuels are gases, gasoline, diesel, heavier oils and biofuels. These fuels can also be burned in boilers to power steam turbines similar to coal fired power plants. Small and medium sized engines work according to a four-stroke cycle. First air and fuel is let into the cylinder. Second, a piston decreases the volume of the cylinder by moving, effectively compressing the fuel mix. Third, a spark ignites the fuel mix, inducing mechanical power on the piston. Fourth, the burned fuel mix is exhausted from the cylinder. Large installation typically make use of a two-stroke cycle. In a two-stroke cycle, the piston compresses the fuel mix which is subsequently ignited. The intake and exhaust happen simultaneous during the high volume phase of the cylinder [109]. Using oil in reciprocating engines for electricity generation is not efficient as much heat is exhausted from the engine. This heat can be used to produce combined cycle generation, but this is only economical for very large engines. The technology is fit for use at remote locations as result of the high energy density of hydrocarbon fuels. Furthermore, the engines provide high flexibility and could therefore be used as peak firing plant [110].

A.5 Biomass and waste

Apart from fossil fuels, biomass and waste can be burned to generate electricity. Biomass can be divided into purposefully grown energy crops and waste streams including urban, agricultural, livestock and wood waste. Depending on the type of biomass, it can be directly burned in a furnace, or indirectly by creating bio-fuels through fermentation or pyrolysis. The predominant method is burning the biomass in a furnace to create steam and drive a steam turbine [111]. The biomass, often types of wood, has to be analysed and adequately prepared for burning. The preparation process includes drying, screening and grinding [112]. Optionally, the biomass can be burned together with coal in efficient large coal-fired power plants. This process is called co-firing. Biomass processes that are not (or very rarely) used for generation of electricity are bio-gas production through digestion of manure, production of bio-alcohol from crop fermentation and ethanol production from crops containing oil [111]. Urban waste provides a another potential source of electricity. This waste can be recycled, burned or land-filled in decreasing order of environmental desirability. It differs per geographic region and waste composition which processing method is predominantly used. Municipal solid waste and industrial waste are main sources of electricity from waste [113]. These waste streams are sorted, burned and resulting gases are filtered to limit the emissions of harmful flue gases [114]. The heat as result of the incineration is used to drive a steam turbine.

A.6 Nuclear power

Nuclear energy is released by a change in elemental form of an atom. This effect can be observed in natural occurring radioactive isotopes, but this process is too slow an rare to provide a practical source of energy. In a nuclear reactor, a faster and more intense variant of this process is created, called nuclear fission. Radioactive decay is a process where a nucleus decreases in energy by radiation. Part of this transition is the emission of one or more neutrons. In nuclear fission, this neutron is used to collide with a another heavy nucleus, causing it to split, decreasing in energy and emitting several more neutrons. When a big enough mass of heavy nuclei is available, a chain reaction of mass to energy conversion can be created. The nuclear reactor, shown schematically in Fig A.2, is built around a fuel element, often consisting of uranium in a sealed cylinder, which provides energy to the system as result of the nuclear fission process [115]. The fuel element must be replaced when the fissile uranium is depleted [116]. The fuel element is surrounded by a moderator material that converts the fast neutrons into thermal neutrons, heating up the system. This heat is extracted by a continuous stream of coolant which is used to drive a steam turbine. Furthermore, control rods are installed in the reactor core to control the neutron population and therefore the stability of the reaction. The reactor core is surrounded by a concrete body to contain the effects of a possible core failure [115]. What stands out in using nuclear power as electricity source is the minimal amount of fuel used for a large electricity production. 140 GWh of energy could be theoretically gained per kilogram of naturally occurring uranium [116].

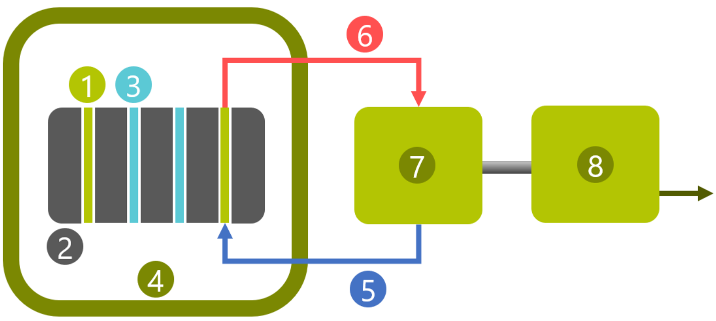

Fig. A.2.: Schematic representation of nuclear power plant. (1) Fuel element containing fissile uranium, (2) moderator material, (3) control rods, (4) concrete encapsulation container, (5) coolant stream, (6) steam flow, (7) steam turbine, (8) generator. Adapted from [115].

A.7 Geothermal power

Our planet consist of four main layers, the inner core, outer core, mantle and crust. The crust has a thickness of 30 km on land and 5 km from the ocean floor down [117]. The temperature profile across ground layers is called the geothermal gradient. The geothermal gradient varies per location from 20-30 $\circ Ckm^{-1}$ in continental areas to 40-80 $\circ Ckm^{-1}$ in vulcanic areas with relatively thinner crust. Commonly around tectonic plate boundaries, water heated by geothermal energy naturally arise in the form of springs and geysers. At other locations with varying geothermal gradients, geothermal wells can be created using fracking, creating faults and cracks for liquid to flow through [118]. At shallow depths, the ground temperature is stable at the year round average air temperature. Technologies that make use of this stable temperature at small depths are called shallow geothermal technologies. All other geothermal heat retrieving methods are characterised as deep geothermal. Heat is retrieved by circulation of water between the surface and hydro-thermal reservoirs [119]. Most geothermal installations serve heat demand as their purpose while electricity can also be generated. Geothermal power plants are predominantly located near geothermal fields at a depths ranging from 100 m to 2 km which produce water, steam or a mix of the two at high pressure. This mix, called brine, contains corrosive and toxic substances. Therefore, the heat should be extracted and the brine re-injected in the geothermal reservoir to limit ground water pollution [118]. Geothermal power plants can be characterised as three types. Dry steam plants directly use the geothermal fluids that are available in vapour state to power a turbine. The most common type of geothermal installations are flash steam systems, shown in Fig A.3, separate the liquid fraction from the vapour fraction, where only the latter is used to power a steam turbine. Lastly, binary cycle technologies make use of heat exchangers to transfer the heat from the geothermal fluid to a working fluid with a low boiling point and high vapour pressure which subsequently powers a turbine. This technology is desirable from an environmental standpoint as minimal interaction with the brine is needed [119].

A.8 Concentrating solar thermal

The sun is the major supplier of energy on earth. Besides making use of the derivatives of solar energy such as wind (result of surface heating), biomass and fossil fuels (result of photosynthesis), electricity can also be generated directly from solar irradiation. One way to do generate electricity from power provided by the sun is by using it directly as a source of heat through Concentrating Solar Thermal (CST) systems. The intensity of solar radiation at the earth surface is too low to practically generate power. Therefore, the irradiation has to be concentrated. Three

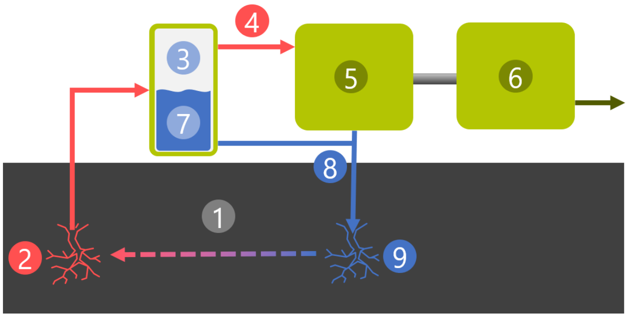

Fig. A.3.: Schematic representation of a flash steam geothermal power plant. (1) Geothermal zone, (2) production well, (3) brine vapour fraction, (4) vapour flow, (5) turbine, (6) generator, (7) brine liquid fraction, (8) waste brine (9) injection well. Adapted from [118].

common CST technologies in order of descending utilisation are parabolic through collector, solar tower and parabolic dish [120]. These technologies all use mirrors to concentrate the irradiation on a receiver. Parabolic throughs make use of a two dimensional parabolic shaped concentrating mirror with a centred receiver tube which collects and transports the heat to a steam turbine using the flow of a heat transfer fluid [121]. A solar dish has the same working principle a the parabolic through, but makes use of a three dimensional parabolic mirror, hence the name 'dish'. In the case of solar towers, shown in Fig A.4, a large area of direction controlled mirrors called heliostats are placed to concentrate the irradiation towards a receiver located in a central tower. Essentially, solar towers are large variants of the smaller solar dish [122]. CST systems are often combined with diurnal heat storage systems, e.g. molten salt storage, to provide a stable electricity generation throughout the day [118, 121]

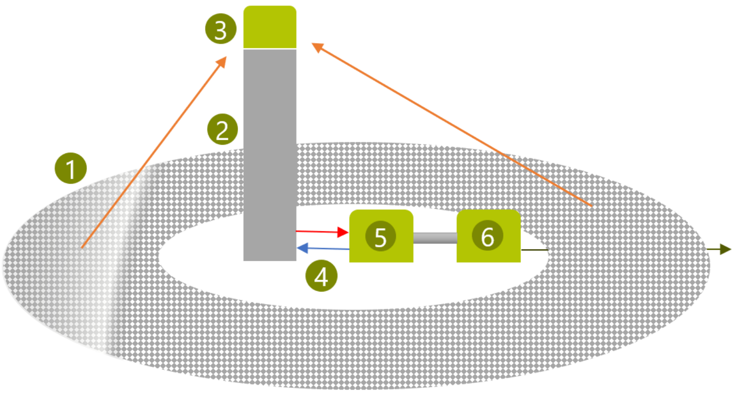

Fig. A.4.: Schematic representation of a concentrated solar power plant. (1) Heliostats, (2) receiver tower, (3) receiver, (4) heat exchange, (5) steam turbine, (6) generator. Adapted from [123].

A.9 Photovoltaic panels

The predominant technology to generate electricity from radiant energy provided by the sun is through the use of photovoltaic panels. PV panels are a collection of PV cells which for the most part consist of semiconductor materials. These materials have a variable conductivity which is sensitive to external factors, including light. These materials consist of crystalline structured atoms bonded by shared valence electrons, electrons in the outer orbit of the atom. By absorbing energy from the incoming sunlight, these valence electrons are able to leave the host atom and move freely through the material, i.e. the material becomes conductive. A so-called hole remains in the crystal structure where the electron originated. The electron and hole are separated by a PN-junction and can only recombine though a circuit. In this way electrical power is created from the impact of photons in the surface of the PV cell.

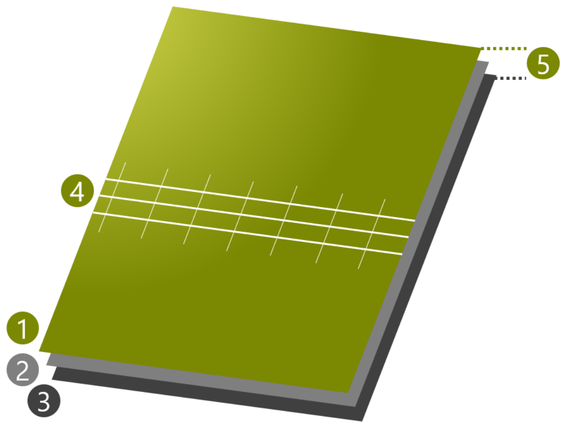

Fig. A.5.: Schematic representation of solar panel. (1) n-type semiconductor, (2) p-n junction, (3) p-type semiconductor, (4) front contact, (5) power output. Adapted from [122]

The power output of PV panels is dependent on solar irradiation. This irradiation consists of direct-, diffuse- and reflective irradiation with describe the direct sunlight and the light that has bounced off of atmospheric particles and the earth surface respectively. Therefore, the movement of earth with respect to the sun and interruption of sunlight by clouds and shadows are major influences of the generation profile of a PV panel. Strategic placement of PV panels allows for optimal power output, by placing the panel such that it is exposed to direct sunlight the longest. Alternatively, the panels can be placed facing multiple sides to stabilise the power output of time. [124]

A.10 Wind power

Humanity have used wind power for centuries to perform a wide range of activities. However, the conversion of wind in electrical energy is a relatively new technology. The technology has been on the rise since the 1960s with a spurge in the 1990s. This is a result of the willingness to reduce the dependency on fossil fuels, the large potential of freely available wind power and technological developments that could be applied to wind turbines. What differentiates wind turbines from windmills is the conversion to electricity in turbines, where windmills make use of mechanical energy.

There are many different wind turbine designs. The most successful and widely used modern wind turbines, Horizontal Axis Wind Turbines (HAWTs) shown schematically in Fig A.6, make use of aerodynamic force of lift to induce a torque on a rotating shaft. This is done by a rotor consisting of two or three blades and hub on top of a tower. The mechanical power is fed to a drive train and transformed into electrical power in generator. Design differences are found in hub design (rigid, teetering, hinged), power control (pitch/stall), rotor speed (fixed/variable), orientation alignment (self/active), generator type (synchronous/induction) and with or without gearbox. [125]

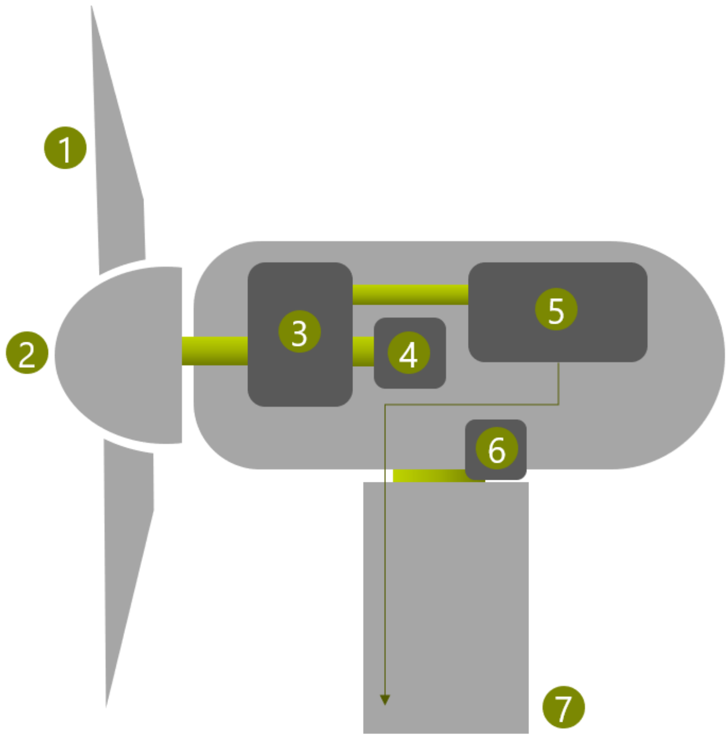

Fig. A.6.: Schematic representation of a horizontal axis wind turbine. (1) Blade, (2) rotor hub, (3) gearbox, (4) brake, (5) generator, (6) yaw drive. Adapted from [126].

Wind turbines exist with a broad range of output capacity. At the time of writing, the largest installed wind turbines have a nameplate capacity of 10MW [127]. Logically, the output of a wind turbine at a given time is dependent on the momentary wind speed. This results in a fluctuating power supply that can only be controlled downwards by curtailment.

A.11 Hydro power

On of the oldest sources of electricity is hydro power. The technology is relatively simple in principle. As shown in Fig A.7, potential energy is water as result of its elevation is converted in mechanical energy by giving the water opportunity to flow downwards. The mechanical energy is then used to power a turbine connected to a generator in order to generate electricity. The elevated water is created by precipitation as thus not endless in capacity. The largest challenge in constructing a hydroelectric power plant is finding a suitable location. A combination of suiting topography, allowed construction, an availability for electricity transmission are essential. The capacity of the hydro power plant can be determined by the volume flow of water and its drop in elevation. Many types of rivers are suitable for hydro power, as construction is cheaper on flatter surfaces and capacity is higher in elevated landscapes. The largest power plants in the world are predominantly hydroelectric power plants. Apart from using a dam and reservoir as shown in Fig A.7 run-of-river installations are used to generate electrical power from a flowing river. Run-of-river installations make use of a artificial steep declining short-cut from a river with a variable inlet. This allows for controlling how much water is diverted through the shortcut and how much power can be generated from the diversion [128].

Additionally to hydroelectric power, tidal, or oceanic, power can be converted into electricity. Many different designs are proposed to convert oceanic flow into electricity. Examples are wave, tidal, Oceanic Thermal Energy Conversion (OTEC) and salinity gradient [129]. The most common is tidal which often consists of essentially a two-way dam which direction inverts with the tides [130]. Although many Tidal Power Plants (TPPs) are currently proposed, only two TPPs with a notable capacity of 240 and 254 MW are in operation in France and South Korea respectively [131, 132, 133, 134].

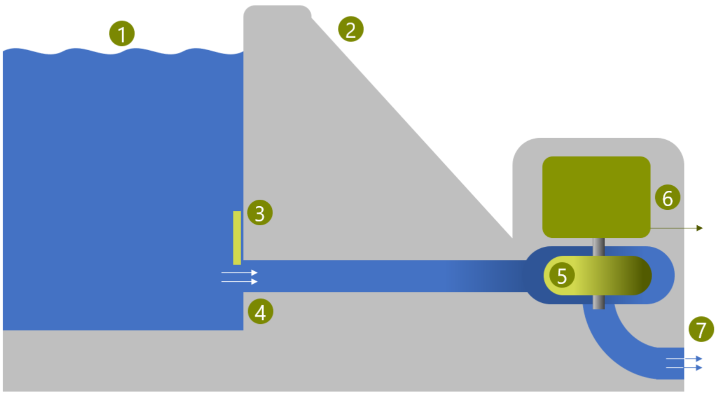

Fig. A.7.: Schematic cross-section representation of hydroelectric dam. (1) Reservoir, (2) dam, (3) inlet valve, (4) intake, (5) turbine, (6) generator, (7) outlate. Adapted from [135]

.

Emission Allocation

B

Allocation of emissions i.e., what product is responsible for which emissions, plays an important role in determining the life cycle emission factor for power generation installations. Every fuel combusting power plant that produces electricity co-produces heat as secondary product. Co-generation, the combined generation of power and heat, is much more efficient that the separate generation of heat and power, in which case residual heat is wasted to the environment.

Demand for heat in industrial processes and houses can be met through the use of a heat network. This usage of heat poses the question whether it is a residual product or not. In the case where heat is transported and put to use it should be determined whether or not the heat is a residual product. When the installation is intentionally build to cover a demand of electricity and heat, the heat is a intentionally produced product and should therefore cover a part of the emissions. A method to determine the intentionally produced heat is to take the benchmark efficiency share of electricity generation when a plant is optimised for electricity production. This baseline share of heat that is produced in that specific plant can be regarded as the residual share. One is not able to produce electricity using this technology without producing this share of heat. Plants with higher shares of heat that cover a heat demand could allocate emissions to the difference of the baseline heat share and their heat share. Alternatively, all heat can be viewed as a resource, even if it is unused, and therefore a emission share could be assigned to all heat.

In the case of Carbon Capture and Storage (CCS), electricity is used to extract carbon emission from the air. This results in a reduction of emissions as result of electricity generation but an increase of consumption. When a CCS installation in directly added to a power plant, its direct emission will decrease but so will its efficiency (kWh per kg of fuel). Overall, the emission factor for a CCS fitted power plant will be lower than one without CCS. Separate CCS installations, using direct air capture, can be excluded from the GHG intensity of electricity because the emission reduction is a result of consumption instead of generation.

C RES coverage example

In order to illustrate the discrepancy between certificate backed claims and real physical delivery of power, an theoretical example of a household is introduced in Figure C.1. In this scenario, the annual aggregated demand of a household is matched with the annual aggregated generation of renewable energy sources [97, 136, 137]. With the use of certificates, the retailer claims that it provides "100% renewable electricity" to the household. In the top graph, the household consumes as much electricity as is generated by a local PV installation on an annual basis. The week in May that is shown, clearly illustrates the problem in timing between consumption and generation of electrical power. During the day, the generation of electricity by PV panels greatly exceeds the demand while at nighttime, the demand is logically not covered by PV generation. Over the year, the consumed electricity of the household consists for only 32% of electricity generated by the PV installation, the other 68% is imported from the grid. Analysing the same scenario with electricity generation from local wind turbines (middle graph) result in a higher coverage with 70% wind against 30% grid imports. The lower graph shows a scenario in which a mix of local PV and local wind is determined to increase coverage of the consumption pattern of the household. An iterative function is used to determine the respective fractions of PV and wind to find the mix with the highest coverage. In this scenario an coverage of 72% is reached, which means that 72% of the annual electricity consumption is sourced from local PV and wind installations. In reality, the procurement of GOs by the retailer is not adapted to cover the household demand.

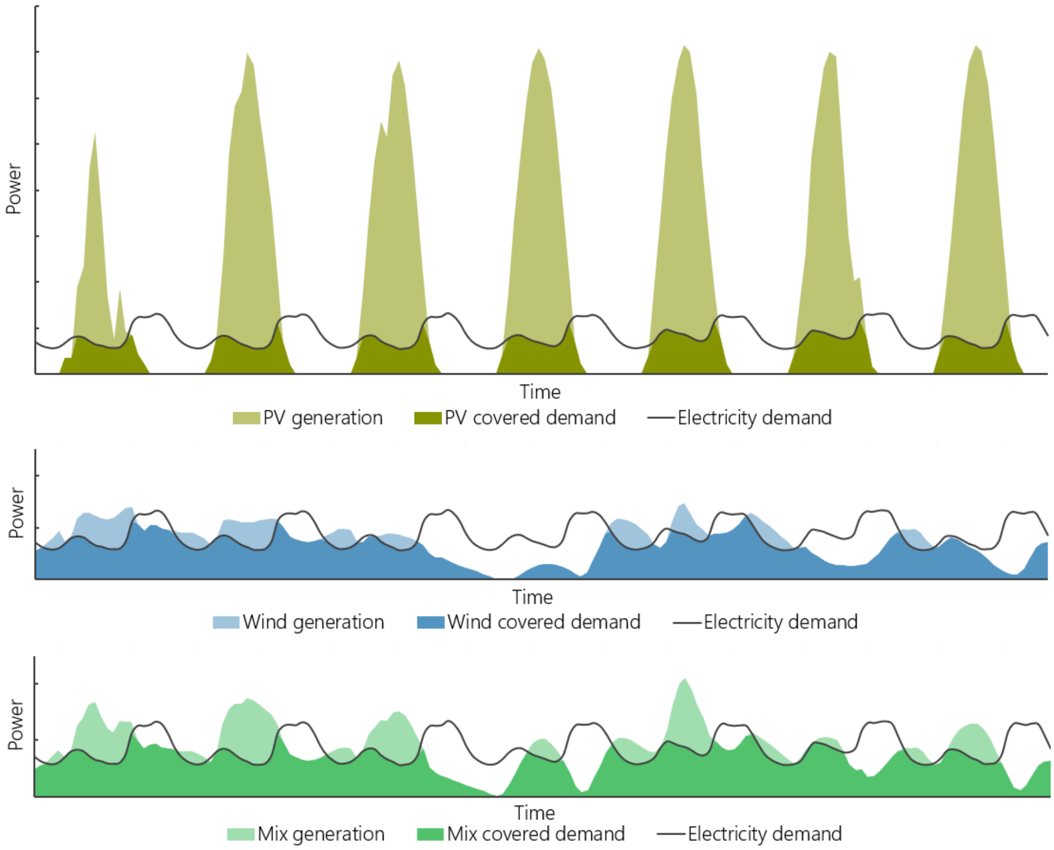

Fig. C.1.: Illustrative example of demand coverage by intermittent renewable electricity generation for a week in May. The mixed generation consists of a combination of 89% wind and 11% solar energy.